1986

Low Strain Shear Measurements of Soft Sediments Using Triaxial Vane Device (Triaxial Vane Testing, Soft Clays).

Sibel Pamukcu
Louisiana State University and Agricultural & Mechanical College

Pamukcu, Sibel

LOW STRAIN SHEAR MEASUREMENTS OF SOFT SEDIMENTS USING TRIAXIAL VANE DEVICE

The Louisiana State University and Agricultural and Mechanical Col. PH.D. 1986

PLEASE NOTE:

In all cases this material has been filmed in the best possible way from the available copy. Problems encountered with this document have been identified here with a check mark ✓.

1. Glossy photographs or pages ✓
2. Colored illustrations, paper or print _____
3. Photographs with dark background ✓
4. Illustrations are poor copy _____
5. Pages with black marks, not original copy _____
6. Print shows through as there is text on both sides of page _____
7. Indistinct, broken or small print on several pages ✓
8. Print exceeds margin requirements _____
9. Tightly bound copy with print lost in spine _____
10. Computer printout pages with indistinct print _____
11. Page(s) _____ lacking when material received, and not available from school or author.
12. Page(s) _____ seem to be missing in numbering only as text follows.
13. Two pages numbered _____. Text follows.
14. Curling and wrinkled pages _____
15. Dissertation contains pages with print at a slant, filmed as received _____
16. Other _____

_____

_____

University
Microfilms
International

LOW STRAIN SHEAR MEASUREMENTS OF SOFT SEDIMENTS USING TRIAXIAL VANE DEVICE

A Dissertation

Submitted to the Graduate Faculty of the
Louisiana State University and
Agricultural and Mechanical College
in partial fulfillment of the
requirements for the degree of
Doctor of Philosophy

in

The Department of Civil Engineering

by
Sibel Pamukcu
B.S., Bogazici University, Istanbul, Turkey, 1978
M.S., Louisiana State University, 1981
May 1986

ACKNOWLEDGEMENTS

The author wishes to extend her most sincere gratitude to her major professor Dr. Joseph N. Suhayda. His guidance, support and expertise were invaluable and made all the difference during the author's academic studies at Louisiana State University. His professionalism and unbiased attitude are some of the traits this author wishes to be able to acquire some day.

Very special thanks are due to my husband Mr. Derya Pamukcu for all the encouragement, patience and devoted, unselfish assistance throughout my academic studies.

Derya, I could not have done it without you, thanks once again !

The author also wishes to express her sincere thanks to Prof. Mehmet T. Tumay for his support and assistance.

To my father

"For us the experimental method is truly an art-that is, it is based on special skills and not on general rules. As such there are never any guarantees of success and one always remains at the mercy of triviality or poor judgment. No methodological principle can eliminate the risk, for instance, of persisting in a blind alley of inquiry..."

from: "Order out of Chaos"

by Ilya Progogine and
Isabelle Stengers

TABLE OF CONTENTS

LIST OF FIGURES

LIST OF TABLES

LIST OF SYMBOLS

B	Skempton's pore pressure parameter
C_v	Coefficient of consolidation
D	Diameter of vane
dV/V_0	Volume change
e	Void ratio
e_o	Void ratio at zero effective stress
e	Void ratio at infinite effective stress
f_n	Natural frequency at resonance
G	Shear modulus
Gmax	Maximum shear modulus
Gmax-d	Maximum dynamic shear modulus
Gmax-s	Maximum static shear modulus
Gs	Specific gravity
H	Height of vane
h	Layer thickness of soil deposit
Ko	At rest earth pressure coefficient
l	Length
N	Finite strain governing equation dimensionless parameter
OCR	Overconsolidation ratio
PI	Plasticity index
P_p	Effective preconsolidation pressure
P_t	Total pressure
Ru	Undrained residual shear strength
S	Shear stress

Su	Undrained shear strength
SF	Load spring factor
T	Torque
T_v	Consolidation time factor
U	Percent consolidation
u_r	Pore pressure ratio
u_{excess}	Excess pore water pressure
w_f	Final water content
w_i	Initial water content
V_0	Initial volume
X	X position of light beam on detector surface
X1,X2	Signals from sensors on the horizontal axis of detector
Y	Y position of light beam on detector surface
Y1,Y2	Signals from sensors on the vertical axis of detector
β	Experimental constant in resonant column test
γ	Shear strain
γ_c	Threshold shear strain
γ_d	Threshold shear strain
γ_s	Bulk density of soil
γ_w	Bulk density of water
γ_y	Yield shear strain
γ_1	Reference shear strain
λ	Linearization constant in finite strain theory
ρ	Mass density
σ'	Effective confining pressure

τ	Shear stress
τ_y	Yield shear stress

ABSTRACT

A new semi-computer aided testing procedure was designed and implemented to determine low shear strain properties of soft saturated clays. Components of the test set-up were a triaxial vane device, data acquisition units to detect small strain amplitudes, and a microcomputer. Real-time data acquisition and interactive computer graphics were utilized to collect and analyze data. The average range of electronically measured strain amplitude was from 10^{-4}% to 1%. Approximately 1500 data points were taken in this range. Testing could be extended to determine undrained shear strength of the specimens, occuring between 10% to 20% of shear strain amplitude, and beyond for residual strength measurements.

Using duplicate specimens, shear moduli reduction curves were obtained through resonant column testing and the new triaxial vane shear testing procedure and they were compared. The dynamically determined low strain shear stress-strain behaviour was found to be substantially influenced due to cyclic degradation for the soft saturated clay specimens. Whereas, static testing using the new procedure resulted in acquisition of better quality and more realistic low shear strain data for these types of soils. For normally consolidated specimens, Gmax-static/Su was found to be 112, and Gmax-static/Gmax-dynamic was 0.85 .

CHAPTER 1

INTRODUCTION

Science of solid materials had already existed a long time when principles of soil mechanics were developed with the need of solving engineering problems. The existing theories regarding failure and deformation were adopted and applied to soils without rigorous analysis of their validity. A major obstacle to confirmation was lack of adequate testing equipment and experimental methods. With the advent of fast computing techniques and development of new elasto-plastic models (21,38,40,57,62,63,65) that are formulated on the grounds of plasticity theory, soil behaviour could be simulated more realistically. However, the experimental methods to estimate soil properties for use in analytic techniques have not reached to the level of sophistication of these models and computational abilities. There exists an accumulation of vast amount of information and data both from laboratory and field investigations. A significant percent of this data lacks consistency, sufficient quality and/or scope (37,73). Uncertainty in the data is the result of various factors, some of which are compliance of equipment, compatibility of testing procedures, ability to simulate in-situ conditions, and the interpretation of behaviour beyond limits of test data. Practical and economical limitations require few laboratory tests yield maximum amount of information. The need for

security when coupled with the already existing uncertainty of laboratory and field data, promotes the use of theoretical models that estimate soil behaviour with some degree of conservatism. This matter brings the investigators back to where they have started from, which is acknowledgeing the need to understand the mechanics of a particular soil with respect to various factors, and obtain realistic data to use in the model. The study reported here addresses this need in one of the areas of soil mechanics where uncertainty of data is significant. The main objective of the study is to investigate some problems associated with acquiring low strain data of soft saturated clays and propose a new technique to obtain more realistic information about these types of soils.

The variety in the nature of failure for soils makes it imperative first to identify depositional characteristics and state variables in order to learn why the soil behaves in the specific manner it does. Depositional characteristics consist of fabric, minerological and pore fluid parameters. State variables are stress, strain, time and temperature. This investigation is basically concerned with the first two state variables, stress and strain.

Soft grounds are no longer strictly avoided for building sites, but taken into consideration as long as proper design procedures are formulated. Problems associated with building on soft deposits and on unstable grounds in offshore environment have already been investigated

extensively (8,9,45,50,59,61,64,69,75,77,80). Soft clays are highly nonlinear in stress-strain behaviour, and yield over a considerable strain range. From an engineering point of view, failure condition is preferably defined in terms of deformation or be related to deformation. Although actual failure takes place at high strain levels (10% - 20%) for these soft soils, it is becoming increasingly common to evaluate stress-strain relation at much lower strain amplitudes due to the nonlinear nature of the behaviour (78). In order to test and evaluate stress-strain behaviour below a certain strain amplitude, dynamic testing equipment and cyclic loading principles and formulations are to be adopted. Otherwise, analytical estimation procedures (41), or empirical relations (28) must be utilized to assess low strain parameters and model the behaviour. Therefore, the investigator conducts two separate tests and/or uses an analytical procedure to understand the nonlinear stress-strain behaviour of these soft soils over an increased scope of data. This certainly accomplishes expansion of data range however at the expense of introducing new uncertainty to the data with assumptions and/or estimations. In addition, small variations in the estimated values of the parameters or shape of data curves may change computed results in analytical model as much as by factor of 2 (43). This is a serious consequence, because it is the accuracy of the total analysis and not the uncertainty that is of major

concern.

This investigation reported here is aimed to focus on improving ability to directly obtain shear stress-strain relation data for soft clay soils at low shear strain amplitudes through static testing. Related areas of investigation are:

1) Expanding scope of data collection from low strains (10^{-4} %) to failure strains (20 %) within same testing,

2) Compare low strain static and dynamic behaviour of soft clays and identify parameters applicable in numerical modeling,

3) Effect of stress-history, and existing excess pore water pressures simulated as in fast deposited soft marine clays,

4) Prediction of a realistic maximum shear modulus, Gmax, of monotonic soft clay behaviour,

5) Comparison of shear moduli and shape of shear stress-strain curves pertaining to dynamic and monotonic (static) loading,

6) Prediction of a realistic Gmax/Su (Su = undrained shear strength) ratio which is frequently used in soft clay analysis,

7) Gain some insight into laboratory vane shear testing of soft clays with the new testing method.

It is very important for an individual investigator to identify soil state parameters and loading conditions before

choosing a testing technique or an empirical procedure to predict soil parameters to use in numerical models when working with soft soils. As the nonlinearity of the material increases, small variations in parameters will introduce large deviations of the end design from optimum. In the study reported here, a resonant column device was utilized for dynamic testing and a modified triaxial laboratory vane device was used for static testing. Basic compatibility criteria were satisfied either by inherent operation process of each device (stress-controlled testing, similar strain rate effects), or making the necessary operational modifications (similar strain amplitude ranges, triaxial confinement, drainage and consolidation). Duplicate specimens trimmed from artificially prepared Georgia kaolinite samples were used in each device to obtain comparative data.

The significance and originality of this study lies in the fact that the ability to obtain good quality and repeatable data over a large range of strain amplitude was improved using a new testing method and data acquisition technique. A "semi-computer aided" experiment was designed and implemented. Both the modified testing equipment, namely triaxial vane, and the unique data acquisition technique possess high potential for use in further research in a variety of soil investigations. The current set-up can easily be modified for specific needs of different tests. The results obtained in this study are the results of a

pioneering testing method. In spite of this fact, the scatter and uncertainty in data obtained is certainly not any larger than the results encountered in other laboratory or site-investigation methods. In this sense, the proposed method may not offer improvement, however it does put in perspective certain criteria to watch for when predicting and analyzing soil behaviour and aid to obtain data accordingly.

CHAPTER 2

BACKGROUND

This chapter focuses on two major subject areas of interest to this study. One area is the previous investigations on correlating dynamic and static behaviour of clays, the other area is recent investigations on vane shear testing and in particular on triaxial vane shear tests. Discussions on dynamic and static laboratory testing of soft clays are presented initially.

2.1 DYNAMIC TESTING OF SOFT CLAYS

The common existing laboratory dynamic soil testing equipment are resonant column (using either solid or hollow samples), cyclic torsional shear, cyclic triaxial, cyclic simple shear, and shake table. Typical range of shear strain application vary from one device to the other. Amongthe equipment cited above, only resonant column and cyclic torsional device are capable of low shear strain applications ($<10^{-2}$%).

An earlier study conducted and co-investigated by the author (53,54,55) revealed that degradation of shear moduli is a factor that complicates results significantly in dynamic testing of soft offshore sediments. Degradation increased with increasing number of cycles of loading at high shear strain amplitudes ($>10^{-2}$%), and decreasing effective stress state of the soil specimen. Fig. 2.1 shows the actual shear moduli vs shear strain data superimposed on

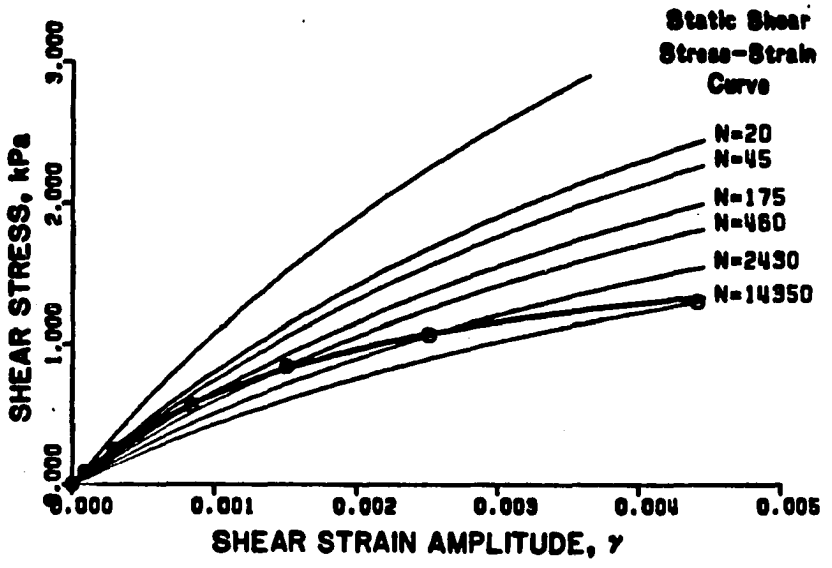

Fig. 2.1 Degraded Backbone Curves with Actual γ vs τ Data Points and Fitted Hyperbolic Curve [reproduced from Pamukcu and Suhayda (55)]

the analytical curves illustrating the degradation of initial shear stress-strain curve for each measurement. These data were obtained using a resonant column device in which very low amplitudes of strain can be measured. A hyperbolic curve was fit to the data in order to interpolate a maximum value of shear modulus at 10^{-4}% shear strain amplitude at which G is considered to no longer vary with shear strain (28). However, at typically applied low stress levels the specimen would exhibit high strains (>10^{-2}%), promoting degradation and subsequently complicating the estimation of a realistic maximum shear modulus. Degradation problem have long been recognized and investigated for soft clays (30), however the significant effect it has on predicting Gmax and the shape of backbone curve for the

soft offshore clays has not been documented well. Progressive pore pressure increase (dynamic pore pressure) during dynamic testing becomes more pronounced at high cyclic strain (22), which in turn promotes reduction of shear moduli by decreasing the effective stress. Stress reversal and break down of inherent soil structure during cyclic loading contribute to degradation of shear moduli also (33,67). Considering the factors discussed above, it is imperative to evaluate the dynamic test data of soft offshore clays very carefully in order to predict realistic parameters and stress-strain curve shapes. Dynamic testing procedures are generally used to predict dynamic parameters, Gmax and the damping ratio. The data obtained through these tests are utilized in designs for dynamic loading, such as earthquake, machine vibration, blasting, or wave loading. Maximum shear modulus is assumed to be unique for both dynamic and static shear stress-strain curves because the first cycle dynamic curve (backbone curve) is assumed to coincide with the static (monotonic load) curve up to the value of the cyclic stress applied (28,29). This is a valid assumption for most types of soils. However, when soft soils bearing excess pore pressures are considered, careful examination of this assumption is needed due to the testing and subsequent data interpretation difficulties discussed above. Moreover, the highly nonlinear nature of these soils is a significant factor which makes it more difficult to validate the existence of an elastic region on shear stress-

strain curve, and the assumption that loading rate will have no or minimal effect.

2.2 STATIC SHEAR TESTING OF SOFT CLAYS

The common laboratory soil shear testing equipment are translatory direct shear, torsional direct shear, simple shear, and triaxial using solid, prismatic or hollow specimens. All of these devices operate above strain amplitude of 10^{-2}%. In translatory and torsional direct shear, and simple shear, only Ko consolidation can be acheived while in triaxial, isotropic and anisotropic consolidation are possible also. In direct and simple shear tests, normal and shear stresses and strains are obtained from measured or applied axial and tangential forces. In triaxial tests (using solid specimens) only the normal stresses and strains are measured and shear components are calculated based on various assumptions.

An in-situ instrument which is widely used to measure undrained shear strength of saturated soft clay beds is the vane shear device (1,42,46,66). Laboratory vane shear device is also used frequently on soft saturated soil samples without extracting or trimming the samples retrieved. The apparent advantage is avoiding sample disturbance induced by specimen preparation. Over the years, many investigators have focused on analyzing vane shear mechanism based on experimental data, and determining the factors influencing the data (1,4,7,14,17,25,36,42,47,49,60,

66,70,79,81). Other investigators compared laboratory and field tests (20,23,35,71,72) accumulating a bank of data. Concerns in relation to over prediction of Su in soils with high plasticity (7,12), disturbance effects due to insertion of vane (7,36), pore pressure distribution and assessment of effective stress state on vane shear plane (36,44,66,71,82) have been investigated. Studies indicate that there is confirmation between unconfined compression data and laboratory vane shear data, and in case of soft saturated clays there is some confirmation even with undrained triaxial data. Wide use of the equipment over the years resulted in vast amount of data collected both in lab and in-situ which is validated by other test data in general. Meaningful shear strength data for soft saturated clays can be obtained with relative ease and speed using the vane shear device. This favorable characteristic brought about the interest to utilize the equipment for a wider range of applications (26,76). In this study, vane shear device was utilized in an unconventional manner also, that is, predicting and accentuating low strain shear parameters.

2.3 IMPORTANT ASPECTS OF DYNAMIC AND STATIC PARAMETER CORRELATIONS

Determining dynamic properties of soils experimentally can be costly. Laboratory procedures are sophisticated and geophysical methods not readily available. As a result, a number of investigators have worked on correlating static parameters, which are more easily obtained, to dynamic

parameters to establish emprical relations, or mathematical models (5,18,26,27,34,56,58,74,76).

A popular approach to correlation is determining Gmax/Su ratio (3,6,18,19,27,28,39,52,64,68). Both variables of this ratio are functions of void ratio, effective confining pressure, overconsolidation ratio, and both exhibit time dependent variations. However, there is not a high degree of agreement among the results as well as testing methods used. Generally, maximum shear moduli obtained from resonant column tests are normalized by undrained shear strength values from triaxial tests. Some values of the ratio measured using different methods are:

1) Hardin et al. (28) reported ratios ranging from 380 to 1500 with a mean value of 760.

2)Wilson and Dietrich (83) reported ratios ranging from 178 to 550 with a mean value of 390.

3) D'Appolonia et al. (19) reported ratios ranging from 53 to 833 with a mean value of 420.

4) Hara et. al (27) reported ratios ranging from 250 to 1430 with mean value of 548.

5)A previous study conducted by the author (52) revealed ratios ranging from 150 to 500 with mean value 250 using one set of data and ratios ranging from 500 to 2500 with a mean value of 1000 using another set of data.

6)Using a different method of approach, a study

conducted by Schapery et al. (64) revealed a ratio of 32, for marine clays.

7) Chae et al. (18) used mathematical relations between deviatoric stress and shear modulus and found an approximate range for Gmax/Su ratio of 260 - 1200.

The scatter in the values reported above may be due to various factors, an important one being differences in testing and data evaluation procedures. This is illustrated in Fig. 2.2, which shows how results vary substantially from one device to the other. Moreover, other investigators report that the scatter is due to the fact that Gmax/Su is not a constant value but strongly depends on overconsolidation ratio, void ratio and effective confining

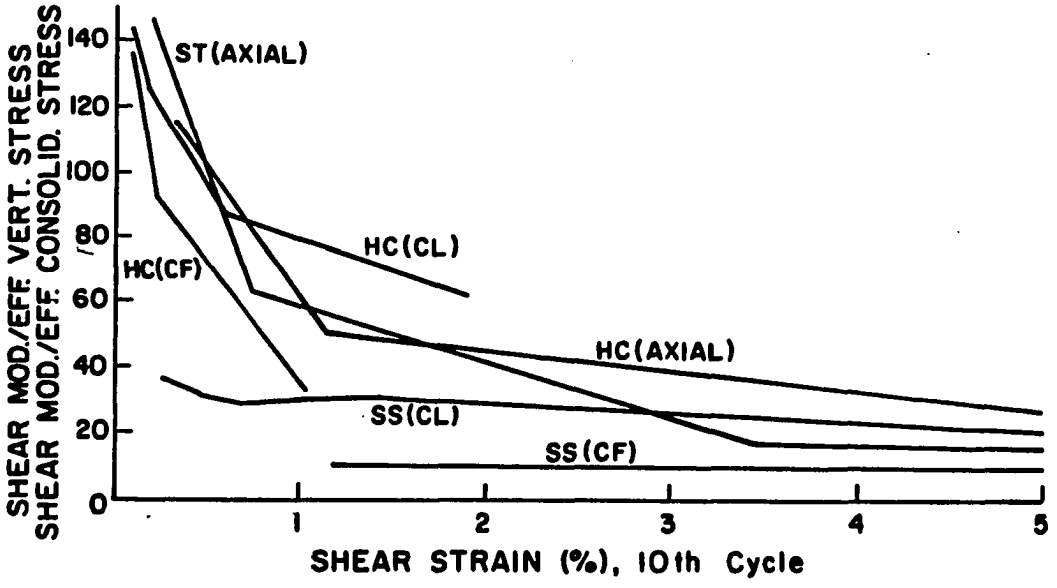

Fig. 2.2 Normalized Dynamic Shear Moduli Corresponding to the 10th Cycle and Various Levels of Strain in the Standard Triaxial (ST), Hollow Cylinder Torsion (HC), and Simple Shear (SS) Test (CF=Constant volume or length, CL=Constant Force or Undrained) [reproduced from Adel Saada (1981)]

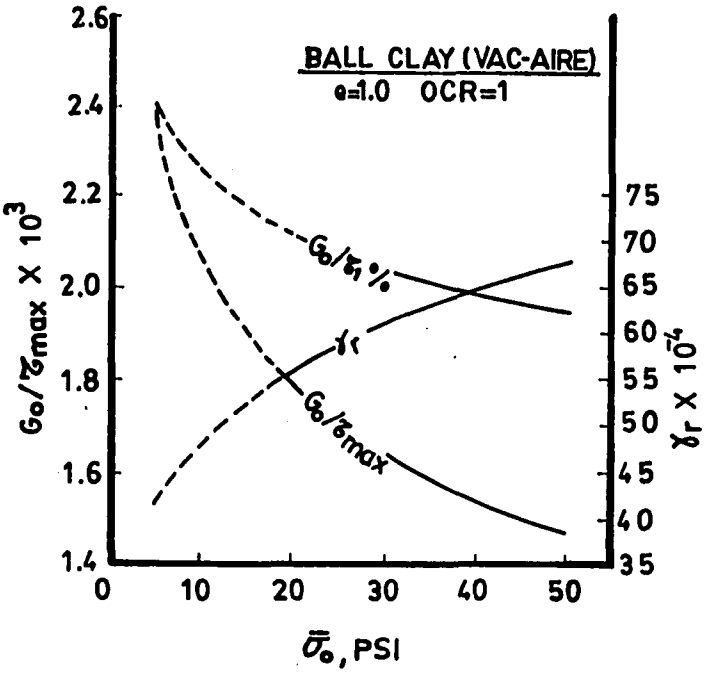

Fig. 2.3 Dependence of G_o/τ_{max}, $G_o/\tau_{1\%}$, and γ_r on the Confining Pressure σ_o (G_o= maximum shear modulus, τ_{max}= maximum shear strength, $\tau_{1\%}$= shearing stress at 1% strain, $\gamma_r = \tau_{max}/G_o$) [reproduced from Athanaspoulos and Richart (5)]

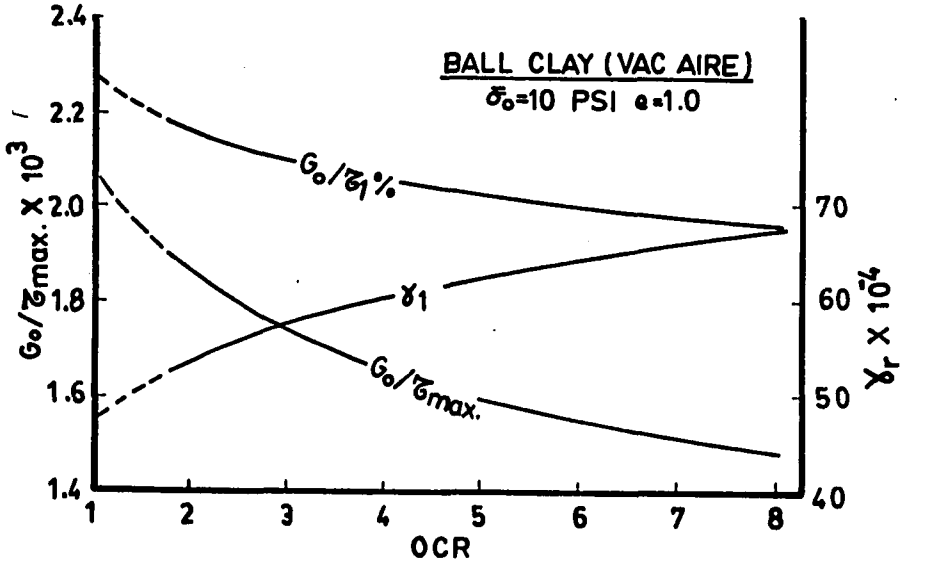

Fig. 2.4 Dependence of G_o/τ_{max}, $G_o/\tau_{1\%}$, and γ_r on OCR [reproduced from Athanaspoulos and Richart (5)]

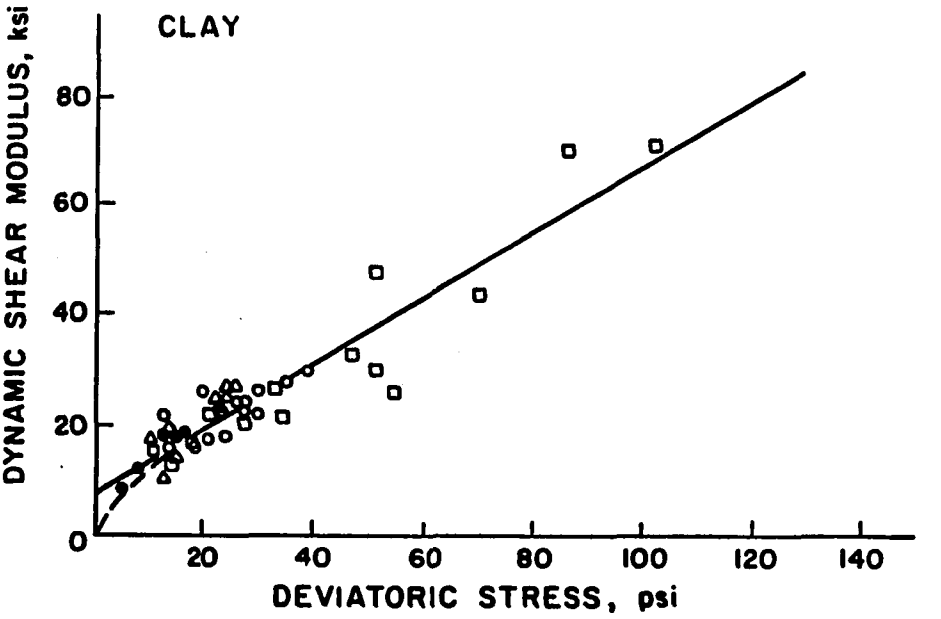

Fig. 2.5 Dynamic Shear Modulus vs Static Strength Variation [reproduced from Chae et al. (18)]

pressure. Figs. 2.3 and 2.4 illustrate these effects. Fig. 2.5 shows that a straight line relationship between Gmax and deviatoric stress may not be valid for lower stress ranges (<10 psi [~70 KPa]).

Shear modulus is a parameter that has a wide range of use in numerical modelling techniques . Its sensitivity with respect to loading patterns and some state variables of soils has been examined by a number of investigators. It is well established that the shear modulus strongly varies with shear strain, number of cycles of loading and confining pressure. Sensitivity with respect to effective stress, dynamic pore pressures and strain rate effects are more recent areas of research.

A study conducted by Dyvik et al. (22) concludes that pore pressure is a basic indication of the level of

degradation of shear modulus of a soil specimen subjected to cyclic loading. Figs. 2.6 and 2.7 show variation of cyclic shear stress and shear modulus with dynamic porepressure ratio, from tests conducted on Gulf of Mexico clays using simple shear device modified for cyclic loading (22). Some geotechnical data for the clay used in that study were given as follows:

Water content = 70-105 %, PI = 75 , Su = 13 kPa

The consolidated, constant volume (CCV) cyclic laboratory shear test used was a strain-controlled type of test in which strain rates did not affect the results. Pore pressure predictions were made by changing normal stress to keep the height of specimen constant. It was assumed that the change in vertical stress is equal to the change in pore pressures that would have occurred during an undrained test. As seen in Fig. 2.6, dynamic pore pressures increase with increasing cyclic shear strain, and they decrease with increasing cyclic shear stress. Degradation of shear modulus with increasing dynamic pore pressure is clearly illustrated in Fig. 2.7.

In relation to the effects of strain rate on shear moduli measurements of soft clays, a study done by Isenhower and Stokoe II is quite illustrative (32). Figs. 2.8 and 2.9 show the variation of shear moduli with shear strain rate and, comparative results of two different tests illustrating strain rate effect, respectively. As seen from Fig. 2.8, at

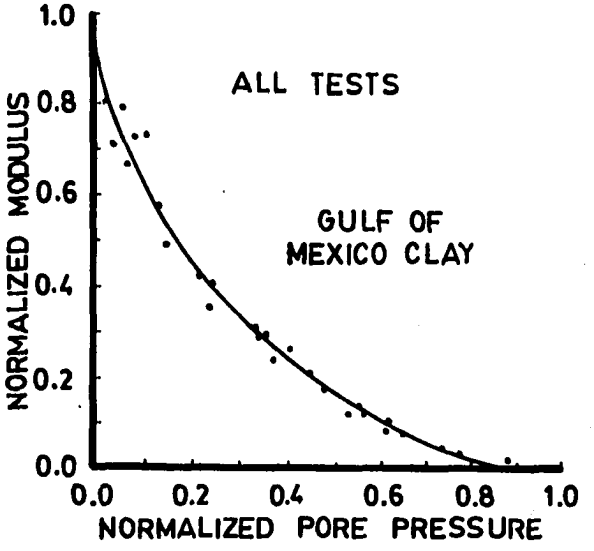

Fig. 2.6 Cyclic Shear Stress versus Normalized Pore Pressure Variation [reproduced from Dyvik et al. (22)]

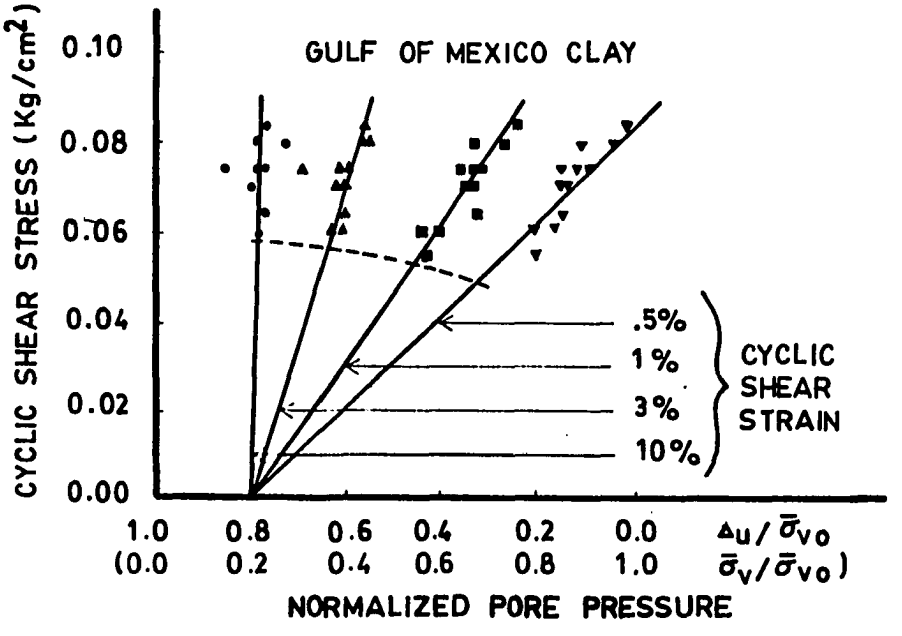

Fig. 2.7 Normalized Modulus versus Normalized Pore Pressure Variation [reproduced from Dyvik et al. (22)]

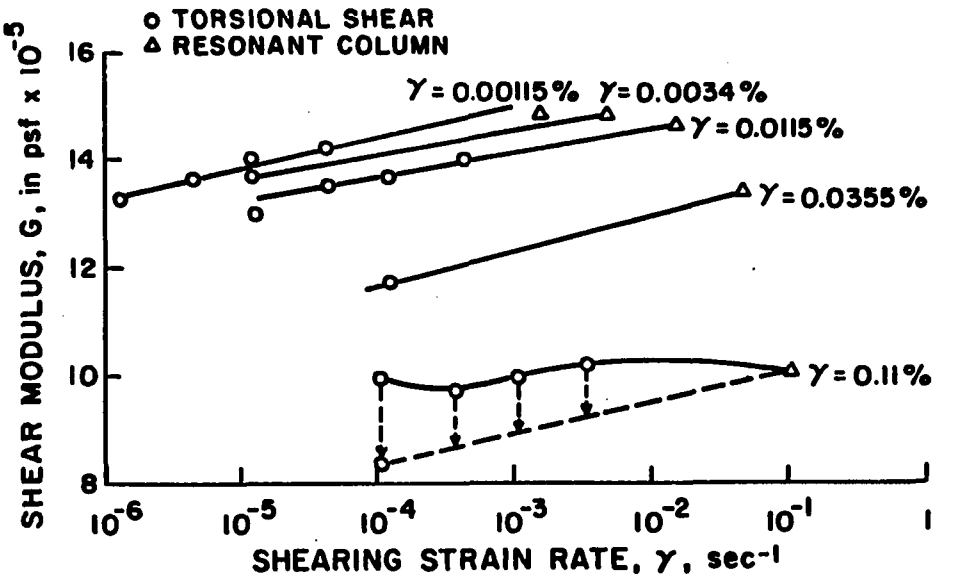

Fig. 2.8 Variation in Shear Modulus With Shearing Strain Rate [reproduced from Isenhower and Stokoe II (32)]

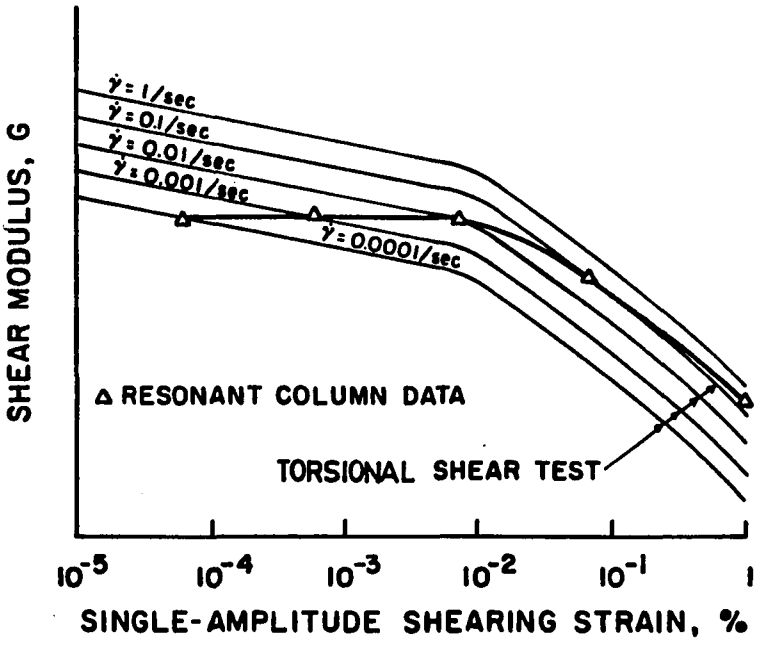

Fig. 2.9 Combined Parameter Effects on Shear Modulus [reproduced from Isenhower and Stokoe II (32)]

a constant shearing strain amplitude, the shear modulus increases as the logarithm of shear strain increases. In Fig. 2.9, the shear modulus increases with decreasing shear strain amplitude. When shear strain rates are considered, measurement of maximum shear modulus is found not to be affected substantially due to the counterbalancing action of low strain amplitudes. Influence of shearing strain rates becomes more pronounced at strain amplitudes greater than 10^{-2}% .

Other methods encountered in the literature that correlate or compare, either experimentally or numerically, static and dynamic behaviour of clay, utilize the initial stress-strain relation at low strains (26,31,33,34).

A general analytical model proposed by Prevost (56) describes the anisotropic , elasto-plastic, path dependent stress-strain-strength properties of saturated clays under undrained cyclic or monotonic loading. The frequency of cyclic loading simulates the conditions of wave loading rather than earthquake type of loading. Loading frequencies used in the model are 0.5 and 0.05 Hertz. The model parameters were determined through slow monotonic (strain rate 4.5 % /hr), and rapid cyclic (frequency 0.1 Hertz) strain-controlled simple shear tests of Drammen clay (OCR=4). Fig. 2.10 shows the experimental test results, slow monotonic and rapid cyclic stress-strain curves and typical hysteresis loops obtained at a constant strain amplitude. Prevost reports that the hysteresis loops develop an S-shape

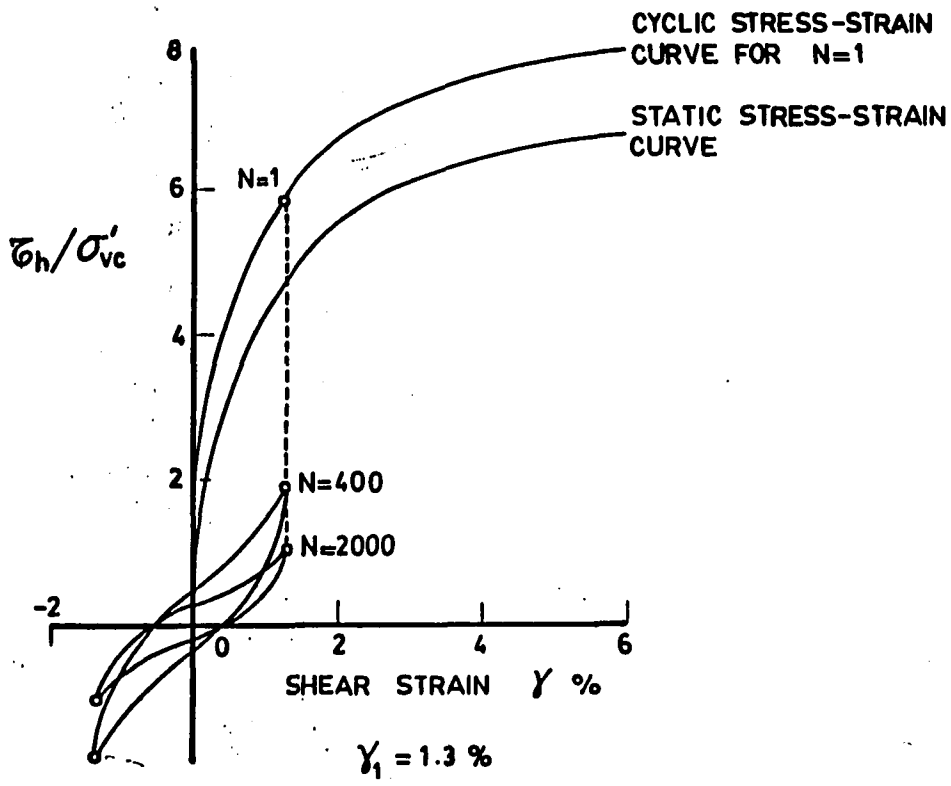

Fig. 2.10 Rapid Cyclic and Slow Monotonic Stress-Strain Curves Obtained From Tests of Drammen Clay [reproduced from Prevost (56)]

which becomes even more marked as the number of cyles of loading increases. Also reported is an experimental finding that the gradient of the hysteresis loops at the peak shear stress remains constant and is approximately equal to the gradient of the static curve at the corresponding strain.

Some of the results of a study conducted by Ishihara and Yasuda (33) on alluvial clay are given in Fig. 2.11. The testing method used in this study was cyclic triaxial and the stress-strain curves for various number of cycles of loading (frequency 1 Hertz), and monotonic loading were obtained. Specimens were first consolidated isotropically to a certain effective stress value and than cyclicly loaded in

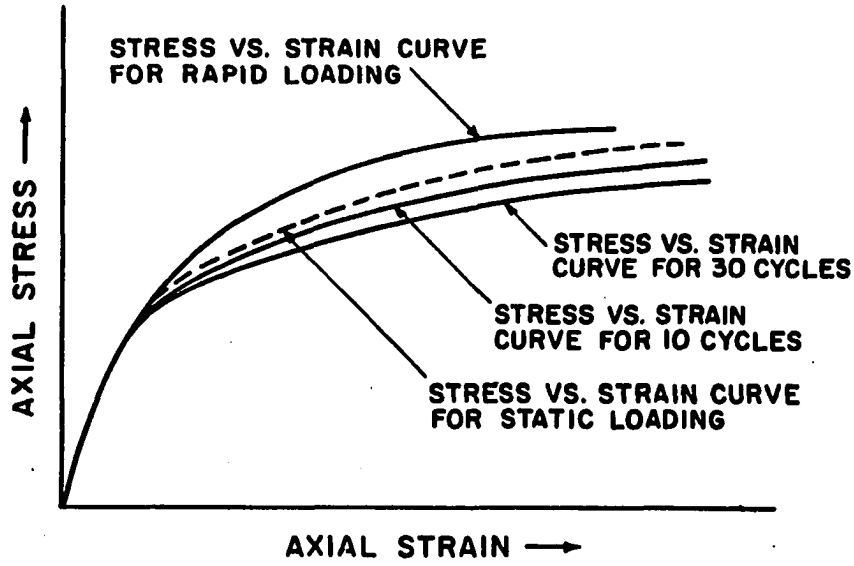

Fig. 2.11 A set of Cyclic Stress-strain Curves With Different Number of Cycles [reproduced from Ishihara and Yasuda (33)]

steps of increasing magnitude to failure. As seen from Fig. 2.11, the degraded stress-strain curves at 10 and 30 cycles of loading fall below static curve. The curve labeled "rapid loading curve" corresponds to first cycle stress-strain curve (backbone curve). An important result of this study are given in Figs. 2.12a and 2.12b which show the variation of the ratio of cyclic strength to static strength versus the ratio of initial shear stress to static strength for the two types of clays tested. In these set of tests, before applying the cyclic load, the specimens were loaded up to a fraction of the static failure stress which was labeled as "initial shear stress". It is already been shown through a number of investigations that strength of cohesive soils under rapid loading conditions is greater than the strength obtained in static loading conditions in which the

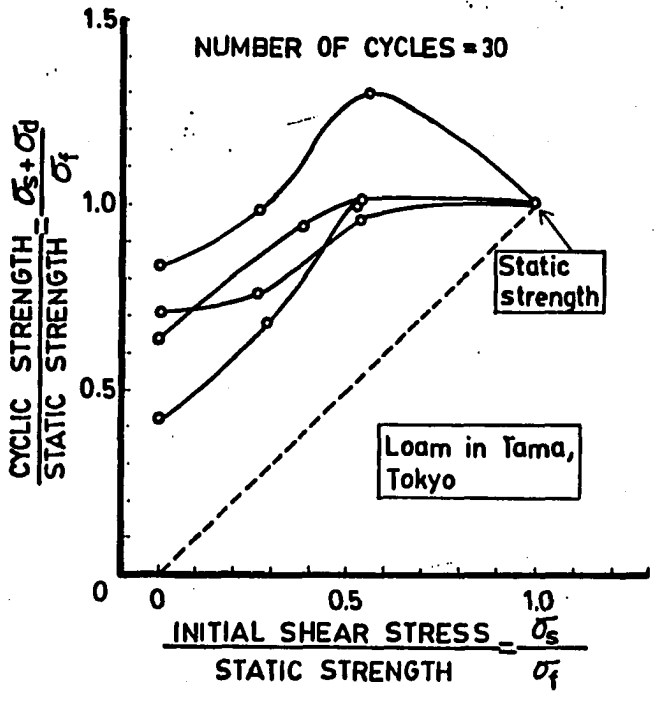

(a)

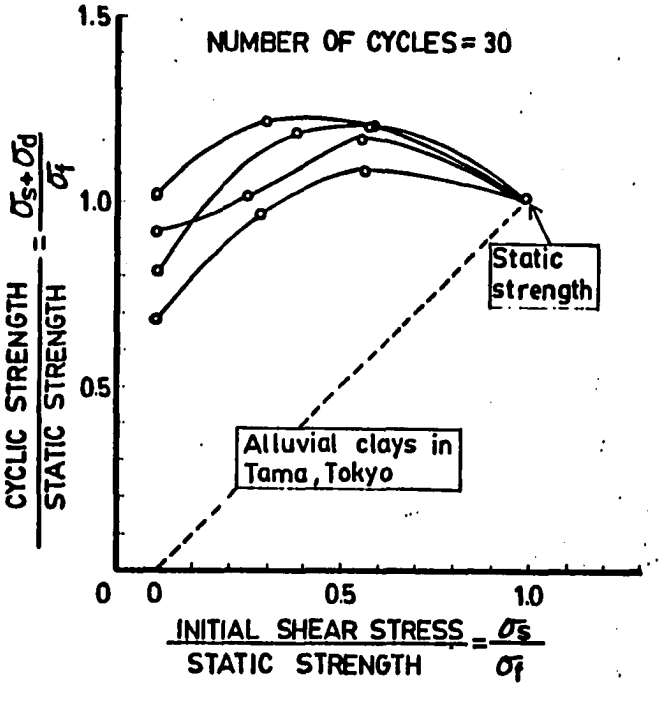

(b)

Fig. 2.12 Cyclic Strengths versus Initial Shear Stress [reproduced from Ishihara and Yasuda (33)

application of loading is slow. This is known as the rate effect. However, as seen in Fig. 2.12 the cyclic strength to static strength ratio is less than 1 for zero or small initial shear stress ratios. This is a result known as "strength deterioration" and it is attributed to pore pressure buildup, breakdown of inherent structure in cohesive soil, and/or stress reversal during cyclic loading. This occurrence was observed by other investigators also (52,67). The effect becomes more pronounced when stress reversal is at the origin or at an initial stress level close to the origin forcing the specimen to experience negative stresses at each cycle. The effect of strength deterioration is correlated with plasticity, and the results are given in Fig. 2.13.

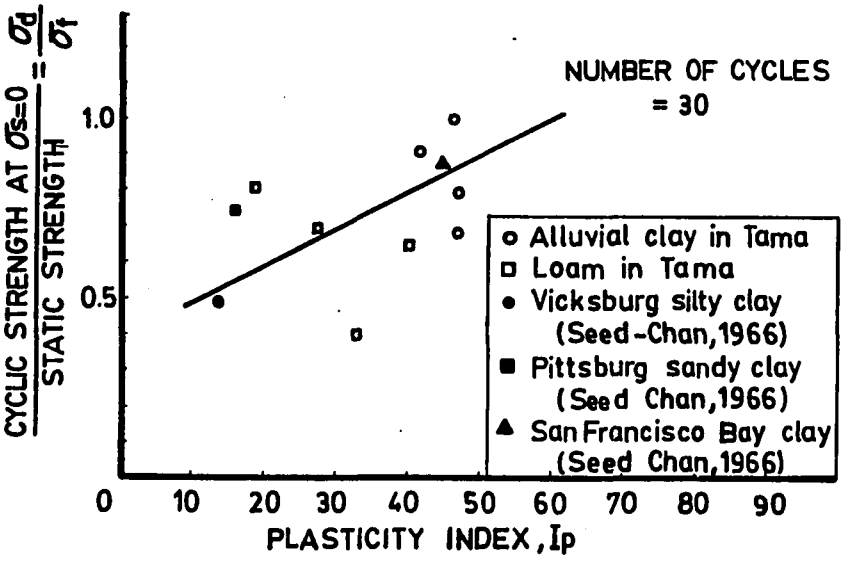

Fig. 2.13 Cyclic Strength in Reversing Cyclic Loading as Functions of Plasticity Index of Soils [reproduced from Ishihara and Yasuda (33)]

Kavazanjian and Hadj-Hamou (34) conducted an investigation in which they correlated and compared dynamic and static behavior using results of resonant column tests and empirical methods. Using existing data and a simple procedure to estimate static modulus through empirical relations they were able to produce comparative curves for San Francisco Bay mud, as shown in Fig. 2.14. They concluded that resolution of most laboratory shear tests prohibits definition of static stress-strain curve below shear strains of 10^{-1}%-10^{-2}%,therefore the maximum static shear modulus is to be estimated using emprical relations (28,41).

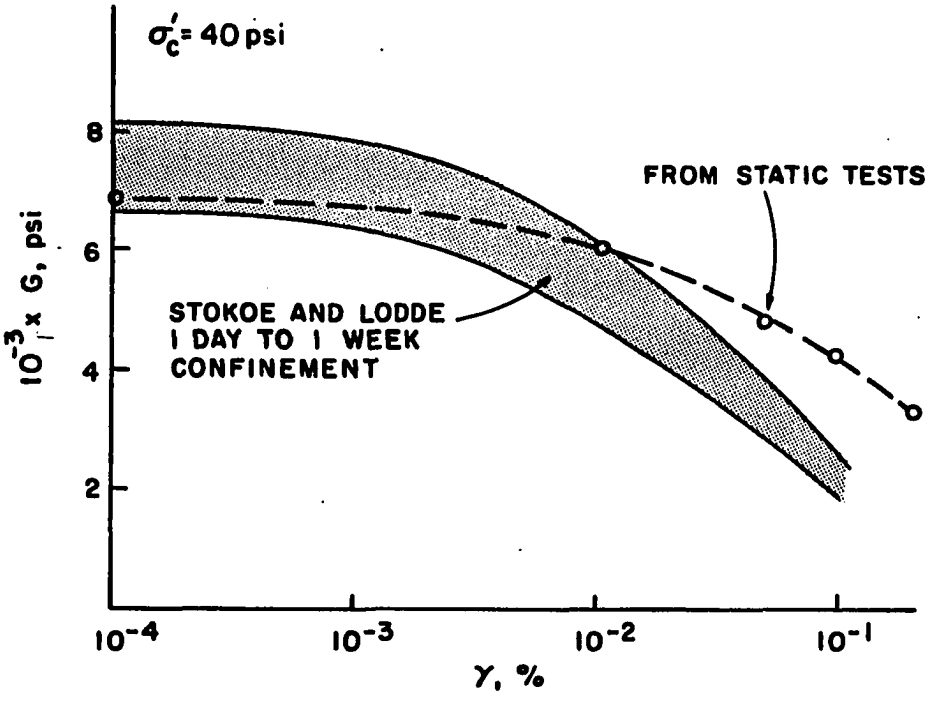

Fig. 2.14 Modulus of San Fransisco Bay mud [reproduced from Kavazanjian and Hadj-Hamou (34)]

2.4 VANE SHEAR TESTING

Vane shear testing is frequently used in estimating undrained shear strength of soft saturated clays in-situ. It is known to perform especially well in soft seabed clays. In-situ vane test results compare well with other in-situ testing methods when used in these types of soils (46), and it is economical and fast. Several investigators have shown that vane testing overestimated Su in highly plastic clays. Bjerrum (12) formulated a correction relating in-situ vane shear to plasticity index through back calculating shear strengths from several embankment failures. Arman et al. (4) showed that Su predicted through vane tests was two times the undrained shear strength of soft Mississippi Delta clays. Azzouz et al. (7) revised field vane correction from past case histories and formulated a new one which they predict to represent results that will compare better with other in-situ (cone penetration) or laboratory test results.

Laboratory vane shear device was generally regarded as a practical tool used to estimate undrained shear strength of retrieved samples with minimum disturbance. Little was known and researched with respect to stress-strain mode, disturbance and strain rate effects. However, with increased number of research on vane shear mechanism,pore pressure, disturbance, shear rate, and vane shape effects, laboratory vane device is slowly being upgraded from a practical tool to a better soil shear testing device. Moreover, with the

introduction of triaxial vane apparatus (35), duplication of the in-situ stress conditions on specimens could be achieved. Inherent problems of classical lab-vane testing, such as upheaving of soil surface during insertion of vane, drying of soil surface during slow rate-long term tests, and boundary effects due to size and rigidity of soil container are eliminated automatically in a triaxial vane device. Several important investigations related to vane shear testing which are of interest to this study are discussed below.

2.4.1 Shear Mechanism of Vane Test

The classical assumptions for shear mechanism of vane test are: the shear surface is a cylinder of the same dimensions as the vane; the vane is replaced by a rigid cylinder onto which the soil adheres ; the stress distribution is uniform across the surface of rupture (15). It is a stress-controlled test in which the only stress known is the shear stress on the rupture surface. Circular shear surface is a valid assumption for soft saturated clays, however it deviates significantly for sands and silts (82).

Matsui and Abe (47) tested Ko consolidated clays using an instrumented vane shear device in which total stresses and pore water pressures around the vertical shear plane could be measured. The experimental results were compared with results obtained from a numerical analysis. The device

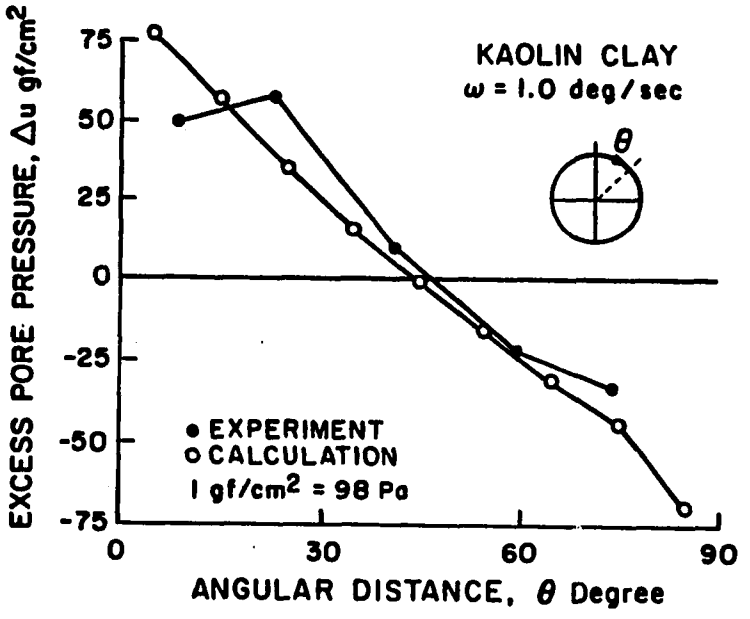

(a) Excess Pore Water Pressure Distribution

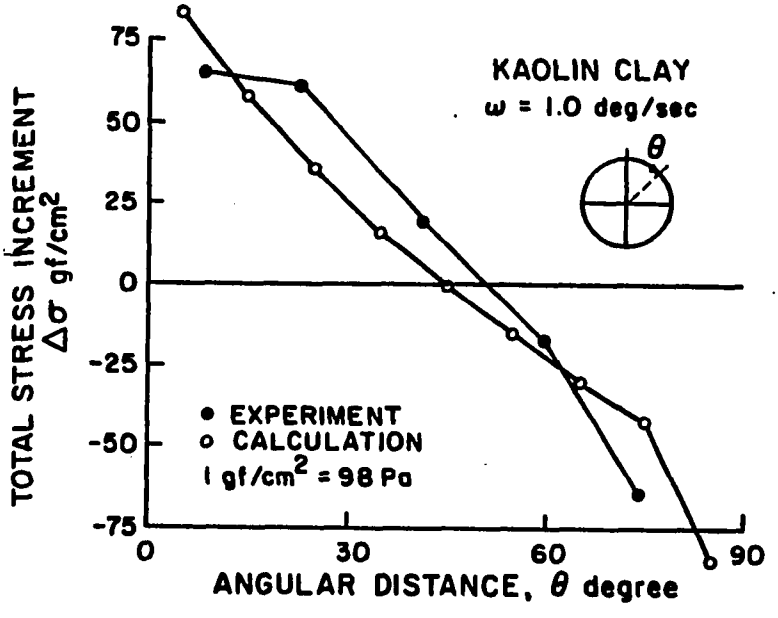

(b) Total Stress Distribution

Fig. 2.15 Analytical and Experimental Distributions of Excess Pore Water Pressure, Total Stress and Effective Stress Increments on the Vane Shear [reproduced from Matsui and Abe (47)

was of the rotating type turntable on which the specimen was placed. It could be operated at constant angular velocities ranging from 0.002 degrees/sec to 5.0 degrees/sec. Pore pressure transducers positioned near or on the vane blade, and lateral earth pressure transducers on the wall of the cell were used to measure pore water and total pressures. Figs. 2.15a, 2.15b, and 2.15c show the variations of pore pressure, total stress, and normal effective stress increments with angular rotation both as predicted by numerical analysis and measured in test, respectively. As the vane blade turns, pore pressure and total stress increase in front of the blade and decrease behind the blade by approximately the same amount, therefore the resulting normal effective stress increment remain distributed around

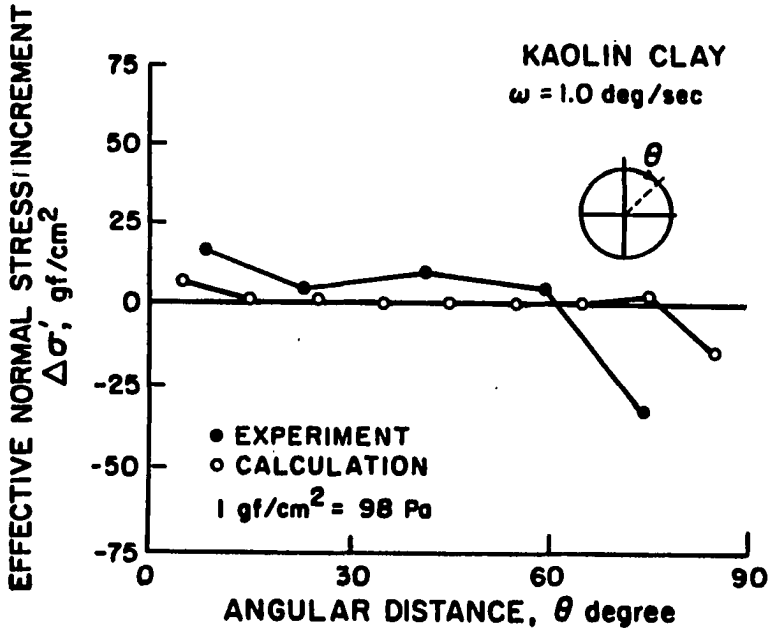

(c) Effective Stress Distribution

Fig. 2.15 (cont.) [reproduced from Matsui and Abe (47)]

zero, and the normal effective stress itself does not change significantly. Fig. 2.16 shows the analytical results of pore pressure distribution for various cases of local pore pressure migration. The slower the angular rotation the smaller the changes in excess pore water pressure. The case for larger angular rotation rate of 1 degree/sec is very close to that of undrained case. One important conclusion from this investigation was that because of pore pressure gradient distribution around the shear plane, if angular rotation is slow enough, pore pressure migration will take place resulting in consolidation of soil in front of the blade and swelling dilation behind the blade. The undrained condition (no pore pressure migration) for the kaolin clay

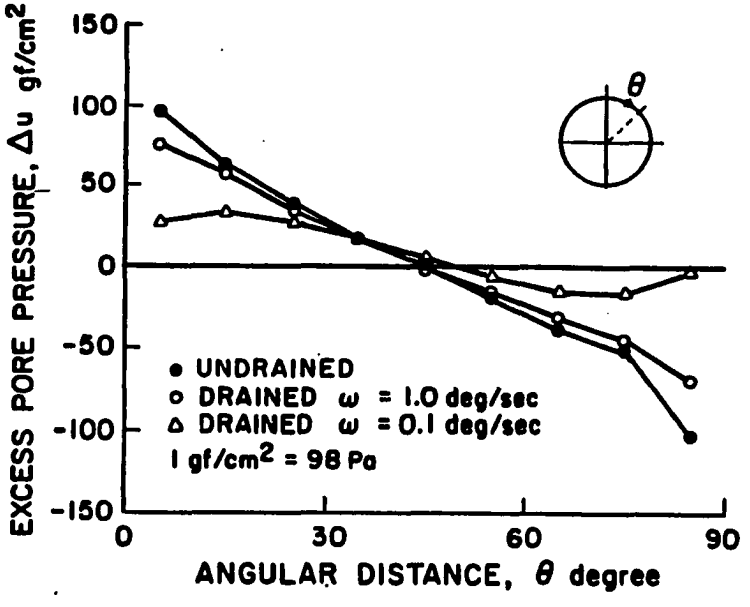

Fig. 2.16 Effect of Local Pore Water Migration on Excess Pore Pressure Distribution on Vane Shear Surface [reproduced from Matsui and Abe (47)]

tested was predicted to occur at angular rotation rates of 1.0 degree/sec or higher. In the case of slower angular rotations, it is predicted that soil in front of the vane blade does not reach failure because of consolidation effect, however soil behind the blade reaches failure at a lower stress level because of swelling dilation.

Menzies and Merrifield (49), using an instrumented vane measured the stress distribution on the vertical and horizontal edges of the vane. Figs. 2.17a and 2.17b show these results along with theoretical shear distribution curves. A concentration of shear distortion in a band of shear at the blade edges was observed.

2.4.2 Disturbance Effect Due to Insertion of the Vane

A number of investigators have observed the effect of vane insertion either in terms of pore pressure increase, up to 50 % of vertical consolidation pressure in some cases (47), or in terms of the reduction in undrained shear strength (42) partially due to breakdown of clay bonds. Aas (1) conducted a study in which the vane was left in the soil for 24 hrs before starting rotation. Results showed a 40 to 50 % increase in the shear strength in comparison to that of a standard test. Torstensson (79) and Shibata (71) made similar conclusions. The time elapsed between vane insertion and beginning of rotation was a critical factor that controlled vane shear strength.

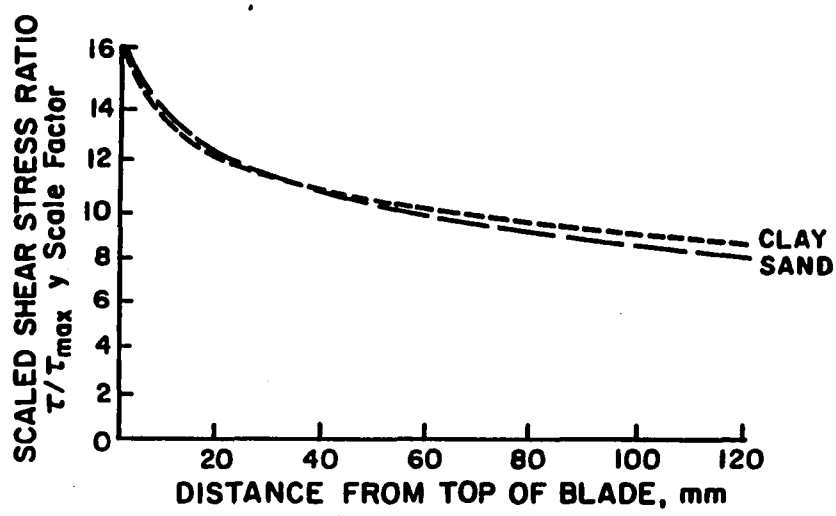

(a) Vertical Blade Edge

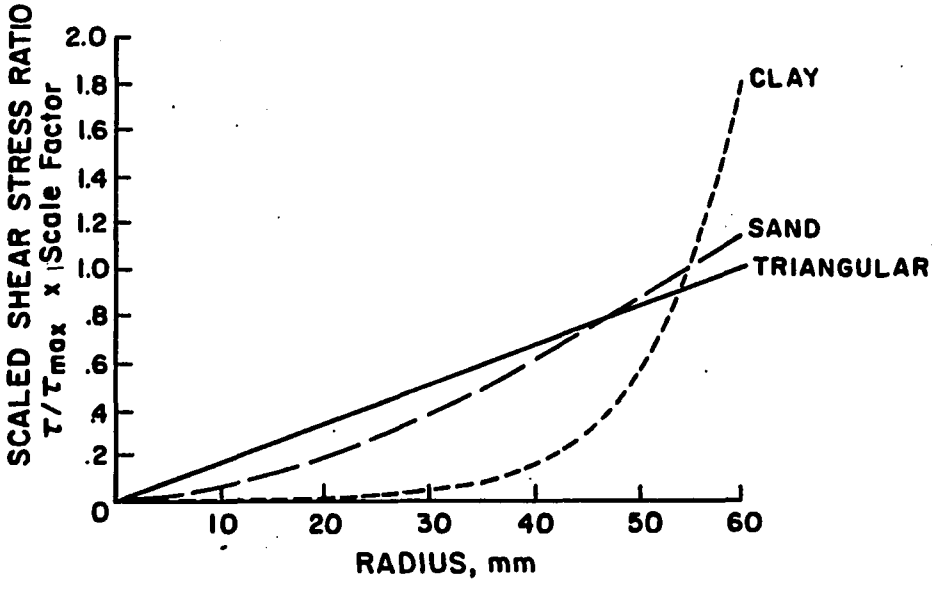

(b) Horizontal Blade Edge

Fig. 2.17 Normalized and Linear Distributions of Equivalent Shear Stress Scaled to Give Equal Torque [reproduced from Menzies and Merrifield (49)]

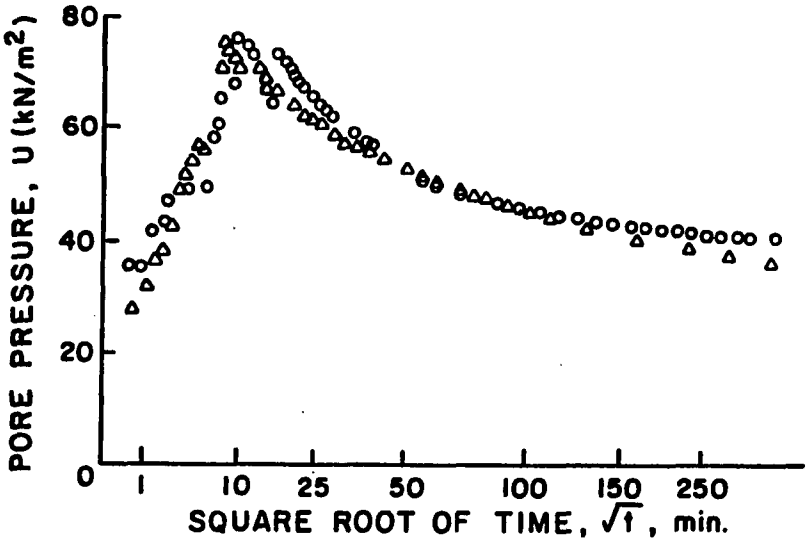

Fig. 2.18 Variation of Pore Pressure During Vane Insertion and Subsequent Dissipation [reproduced from Kimura and Saitoh (36)]

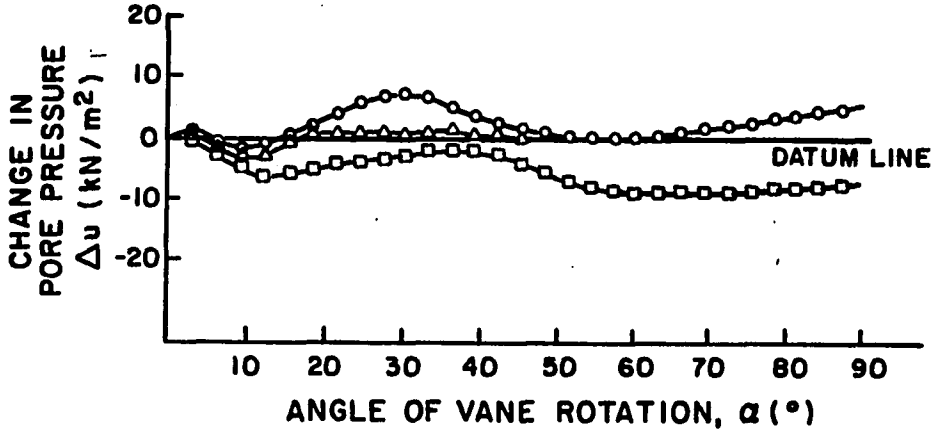

Fig. 2.19 Variation in Pore Pressure During Rotation of Vane [reproduced from Kimura and Saitoh (36)]

Kimura and Saitoh (36) consolidated two types of clay out of a slurry and tested the effect of vane insertion using a transducer instrumented vane. Pore pressure response was monitored over time during vane insertion, elapsed time to rotation, and during rotation. The angular velocity of vane rotation was 0.1 degrees/sec. Fig. 2.18 shows variation of pore pressure during insertion of the vane and the subsequent dissipation. Fig. 2.19 shows a typical angular rotation versus pore pressure response. High pore pressures developed during insertion of vane, dissipated to an equilibrium level in approximately four hours for both clays with PI values of 50 and 20. Pore pressure changes during vane rotation were small. For short dissipation period tests, pore pressures during rotation were lower than the values immediately before due to the fact that dissipation would continue during rotation also.

2.4.3 Shear Rate Effects

Ordinarily torque is applied at a standard rate of 0.1 degree/sec. Earlier studies have shown that measured shear strengths increase with increasing shear rate in plastic clays (1,51,79). A relatively recent study shows that the shear strength of low plasticity clays will increase with decreasing shear rate (70). This occurrence is shown in Fig. 2.20. For low plasticity clays partial drainage is predicted to take place at low rates of shear. At higher rates less dissipation occurs and ultimately decreases the effective

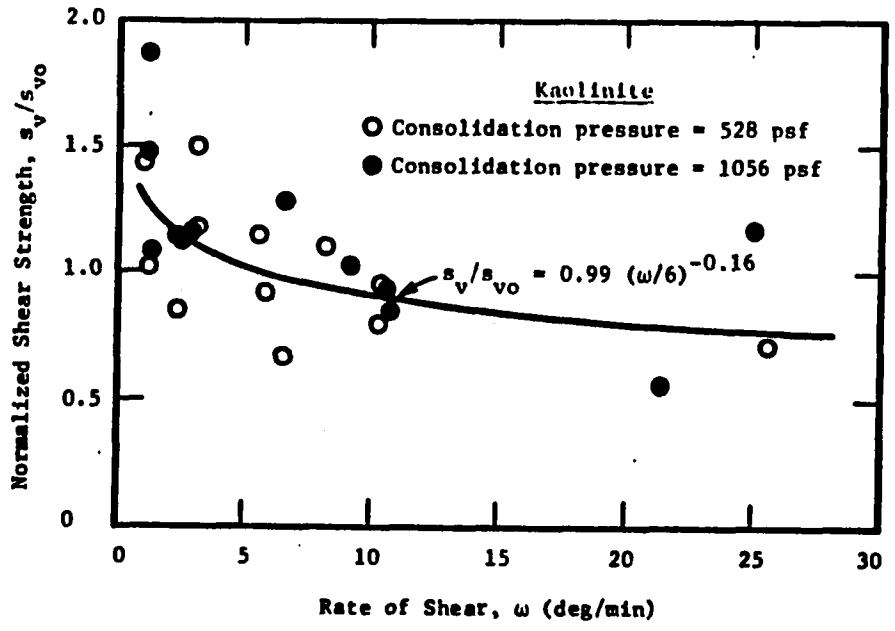

Fig. 2.20 Normalized Shear Strength vs Rate of Shear for Kaolinite [reproduced from Sharifounnasab and Ullrich (70)]

stress and the shear strength. Shear rate is an important factor in determining completely undrained conditions. Since partial drainage can occur in low plasticity clays, it is imperative to establish a threshold shear rate value for these types of soils to ensure undrained conditions.

2.4.4 An Important Utilization of Vane Shear

Undrained residual strength is an important parameter that is generally referred to as the minimum value of shearing resistance that is reached after large strains occur at constant volume on a shear zone. Vane shear testing is generally chosen to measure this property of cohesive soils because a shear zone developes at the edges of the vane blades and it is capable of producing large strains.

Pyles (60) used a vane shear device, operating at different shear rates (0.025 - 0.3 degrees/sec), to measure undrained shear strength and residual strength of San Fransisco Bay mud samples. Results showed that undrained residual strength measured in field and in lab did not differ as in shear strength measurements, and correlation of Ru/Su (Ru = undrained residual strength) with liquidity index revealed a constant value of the ratio over a wide range of water contents.

2.4.5 Triaxial Vane

The triaxial vane was first developed in the Norwegian Geotechnical Institute in 1965 by Kenney and Landva (35). Isotropic, anisotropic and Ko stress conditions can be simulated, and isotropic consolidation can be carried in a triaxial vane device. Moreover, it eliminates some problems associated with regular vane testing as explained earlier.

Law (44), modified a triaxial cell and a vane machine to build a triaxial vane set-up. The vane was designed to be detachable from the vane rod, so that friction pertaining to seals and rod could be measured separately and subtracted from vane shear measurements. This new equipment was used to measure effects of lateral and vertical pressures on torque measurements. The basic design of the triaxial vane unit used in the study reported here is very similar to Law's design with some operational differences.

CHAPTER 3

METHODOLOGY

Equipment, preparation of the artificial samples, testing and data acquisition method pertaining to triaxial vane device are described in this chapter. A schematic diagram showing the testing procedure is given in Fig. 3.1.

3.1 EQUIPMENT

3.1.1 Consolidation Units

In order to accomplish the objectives of this study, a number of duplicate test specimens were needed. They were produced in the custom-made consolidation units as shown in Fig. 3.2. These units after being filled with soil slurry were placed in separate buckets and submerged in water. They were loaded with 10 kg weights in steps up to the desired stress of 1 kg/cm^2. This system proved to be simple and practical. The advantage was that quite a few number of samples could be consolidated within the same period of time. Although time and amount of consolidation could not be measured directly approximate time for 92% consolidation was estimated to be 15 days using linearized finite strain theory (16), soil index properties (see Table 3.1) and formerly obtained consolidation parameters for the same soil.

3.1.2 Modified Triaxial Laboratory Vane Device

The reasons that contributed to the choice of triaxial

vane testing to measure low shear strain properties of soft soils are listed as follows :

1. Vane shear testing is extensively used to determine shear strength properties of soft clays, especially seabed soils,
2. It is a stress-controlled test and is compatible in that aspect with resonant column testing.
3. The new data acquisition system put together to detect minute strain amplitudes was readily adaptable to vane testing in terms of mechanics of operation.
4. Shear stress and strains could directly be measured without the need for evaluation of soil parameters such as Poisson's ratio, or detailed analysis of principles of shear mechanism involved in testing.
5. Some disadvantages in relation to sample disturbance, and interpretation of data, encountered in classical laboratory vane testing was eliminated by modifying and making it a triaxial test.

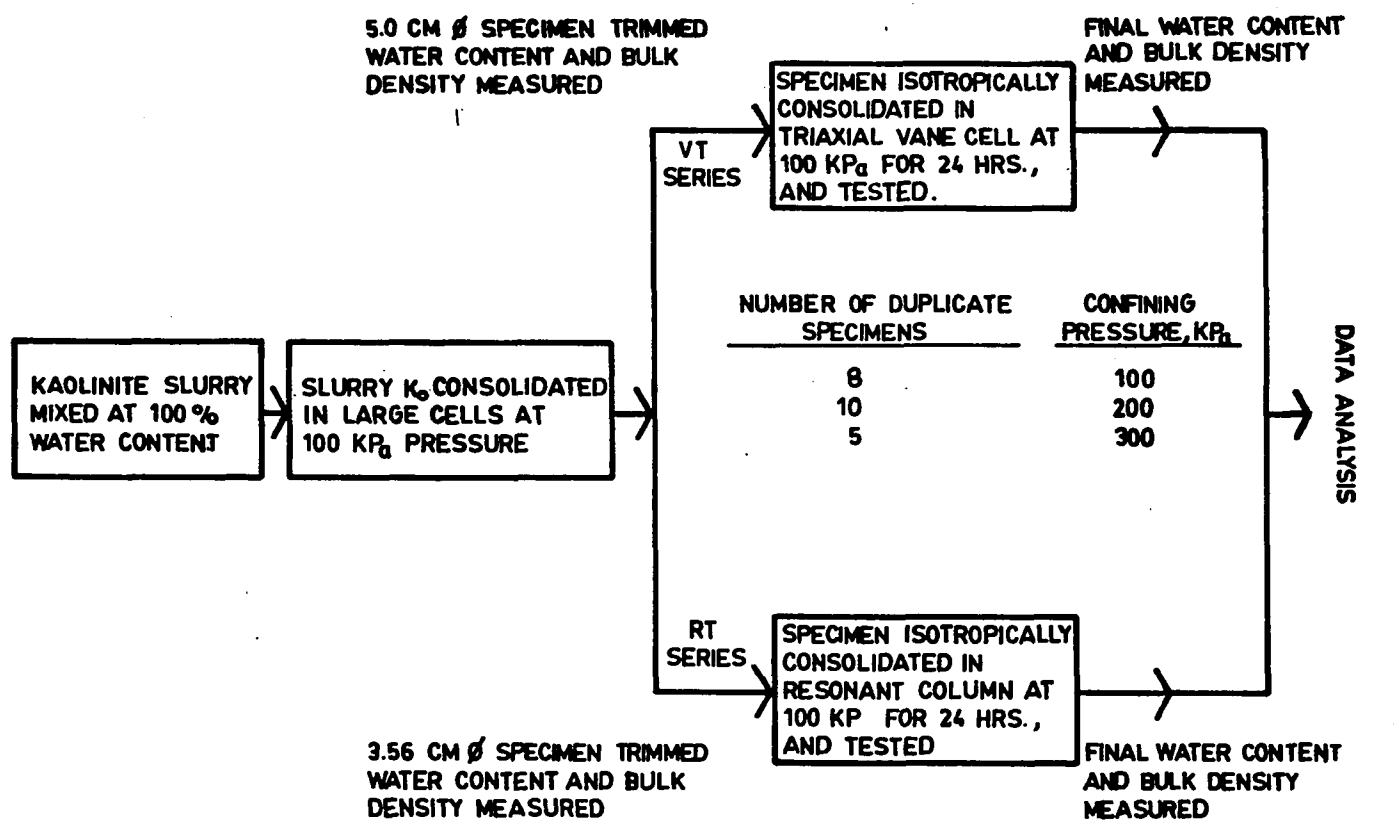

TESTING PROCEDURE

Fig. 3.1 Flow Chart of Testing Procedure

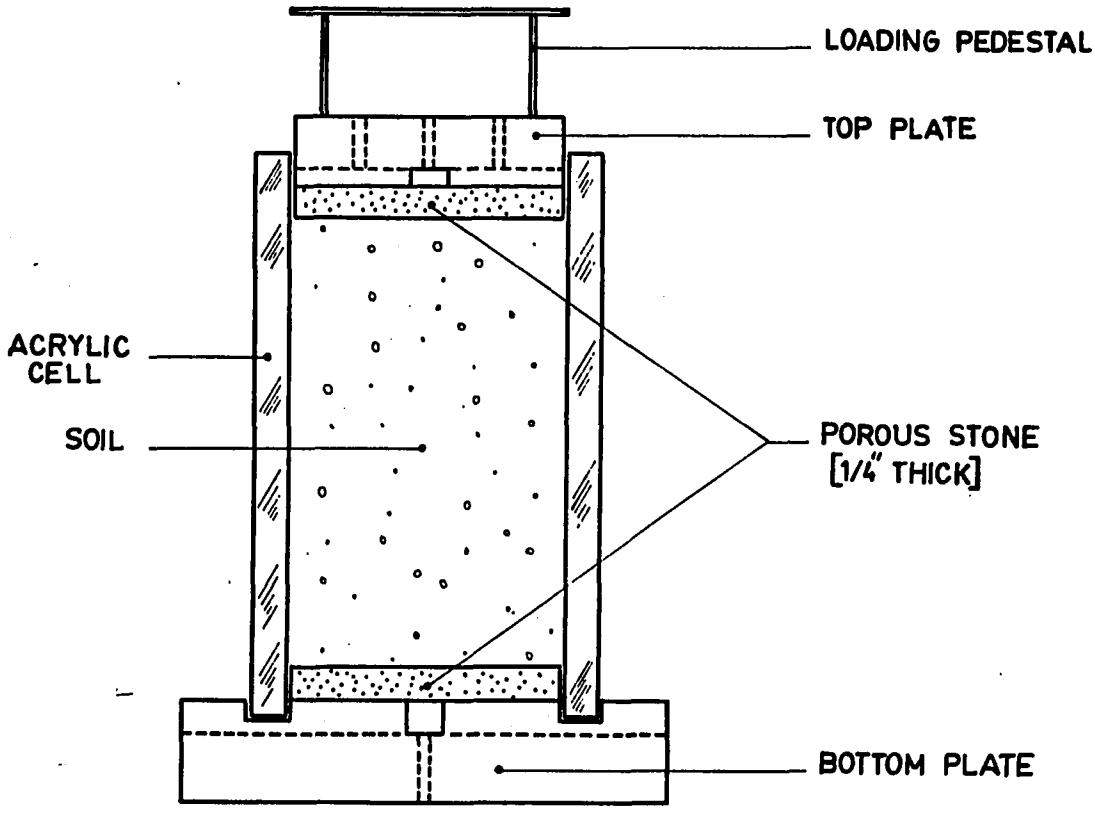

Fig. 3.2 Large Consolidation Cell Used in Preparation of Samples

The apparatus basically consisted of a large triaxial cell, 150 mm nominal diameter, connected to a constant pressure unit, and a laboratory vane machine. Several parts of both the triaxial cell and the laboratory vane machine were either modified or redesigned in order to couple the two separate units. Some of the modifications made were similar to the ones in the triaxial vane apparatus constructed and tested by Law (44) at the Division of Building Research, Geotechnical Section, National Research Council of Canada, Ottava. The set-up used in this study is shown in Fig. 3.3.

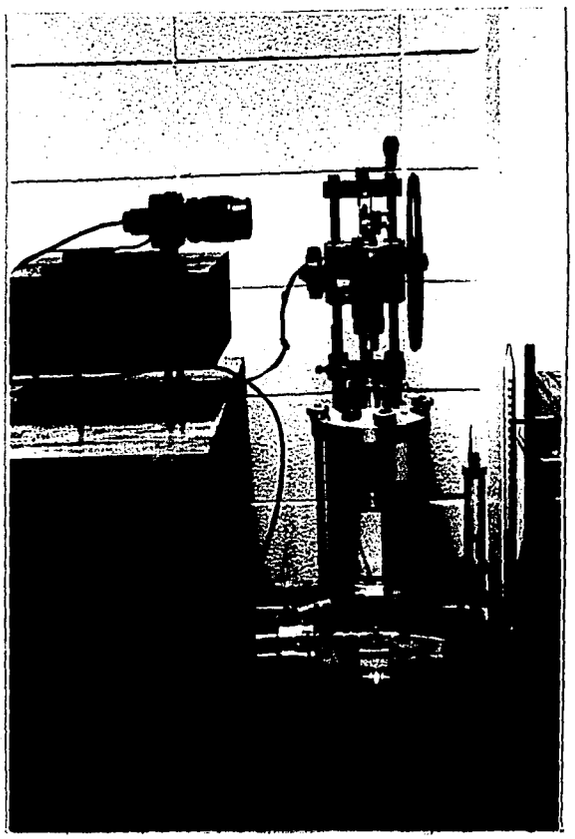

Fig. 3.3 A View of the Triaxial Vane Device

3.1.2.1 Triaxial Cell and Parts

The triaxial cell used was an Engineering Laboratory Equipment Inc. (ELE) cell of model (EL25-406). Confining pressure was applied through an ELE constant pressure apparatus (EL27-432). The schematic diagram of the cell assembly is shown in Fig. 3.4. The modified and new parts of the cell are described below.

3.1.2.1.1 Piston

A stainless steel piston identical to the original ELE loading piston was used to house the vane rod within a narrow duct drilled throughout the length of the piston. A ring shaped, spring loaded teflon seal (Bal-Seal, see Appendix A for specifications) placed in a housing at the top of the piston provided the necessary sealing of the pressure within the cell while allowing the rotation of the vane rod with minimum friction. Schematic details of the piston are given in Fig. 3.5.

3.1.2.1.2 Top Cap

Schematic details of the top cap are shown in Fig. 3.5. The top cap was designed specifically to house a detachable vane. A narrow duct that led into the vane housing was used to fill the housing with distilled water initially, and then to measure the pore water pressure on top of the specimen. The duct connected to a teflon water line which separated into two lines outside the cell, one to the distilled water reservoir and the other to pore pressure transducer. A valve

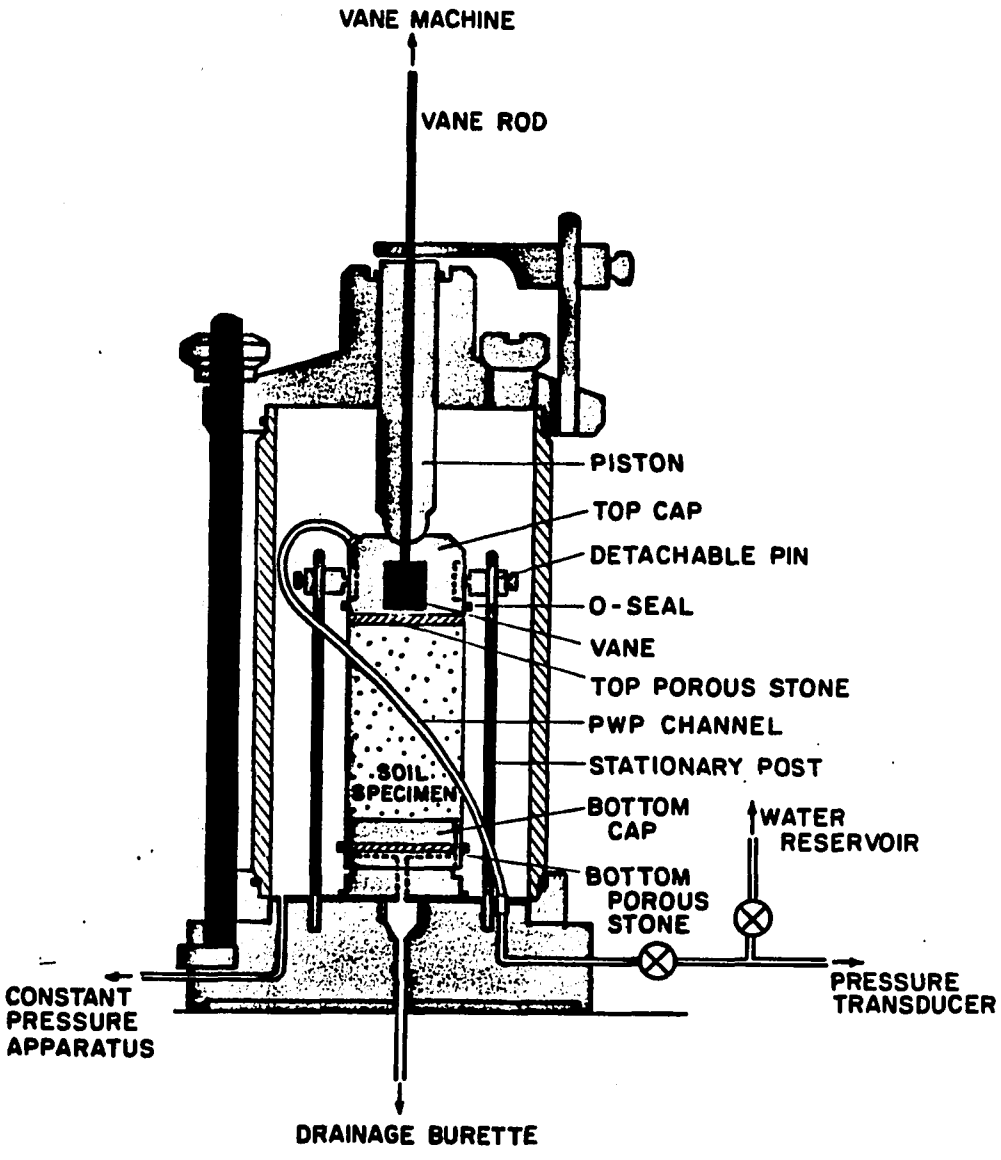

Fig. 3.4 Schematic Diagram of Triaxial Cell Assembly

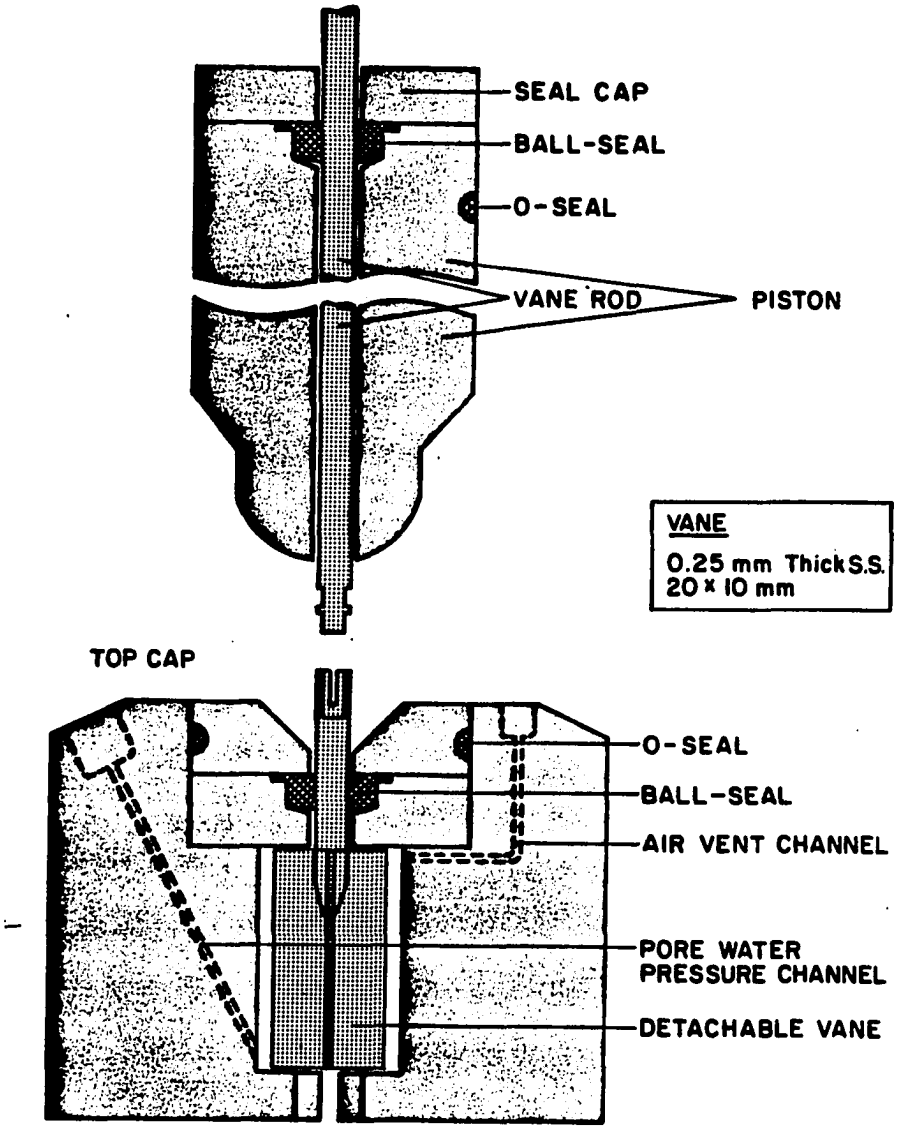

DETAILS OF TRIAXIAL VANE TOP CAP AND PISTON

Fig. 3.5 Schematic Diagram of Cell Assembly Parts [Vane, Vane Rod,Piston,Top Cap]

between the reservoir and the transducer provided the necessary control to use the same water line for both purposes as described above. The housing could be filled with water completely with the aid of an air bleed outlet at the top of the cap which was tightly sealed after filling. Another Bal-Seal, identical to the one in the piston, was placed in a separate housing inside the cap, on top of the vane housing. The purpose of this seal was to block the infiltration of pressurized cell water into the vane housing, therefore be able to correctly measure the pore water pressure changes on top of the specimen during testing. This seal also allowed rotation of the vane rod with minimum friction.

Four perpendicular slits situated around a circular hole at the bottom of the vane housing allowed the passage of the vane blades when lowering the vane into the specimen. Initially, the vane would rest on recesses inside the housing and turned to meet the slits and pushed through at the appropriate time during testing. A brass porous stone, 1/6 " thick, with a circular hole cut through the middle of it, was placed between the top cap and soil specimen. This helped to eliminate slippage and rotation of the top cap.

3.1.2.1.3 Bottom Cap

The bottom cap was specifically designed to prevent the rotation of the specimen. It was designed to fit tightly on top of the original ELE bottom adaptor with the coinciding

drainage holes. The schematic drawing of the part is shown in Fig. 3.4. The bottom cap housed a 1/4" thick corrundum porous stone. A trimmed specimen would be pushed into the housing section until it was firmly set on the porous stone. The extra soil trimmed by the edges of the cap would be removed and sides of the specimen would be leveled with the sides of the cap. In order to ensure the saturation of the porous stone and avoid air be trapped between the specimen and the stone, the housing of the bottom cap would initially be filled with water by opening the drainage valve that led to a graduated burette. Water filling the housing would immerse the porous stone and be allowed to move up to the top edge of the cap ; and then while pushing the specimen into the housing , the extra water would move back up into the burette.

3.1.2.1.4 Side Rods With Detachable Pins

Two alluminum rods were utilized to prevent rotation of the top cap. These rods were threaded at the bottom end and they were screwed into the base of the triaxial cell. Detachable pins, free to move vertically on the rods, would be lined up with two vertical narrow slits on opposite sides of the top cap and secured in place by fixing screws. The vertical slits on the top cap were wide enough to accomodate the pins tightly so that they were not free to move horizontally. However, the top cap was free to move vertically as much as the length of the slits to allow for the vertical consolidation of the specimen. A schematic

diagram of the side rods are shown in Fig. 3.4.

Note that positioning the pins against the slits was an important procedural detail to follow before placing and sealing the latex membrane over the specimen and the caps. It was also necessary to preserve the initial positioning as much as possible and not to introduce significant bending or rotation of the top cap when tightening the fixing screws on the pins. Deviation from the perpendicular positioning of the top cap would result in off-setting the vane to vane-rod coupling point thus introduce excessive friction , disturb the specimen, and make it very difficult to line-up the vane blades with the narrow slits at the bottom of the cap.

3.1.2.2 Laboratory Vane Device

3.1.2.2.1 Vane Machine

An ELE laboratory vane machine (model EL28-180) was modified slightly and utilized for testing. The modification consisted of replacing the original torque wheel attached to the rotating handle with one larger in diameter, and replacing the original electric motor by a variable-speed, reversible motor with remote control panel. The diameter increase in the torque wheel was approximately ten times the original one therefore aided in reducing the speed of rotation significantly. The variable-speed motor made it possible to vary and choose an appropriate rotation speed that would ensure low angular rotation rate for the vane, with the assupmtion that no excessive pore pressures would

develop in front of the vane blade. The reversibility feature was used in conjunction with proper calibration of the data acquisition system. The speed control panel and the reversing switch was wired and placed remotely from the motor which was attached to the vane machine. This set-up provided simultaneous workability with the data acquisition system and it also prevented disturbance to the test set-up by manual interference.

The vane machine was mounted on a stable stand with rubber padding underneath which helped to damp building vibrations. The stand was designed to vertically adjust within the range of 10 cm. The vertical steel rods of the vane machine that carry the motorizing unit, pulley arrangement and the vertical square thread were replaced by longer rods to accomodate the large triaxial cell.

The overall view of the vane machine is shown in Fig. 3.3.

3.1.2.2.2 Vane and Vane Rod

Details of vane and vane rod are shown in Fig. 3.5. The vane was made of 0.25 mm thick stainless steel plate. The diameter to length ratio was 0.5. Two longitudinal slits and two horizontal pins located on the rod provided adequate coupling and decoupling as necessary thus making it possible to detach the vane from the longer portion of the vane rod. The shorter portion of the vane rod extending from the center of the vane and bearing the longitudinal slits at one

end, tapered to a point at the other end at about 1/4 th the height of the vane from the top. The ratio of the diameter of the rod embedded into the vane to the diameter of the vane was 0.32. This ratio is larger than the the desirable ratio of 0.1, which was utilized in a similar design (44). A smaller diameter ratio would introduce less disturbance as the vane is inserted.

3.1.2.2.3 Mirror

As part of data acquisition, the vane machine was equipped with a 51 mm diameter, 13 mm thick, 1/4 wave first surface plane mirror. The mirror was mounted on a miniature mount which allowed position adjustment by rotation about vertical and horizontal axes. The miniature mount was permenantly fixed on the knurled knob at the center of the graduated scale of the vane machine such that the mirror was perpendicular to the dial. Rotation of the vane was directly indicated by the rotation of the mirror connected to the vane via shaft that ran through the load spring and attached to the knurled knob on the opposite side. The total mechanism was lubricated and checked for friction spots thoroughly in order to assure correct transmission of vane rotation to the mirror. Fig. 3.6 shows the details of the mirror and mount set-up on the vane machine dial.

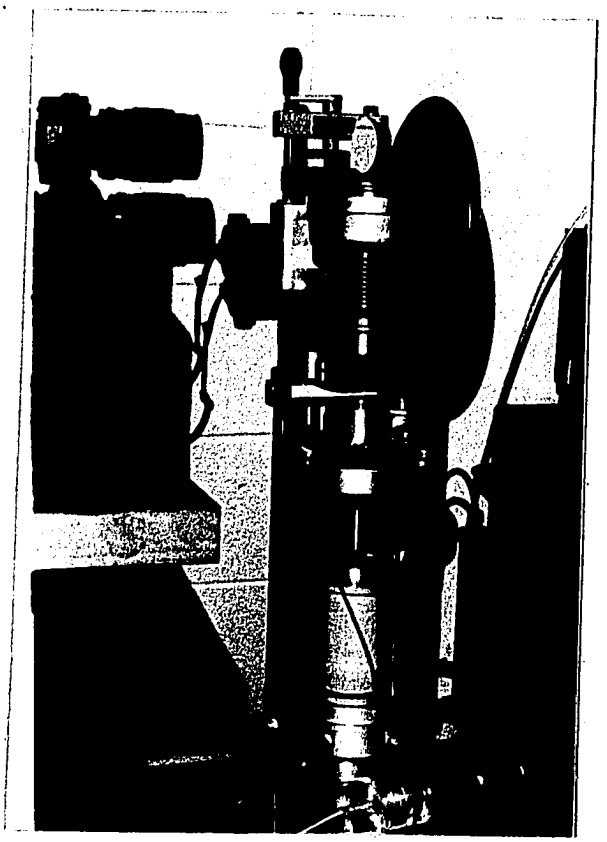

Fig. 3.6 A View of the Vane Mirror and Mount Assembly on the Triaxial Vane machine

3.1.3 Resonant Column

The resonant column test for determining soil moduli and damping of soils is based on the theory of wave propagation in elastic rods. In a resonant column apparatus soil response is monitored for a range of frequencies of both longitudinal and torsional modes of excitation to determine the resonant frequency of the soil specimen. The modulus is determined from the resonant frequency and the geometric properties of the specimen and the driving apparatus. The following equation was used to determine shear modulus, G, using a torsional vibration mode resonant column :

$$G = \left[\frac{2 * \pi * f_n * l}{\beta}\right]^2 * \rho \qquad (1)$$

where, ρ = mass density, f_n = natural frequency measured at resonance, l = specimen length, β = experimental constant.

A Drnevich resonant column apparatus was used in this study. Theory and procedural details of the testing method are discussed in depth in an earlier study (52). These aspects will not be included within the scope of this study.

3.1.4 Equipment Used in Measuring Low Strains

A general layout of data acquisition system is shown in Fig. 3.7. This system was chosen specifically to sense and

record very small angular displacements of the vane via mirror. Ordinarily, autocollimator and the optical position indicator (OP-EYE) duo is used in automated manufacturing industry to measure spatial location, orientation, surface contour, vibration in conjunction with robot arms, control machine tool operations and other production purposes. Another requirement of the data acquisition system was the capability to collect and file vast amount of numerical data. Interfacing a microcomputer to the detection system was necessary to establish the dedicated data acquisition and analysis unit. Individual parts of this unit are discussed below .

3.1.4.1 Electronic Autocollimator

Fig. 3.8 shows a schematic diagram of the autocollimator used. An autocollimator finds application whenever flatness, angle or parallelism is to be measured to a very high degree of accuracy. Position-sensing photodiode is the feature that differentiates the electronic autocollimator from a classical one in which observer's eye is the sensor. The autocollimator used in this study was United Detector Technology (UDT) model (Model 1000-135). The specifications of this unit are given in Appendix A. As shown in Fig. 3.8 , a high power infrared light emitting diode (LED) generates a 15 degrees beam of light which is reflected through a beamsplitter and then collimated by lens. This parallel beam is reflected off the mirror under

test, back through the lens and beam splitter to the detector assembly. A blocking filter is used to prevent ambient light from biasing the detector reading. The detector is a 2 axis position sensor which has electrode connections (photodiodes) at four 90 degree positions around its edge as well as a ground connection. When the return beam from the mirror under test strikes the detector, the signal out of the photodiodes is proportional to the angle of the mirror. The following proximity formulas are used to determine current X and Y positions of the incident light beam on the detector surface :

$$Xposition = \frac{X1 - X2}{X1 + X2} \qquad (2a)$$

$$Yposition = \frac{Y1 - Y2}{Y1 + Y2} \qquad (2b)$$

where, X1 and X2 are signals from sensors on the horizontal axis, and Y1 and Y2 are signals from sensors on the vertical axis (see Fig. 3.9). A sinusoidal response is obtained using the formulas above as the beam of light propagates from one sensor to the other along one axis. The response is most linear in the central region and falls of at the corners of the field of view. For calibration purposes it is imperative either to determine and use this linear portion of the response or correct the nonlinear response within the software that collects and analyzes data. In this study only

the horizontal axis sensor response and the linear portion of this response was utilized both for calibration and data collection. The lens focal length determines the angular coverage and resolution of Model 1000 autocollimator. Focusing is not necessary since only the position of the centroid of the light beam is sensed.

3.1.4.2 Optical Position Indicator (OP-EYE)

UDT OP-EYE is a microcomputer peripheral for IEEE-488 and RS-232C standard buses. The specifications of this unit are also given in Appendix A.

When light falls on the detector surface and causes a current flow in each of the photodiodes proportional to spot proximity, the OP-EYE elóctronics report to the controlling computer the magnitude of current for any channel selected by the computer. Signals from the photodiodes are amplified and then digitized in an A/D converter. The digital values are then converted to ASCII code for transmission to the computer. Communication between OP-EYE and the computer is done through use of a few operational commands interpreted by OP-EYE. Initially a series of set-up commands are sent to OP-EYE for specific instructions that set channel number, gain, operation mode, scan range and start point, etc. for operation. Then each time an "R" command (short for 'read') is sent , OP-EYE measures and replies with data to the computer.

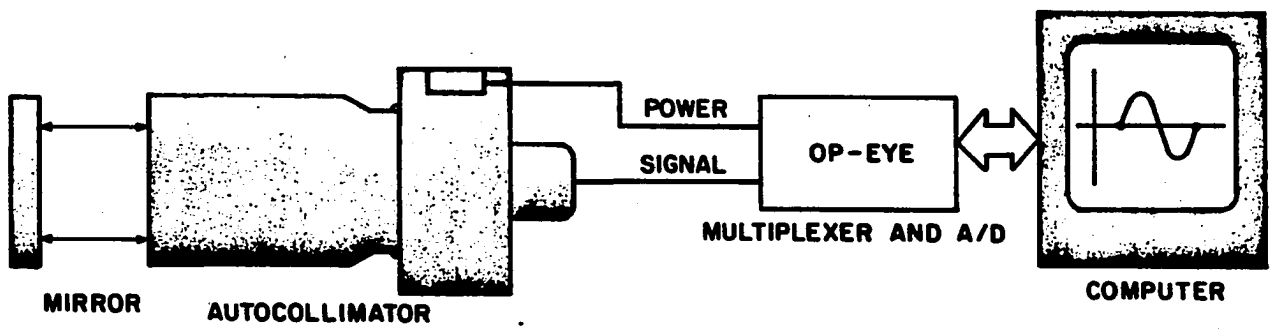

Fig. 3.7 Data Acquisition System

In this study, OP-EYE Model 4 was utilized due to its 16-bit resolution A/D converter capability which made it possible to obtain higher resolution (1 part in 65,536) thus sense smaller angular displacements. Two assembly language routines were used in conjunction with the main software package written in Fortran 77 to read/write to RS-232C ports. Thus the ASCII values transmitted from OP-EYE could be read by the controlling computer via Fortran program, which were than converted to numbers and stored. Fig. 3.9 summarizes the basic operation of data acquisition system via schematic representation.

3.1.4.3 Microcomputer

A 16 bit microcomputer with 256 Kilobytes main memory and 10 Megabytes disk storage was used. Color graphics display capabilities of the computer were utilized through graphics libraries called from Fortran programs. The microcomputer used was a Zenith Data Systems Model Z-100, which runs MS-DOS operating system for which a number of Fortran compilers were available.

The data acquisition and analysis software werewritten in Microsoft Fortran-77. The main segments of programs were:
A. Calibration and data collection programs (OPINIT,OPCALIB)

These programs are used to initially position and calibrate the test set-up interactively and then collect and store data. During testing, positional inputs from the optical sensors are displayed graphically in real-time

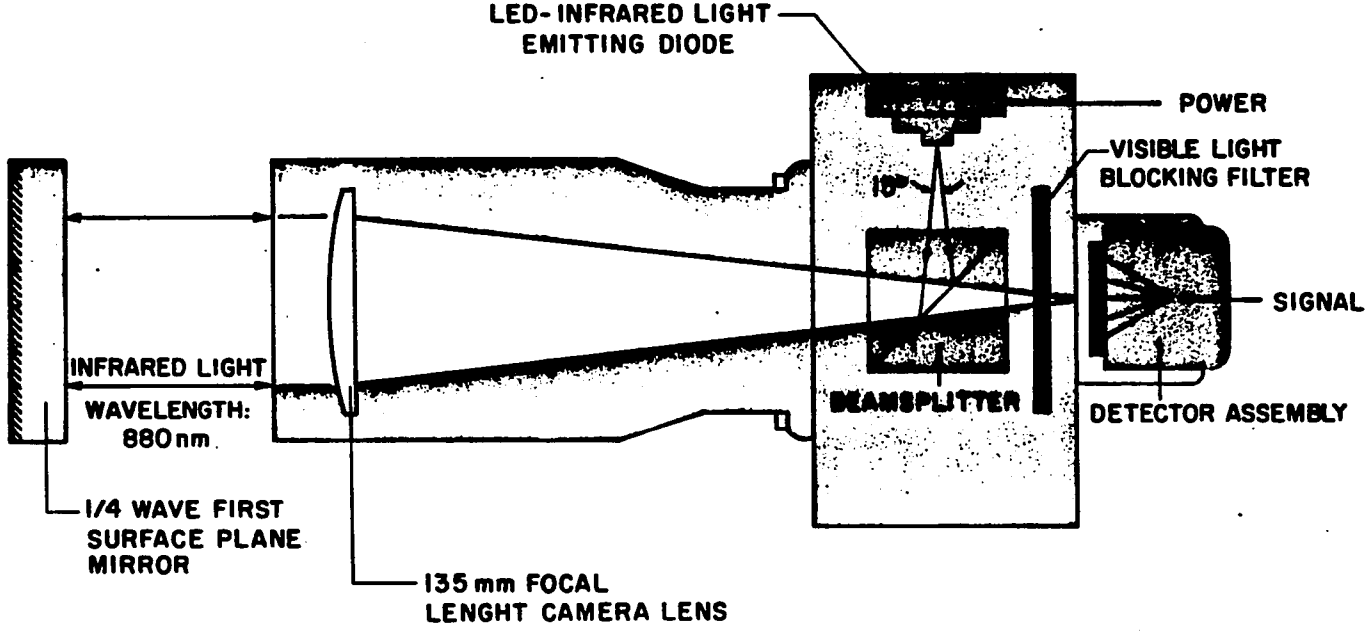

DETAILS OF ELECTRONIC AUTOCOLLIMATOR

Fig. 3.8 Electronic Autocollimator

therefore making it possible to monitor progress of the test.

B. Data smoothing program (OPAUX1)

This program is used to filter excessive noise in data by means of moving averages. The various parameters involved in the method are specified interactively.

C.Data manipulation and analysis programs

(OPAUX2,OPAUX3, OPSTR, RESON)

These programs are used to manipulate large amounts of collected data by use of interactive graphical displays. Curve fitting and regression methods are employed and parameters used by these programs can be changed interactively.

The listings of the programs cited above are given in Appendix B. Fig. 3.10 shows the general view of the test set-up and data acquisition equipment used in this study.

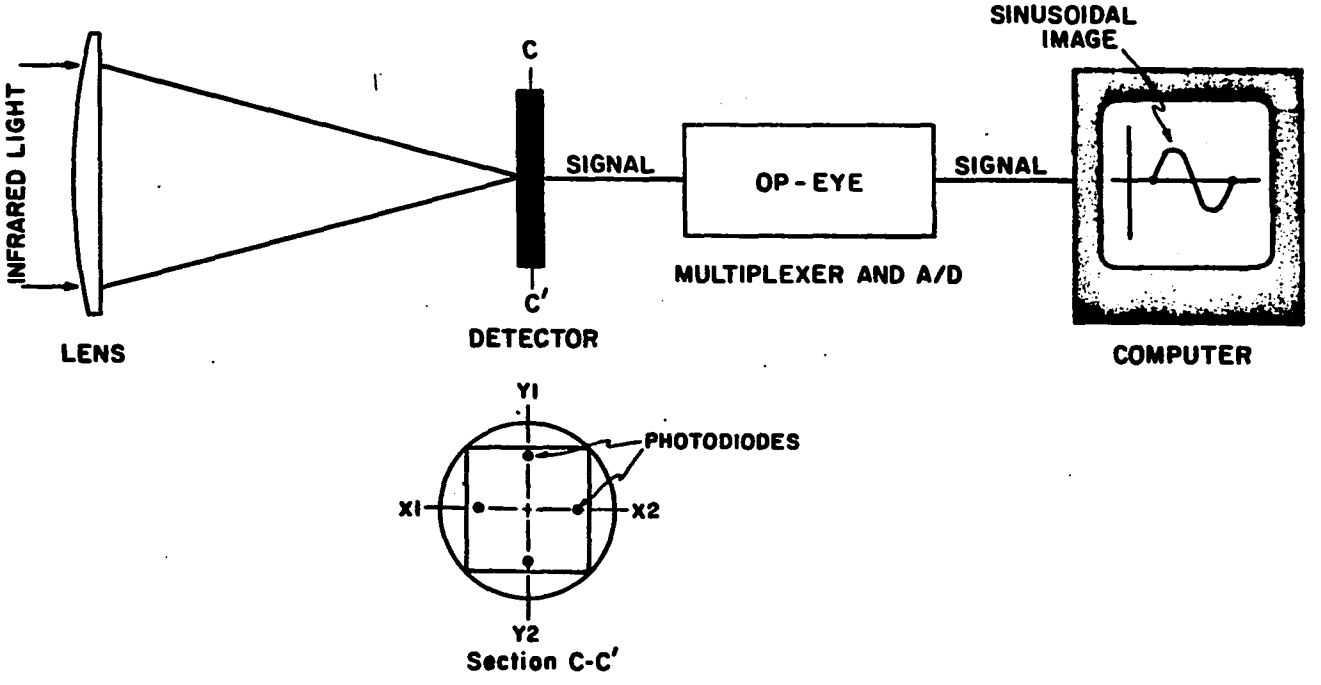

FORMULAS FOR PHOTODIODES:

$$\text{X POSITION} = \frac{X1-X2}{X1+X2} \qquad \text{Y POSITION} = \frac{Y1-Y2}{Y1+Y2}$$

DETAILS OF DETECTION AND DATA COLLECTION ASSEMBLY

Fig. 3.9 Operation of Data Acquisition System

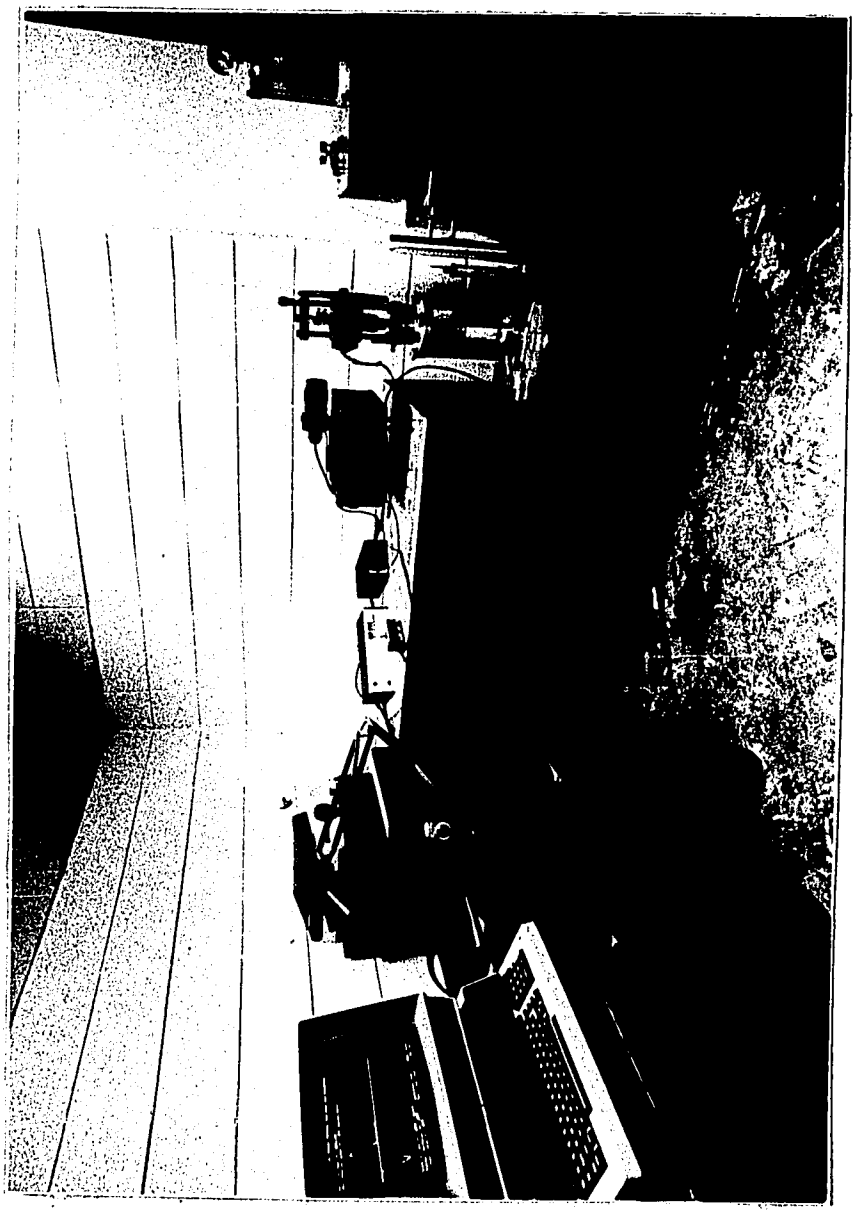

Fig. 3.10 General View of the Laboratory Test Set-Up

3.2 SAMPLE PREPARATION

3.2.1 Slurry Preparation

Artificial samples were prepared from Georgia kaolinite, index properties of which are given in Table 3.1. Dry soil was mixed with distilled water to make slurry at about 100 % water content. The slurry was prepared in a large scale laboratory mixer and left to stand overnight in a covered container. It was poured into plexiglass consolidation cells (see Fig. 3.2) in layers, shaken to force out pockets of air. The consolidation cells were placed in seperate buckets and immersed in water. Loading was done in increments of 10 kg weights at equal intervals up to the desired pressure of $1 kg/cm^2$.

3.2.2 Estimation of Consolidation Time

Finite strain theory and a practical procedure based on this theory (16) was utilized in estimating a conservative duration of loading for approximately 92% consolidation of the slurry material at 1 kg/cm^2 pressure.

Compression curve and Cv values of the same soil mixed at liquid limit were obtained through a standard consolidation test (see Appendix C). Using a relation derived from the governing equation of finite strain theory, a theoretical curve was fit to the compression data (see Appendix C). The theoretical relation is as follows :

$$e = (e_0 - e_{00}) \exp(- \lambda \sigma') + e_{00} \qquad (3)$$

where, e = void ratio, e_0 = void ratio at zero effective stress, e_{00} = void ratio at infinite effective stress, λ = linearization constant , and σ' = effective stress. The best fitting curve to the experimental one was used to estimate a linearization constant value, λ . A basic language program with interactive graphics routine was utilized to fit a curve to experimental data and estimate λ . The value of λ was than used to determine another constant, N, dimensionless governing equation parameter. The relation between N and λ is given as follows :

$$N = \lambda * 1 * (\gamma_s - \gamma_w) \qquad (4)$$

where, l = layer thickness in material coordinates, γ_s , γ_w are unit weight of solids and water, respectively, and

$$l = h/(1+e_0) \qquad (5)$$

where, h = layer thickness as deposited.

A family of dimensionless curves of U, percent consolidation versus T_v, time factor (1), derived from finite strain theory, were used to estimate time factor T_v at 92% consolidation. These curves were functions of factor N, deposition and drainage conditions. Typical curves for normally consolidated, doubly drained and unconsolidated, doubly drained layers of linear finite strain theory are reproduced in Figs. 3.11 and 3.12, respectively. Curves for N=0.0 correspond to material with essentially no self weight. As N value increases the thickness of the layer and self weight of the material increase.

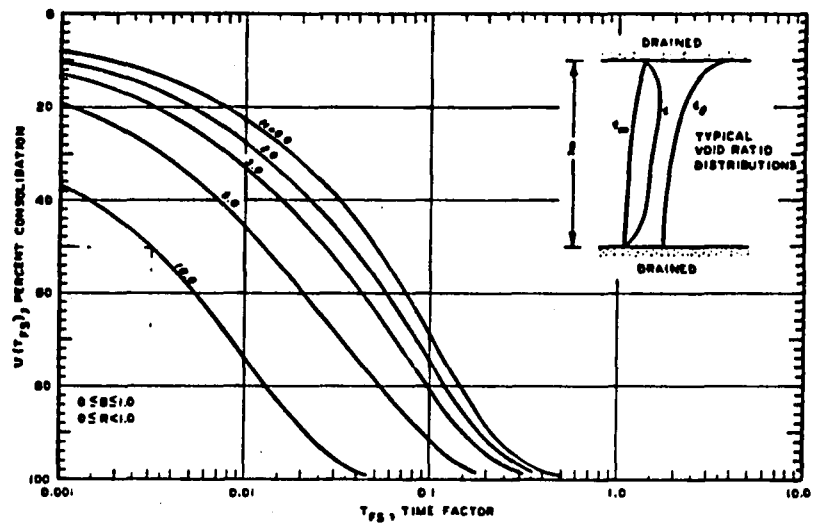

(a) Normally Consolidated Case

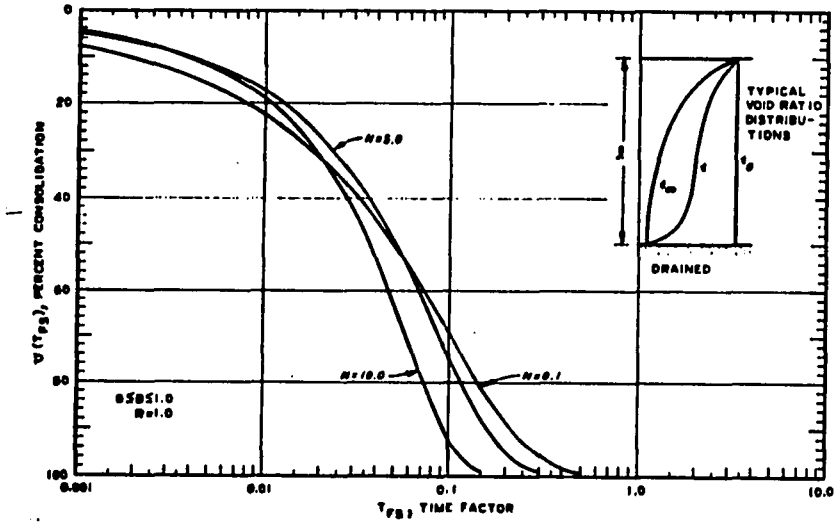

(b) Unconsolidated Case

Fig. 3.11 Degree of Consolidation as Function of Dimensionless Time Factor For Doubly Drained Layers by Linear Finite Strain Theory [reproduced from Cargill (16)]

For the case of slurry material deposited in the consolidation cells, curves for unconsolidated, doubly drained layers were used. The curve fitting to the compression data (see Appendix C) resulted in λ value of 1.07 and a corresponding N value of 9.77, which was rounded to 10. Using the Cv values obtained from consolidation test (see Appendix C) and the time factor estimated from U vs T_v curve for N=10, the 92% consolidation time for the large samples were estimated to be a total of 10 days for final consolidation pressure of 1 kg/cm^2. Using N=0, that is assuming no self weight for the material, the time was estimated to be 20 days. A value of 15 days was chosen for total loading period.

3.2.3 Specimen Preparation

The consolidated soil sample would be extracted out of the plexiglass cell and cut into two portions. One portion was used to trim a 5 cm diameter specimen for triaxial vane test, and the other was used to trim a 3.56 cm diameter specimen for resonant column test. The water content, weight and dimensions of each specimen were measured and recorded. There were 35 specimens tested. A number of these specimens were tested to establish a well defined testing technique and/or for calibration purposes. Complete data pertaining to 23 of them are used and reported in here. The initial average index properties for these specimens are given in Table 3.1.

Table 3.1 Index Properties of Soil Specimens

Water Content (%)	63
Bulk Density (kN/m^3)	15.75
Void Ratio	1.704
Liquid Limit	64
Plastic Limit	34
Plasticity Index	30
Specific Gravity	2.65
% Finer than 2 μm size ...	90

3.3 TESTING

3.3.1 Resonant Column Testing

Resonant column testing generally followed standard procedures. An earlier study (52) documents the theory and procedure of the LSU/Civil Engineering Drenevich resonant column apparatus used in this investigation also. Therefore, description of resonant column testing will not be included herein.

However, it is imperative to note that, in this investigation the current to the driving coils was attenuated significantly to achieve smaller magnitudes of shear strain amplitude. This way degradation of shear modulus reduction curves for the soft specimens could be eliminated significantly due to lower strain vibrations. Difficulty arouse when occasionally calibration limitations of the accelerometer were exceeded due to weak signal, and resonance condition could not be detected accurately. Increasing the magnitude of the driving current slightly

eliminated this condition. Resonant column test specimens were subjected to identical test conditions as triaxial vane test specimens. They were confined and tested under same pressures and drainage conditions.

Although size of the specimens were different because of equipment requirements, duration of consolidation confinement was kept approximately the same. Data obtained from the resonant column testing was reduced and plotted using program RESON (Appendix B).

3.2.3 Triaxial Vane Testing

The following procedure was established and followed to prepare and mount a specimen for triaxial vane testing :

1. Trim a specimen of 5 cm diameter and 8.6 cm length.

2. Mount the bottom cap on the bottom adaptor and place the bottom porous stone inside the cap.

3. Let distilled water rise inside the cap by opening the lower drainage valve which is connected to a graduated burette. Lowering and raising the burette several times will help to extract air trapped within the line and connections.

4. Place the specimen on the edges of bottom cap, push gently into the cap housing. Keep the drainage valve open so that the extra water moves back up the burette. Remove the soil trimmed by the edges of the cap and level the boundary area.

5. Place the top porous stone and the top cap containingthe vane, on the specimen. Rotate the cap such

that the side slits are lined up with the screw holes at the base of the cell where the side rods bearing the horizontal pins are to be installed. Secure the exact place of the top cap by placing a layer of teflon tape around its lower portion in contact with the porous stone.

6. Place the latex membrane and O-seals about the specimen, making sure to cover all of the bottom cap, and part of the top cap without blocking the side slits.

7. Screw in the side rods with the horizontal pins already inserted into the slits on the sides of the top cap. Secure the pins by tightening the fixing screws . Make sure that the top cap does not tilt or rotate from its original position during this process.

8. Connect the line that leads to pore pressure transducer and distilled water reservoir to the top cap. Open the valve to the water reservoir and let the water fill the vane housing by keeping the air vent channel open. Seal the air vent channel and close the valve to the reservoir after filling process is completed. Do not pressurize the reservoir to fill the housing as this may cause water to seep between the latex membrane and the specimen and complicate subsequent pore water pressure measurements.

9. Mount the plexiglass cylinder and the head of the cell with the piston with the vane rod already in place. When mounting the head piece, extend the vane rod such that the pins on the rod would meet the slits on the shorter

portion of the rod. Push against the vane so that that the tip of the piston will gently lower into the depression at the center of the cap. The piston will not rest on the specimen however will help to push against and straighten it if it has deviated from perpendicular position.

10. Turn the vane rod to meet the slits at the bottom of the top cap, however DO NOT insert the vane at this time. When turning the vane make sure the flat side at the top of the rod coincides with the hole on the rotating socket of the vane machine which is used to couple the vane rod and the central shaft leading to the dial assembly of the machine. The mirror at the other end of the shaft, should have already been aligned with the autocollimator lens at this time. In case alignment of the flat side of the vane rod with the rotating socket hole is not achieved at this stage, positioning can be corrected by rotating the triaxial cell.

11. Connect the tie rods of the cell and tighten them securely. Fill the the triaxial cell with the confining liquid (distilled water) and tighten the air vent screw. Adjust the pore water pressure transducer read-out to zero. Adjust the level of water in the drainage burette such that it is approximately aligned with the center of the specimen. (Maintain this level by moving the burette down periodically during the consolidation phase of testing). Record all initial readings; check to make sure valve to the water reservoir is closed, valve to the drainage burette is open,

and the vane rod is properly aligned with the mirror shaft attachment location. Apply the desired cell pressure.

All the specimens were consolidated under 100 kPa (~1 kg/cm^2) confining pressure. Consolidation was monitored by observing the pore pressure dissipation at the top of the specimen and drainage rate at the bottom. Typical pore pressure reduction and drainage rate curves are given in Appendix C. The value of B parameter ranged from 0.95 to slightly over 1.0, indicating nearly 100 % saturation for all specimens.

Three sets of tests were conducted. The initial set of specimens (8 specimens) were consolidated at 100 kPa and tested at 100 kPa of pressure. The second (10 specimens) and third (5 specimens) sets were also consolidated at 100 kPa, however they were tested at 200 kPa and 300 kPa of pressure, respectively. Data pertaining to 3 different pore pressure ratios (u_{excess}/P_t) were obtained. This procedure made it possible to incorporate excess pore pressure effects into the analysis in a controlable fashion.

Vane was lowered into the specimen after the confining pressure was applied. Insertion of the vane was done manually by a slow, steady push. The vane would reach about to the mid-height of the specimen when approximately 2.5 cm of the top end of the vane rod remain above the piston. Since these distances were pre-designed, it was necessary to have a specimen trimmed to the specified length of 8.6

(+/- 0.1) cm, as indicated in the specimen mounting procedures above. Consolidation would progress with the vane already inserted. Duration for dissipation of initial pore pressure to 10 % of the confining pressure (100 kPa) was approximately 24 hrs. This duration of confinement was well above the 4 hrs period of time estimated by other investigators (36) for dissipation of pore water pressures in saturated clays generated by insertion of the vane. A slight increase in pore pressure reading was observed during insertation of the vane, however this increase, measured at the top of the specimen within the vane housing, was due to volume change as the vane rod was pushed through and it did not necessarily show the amount of pore pressure increase around the vane. Since the specimen was allowed to consolidate around the vane, whatever amount of pore water pressure that was generated during insertion was safely assumed to have dissipiated to a constant value when excess pore pressure ratio measured at the undrained boundary (top) had decreased to 10 % of the confining pressure. Disturbance effects were also assumed to have been eliminated significantly by the same reasoning.

Duration of pore pressure dissipation was rather short despite the length of the specimen. This was due to the fact that these specimens were trimmed from samples already consolidated at the same pressure. This occurrance validated the fact that the estimated time for one dimensional

consolidation of the larger samples using finite strain theory was accurate. Since both the confining time (24 hrs) and the pressure (100 kPa) used were relatively small, matters concerning permeability of the latex membrane and compressibility of the water filling the vane housing were not considered to be significant during testing (11).

Vane shear testing would take place at the completion of the consolidation period, which was determined to be at about 90% dissipation of the excess pore pressure under 100 kPa of confining pressure. During testing drainage valve was kept open. Using the variable speed capability of the vane machine motor, the rate of applied torque could be monitored. After several trials the standard rate of torque applied in all tests was chosen to be 20 % of the full rate. This corresponded to approximately the rate of 0.0125 degrees/second torque application. In order to evaluate the correlation between various motor speeds and torque rate, data over long runs of the motor at different speeds were collected manually by observing the free rotation of the torque dial with respect to time. Averaged torque rate data points were than correlated with respective motor speeds. Linear regression analysis was used to fit a line to these data points. Correlation was good as shown in Appendix C. The reasons pertaining to the choice of slow rate of torque application were several. First one was to increase the resolution of small strain data range. The frequency of data sampling by electronic means could not be

altered , and slower rate of rotation resulted in higher number of data points collected within unit time range. The second reason was to achieve low angular rotation speeds of the vane to avoid overestimation of stress values. According to a recent investigation on the shear mechanism of vane test in soft clays (47), it was concluded that undrained loading conditions are satisfied at angular velocities of vane greater than or equal to 1 degree/second. Localized pore water pressure migration could occur at angular velocities below 1 degree/second. The unexpected higher values of shear strength in some tests indicated that there was some amount of localized pore water pressure migration and consolidation around vane due to slow rate of angular rotation. However, this effect was observed only at higher strain ranges and did not influence low strain parameters. Vane assembly is lowered along the square thread of the vane machine to the desired position such that about 1 cm of the flat-sided end of the vane rod would be inserted into the rotating socket of the assembly. The vane rod is not to be attached to the assembly until a calibration procedure, described in the next section, is completed. At this stage, it is imperative that the socket rotates freely about the vane rod for proper calibration. Frictional interferences will be evident in subsequent calibration data therefore repositioning or slight lubrication of the socket interior may be required. The following procedure is followed to

complete testing :

1. Position the vane assembly over the triaxial cell such that socket rotates freely about the vane rod.

2. Run OPINIT program to detect friction interference for calibration. The real-time signal will deviate from producing sinusoidal image if there is interference. Repeat steps 1-2 as necessary.

3. Record the initial position of the dial on the vane machine for both angular rotation and torque scales.

4. Run OPCALIB program and follow the interactive instructions to collect and store low strain data. The program instructs the user when and how to retain the vane rod using the fixing screw.

5. As soon as low strain data collection is complete, record the final position of the dial for both angular rotation and torque scales WITHOUT stopping the vane machine.

6. Record the position of the dial periodically until failure condition is observed. At this stage, the speed of the motor can be increased to 50 % of the full speed without violating compatibility and continuity conditions with respect to low strain data. Angular vane speed will still remain below 1 degree/second. Earlier tests run at 80 % of full speed revealed maximum angular velocity of vane about 1 degree/second, close to the peak strength of the specimens.

7. Record dial readings at peak and residual strengths.

8. Lower the vane assembly approximately 0.5 cm (or 1

to 2 revolutions of the upper hand knob), raise it back up the same distance. This will push the vane to a lower level and when the rod is pulled back the vane will detach from the rod. When the rod is free, it will rotate back to the original position with the unwinding action of the load spring. The mirror attached to the vane rod will also be positioned back at its starting location.

9. Uncouple the vane rod from the rotating socket of the vane assembly by removing the fixing screw, and repeat steps 1-4. This is for the purpose of collecting another set of low strain data (CAL.FILE) to correct the vane shear data (DAT.FILE) for friction between the vane rod and the seals located within the piston and the top cap, and also for friction between the vane rod and soil. The friction data file (CAL.FILE) is determined to be unique for each specimen tested . A standard friction correction was not adapted. This was due to the fact that each friction file, like the data files, displayed high sensitivity with respect to factors like the amount of lubrication in the seals, specific positioning of the vane and the vane rod, minute alterations of the positions and tilt of some data acquisition units (autocollimator,mirror). Consequently, each data file was associated with a unique friction correction file. The maximum seal friction measured was about 10% of the undrained shear strength measured. The factors listed above are also valid for theinitial

calibration procedure, therefore it was incorporated into the data acquisition method as an inherent part.

3.4 DATA ACQUISITION SOFTWARE

The data acquisition system was specifically put together to measure very small angular displacements. Due to large quantity of data collected and the complexity involved to reduce and interpret the data, it was necessary to write software that would help the user to conduct repeatable and fast analysis. Data collection and analysis software involved real-time process and interactive color graphics. Real-time feature made it possible for the user to observe the data simultaneously and monitor the test. Interactive graphics made it possible to manipulate large quantities of data and guide the user in all phases of the analysis. The triaxial vane testing set-up described herein requires the use of this dedicated software. These programs and their operational features are discussed below:

A. OPCALIB

OPCALIB is the data collection program written in Fortran 77. It instructs the user step by step how to calibrate the image, properly position the mirror, collect and file data. It calls assembly language subroutines to communicate with OP-EYE. A separate routine within the main program converts ASCII characters to numbers. Graphics subroutines and libraries are called to plot the signal value against time. The resolution of time step is 1/100

second . The time routine is an external assembly language program which uses the microcomputer's clock. The frequency of data sampling, including all I/O operations and the frequency with which data is furnished by OP-EYE, is 2 data points per second. A typical data collection session, excluding the time spend for calibration and instructions, is approximately 15 min , which correspond to a total of 1800 data points. A typical session using OPCALIB is as following:

1. Figs 3.12a and 3.12b show the progression of the first step in calibration procedure in which the sinusoidal image traces the rotation of the mirror free of vane. The vertical axis is the magnitude of signal from OP-EYE directly proportional to the angular rotation of the mirror. The peaks of the image represent maximum intensity signals from the left and the right photodiodes respectively, depending on rotation direction. The horizontal axis is time in hundreds of seconds.

2. Fig 3.13 show the second step in calibration in which a straight line is fit through the linear section of the sinusoidal image. The slope of this straight line is used to determine the calibration constant as follows:

Calib. Const. = Applied torque rate / Slope of straight line
(radians/unit signal)= (radians/second)/(second/unit signal)

The typical angular coverage from one peak to the other is

0.02 radians as indicated in Fig. 3.13. The linear portion of the sinusoidal image that is employed in data collection is central 75 % of peak to peak distance. Therefore typical usable range traversed by the mirror is 0.015 radians, or in terms of shear strain 1.5 %. The fitted line is also useful in indicating the limits of the linear section .

3. Fig 3.14 show tracing of the mirror rotation in reverse direction. This is necessary to establish a starting location within the boundaries of the linear range, at which the vane rod is affixed to the vane assembly. When the desired position of the mirror is reached, the mirror rotation and signal transfer are terminated simultaneously as instructed by the program. When securing the position of the vane, the rotating socket will move slightly as fixing screw meets the flat side of the vane rod within the socket. This will result in rotation of the original position of the mirror and signal will fall out of the linear range. In order to prevent this happening, OPCALIB allows the user correctly locate the mirror position when securing the vane in place by indicating current signal location with a different colored dot on CRT for each trial.

4. Fig 3.15 shows the completed trace of the mirror rotation with the vane connected. This data is stored in a DAT file with a specific number pertaining to the specimen tested. CAL files are obtained in the same manner as described above however with the vane detached from the vane rod .

B. OPAUX1

This program is used to filter mechanical and electrical noise from the data. OPAUX1 is the first step in data analysis and both DAT and CAL files are subject to filtering. Moving averages with variable parameters is used in filtering process. User is instructed to specify the number of changes, and the values of parameters for each trial. Program is terminated and new data is stored under the same file name only when the user consents on the quality of filtering which is displayed after each trial.

C. OPAUX2

This program is used to manipulate the DAT and CAL curves by means of graphics cursor (cross-hair) so that the starting signal positions coincide. It constitutes the second step in data analysis. Figs. 3.16 and 3.17 show a case where calibration curve is lowered to meet the data curve. Since color graphics is used in this program as well as the other programs, the color coding of individual curves can not be observed in the black and white prints. The manipulation is done simply by pointing the initial and final positions of one point on one of the curves using the graphics cursors and especially coded keys that is recognized by OPAUX2. The key coding is as follows :

D - move down, U - move up, L - move left, R - move right

C - move calibration curve, RETURN - move data curve

(These codes are also recognized by OPAUX3).

Manipulation of data terminates only when instructed by the user. Then, both the calibration and data curves are rotated about their own individual axes, (each bearing the slope of the straight line fit through the linear portion of their initial calibration images produced by OPCALIB), counterclockwise to a vertical line, and the new position values are stored. This procedure was found to be necessary in order to eliminate the effects of calibration slope differences between the CAL and DAT curves and the artificially introduced strain hardening character to torque versus strain curves which are produced in next step.

OPAUX2 reads in DAT and CAL files, and after manipulation and evaluation, creates a temporary file called an INT file, in which are stored the new DAT and CAL values.

D. OPAUX3

This is the final step in analysis. OPAUX3 reads in the INT file which contains both DAT and CAL files as they were altered by OPAUX2. Program converts signal versus time curves to torque versus shear strain curves by use of calibration and torque rate constants. Fig 3.18a shows the first picture produced by the program which is the superimposed torque vs shear strain curves for CAL and DAT files. Manipulation of these curves are still allowed at this stage if they do not coincide properly. Fig 3.18b illustrates this option. The calibration curve is subtracted from the data curve by means of a subroutine that finds the torque values on each curve at equal (or very close) shear

strain amplitudes and interpolates the rest. This subroutine was necessary for subtraction procedure due to the fact that the signals sent by OP-EYE do not bear constant values. Also the calibration constants, though very close, are not necessarily equal. Therefore shear strain values calculated using the signal values and the calibration constants do not coincide discretely point by point for CAL and DAT files. After subtraction , the resulting torque values are multiplied by the corresponding load spring factor, also interpolated from load versus deflection data of the specific load spring utilized. (Load deflection curves of the two load springs used in this study are given in Appendix C). The resulting load values are then divided by vane shear surface to calculate shear stress values. The following standard equation was used to evaluate shear stress :

$$S = \frac{SF*T}{\pi * \left[\frac{D^2*H}{2} + \frac{D^3}{6} \right]} \qquad (6)$$

where, T = torque (degrees), SF = load spring factor (kN/degrees), S = shear stress (kPa), D, H are diameter and height of vane, respectively (m).

Torque data was also corrected with respect to changing angular velocity of vane, however small, since same time base was used to evalute both torque and shear strain values.

Fig 3.19a show the resulting shear stress-strain diagram. Following the instructions given, the graphics cursor is used to point locations that identify a range of data for scale enlargement to evaluate initial modulus and another range of data through which a straight line is fit by linear regression to evaluate yield modulus, or strain-hardening modulus for bilinear representation of the curve. Figs 3.19a and 3.19b illustrate this process.

Fig 3.20a show the enlarged view of the initial part of shear stress-strain diagram. Once again, upper and lower limits are located within an allowed strain range to fit a linear regression curve, slope of which is defined as the initial or maximum shear modulus. Figs. 3.20a and 3.20b illustrate this process.

Fig 3.21 shows the final result of the analysis. Bilinear representation, statistical parameters of the fitted lines, the maximum and strain-hardening shear moduli values, range of shear stress and strain, and resolution of strain values are given in this final picture. This information and the shear stress-strain curve are stored in an OUT file before the program is terminated by the user. If reanalysis is requested, the program moves backward in stages until user specifies where to start the analysis once again.

In all I/O operations of software described above data remains in binary format to save memory space and fasten the I/O processes.

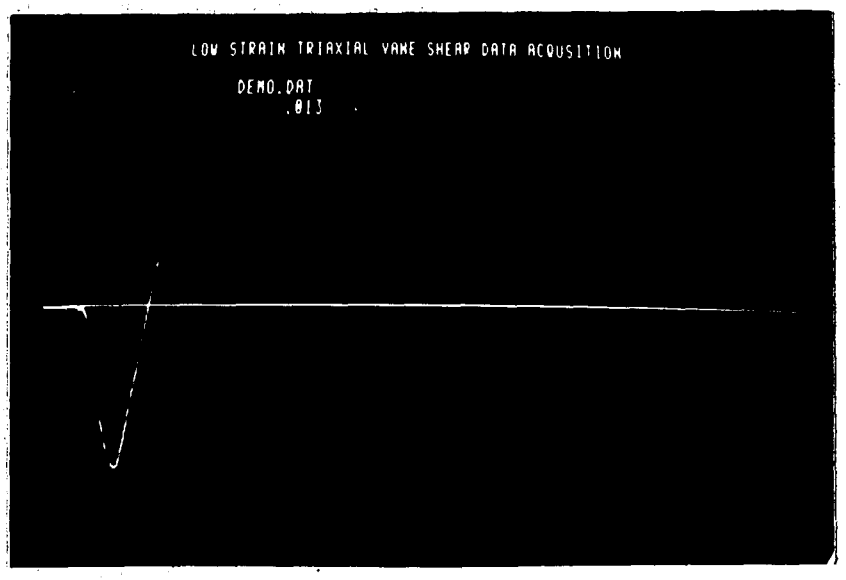

(a)

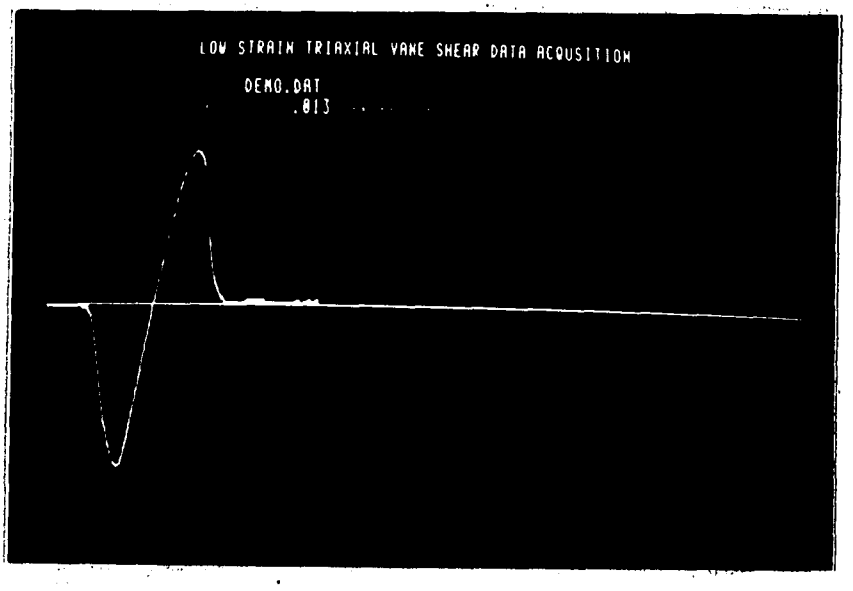

(b)

Fig. 3.12 OPCALIB - Progression of Calibration Step 1

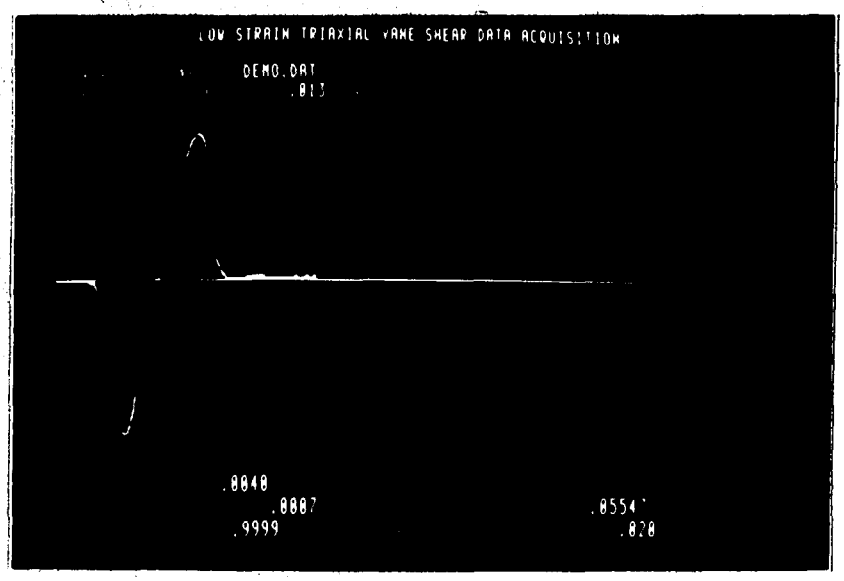

Fig. 3.13 OPCALIB - Calibration Step 2

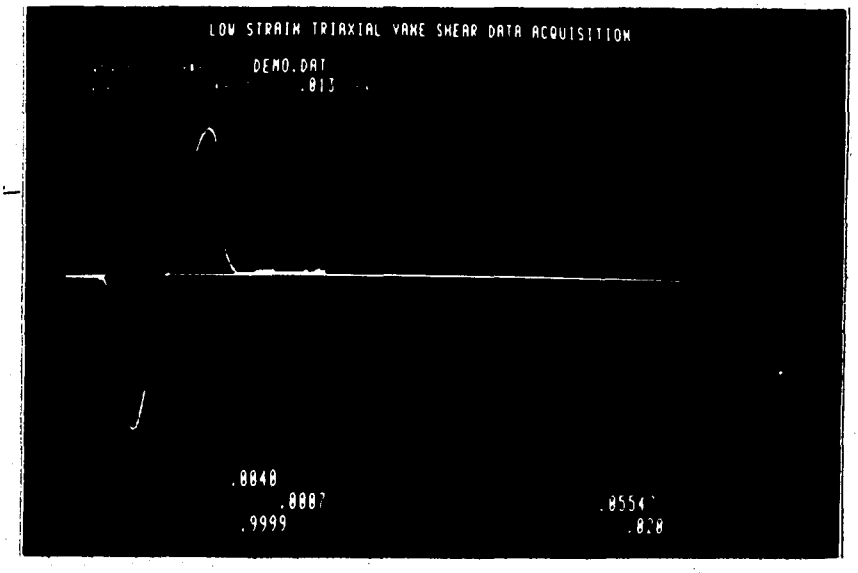

Fig. 3.14 OPCALIB - Calibration Step 3

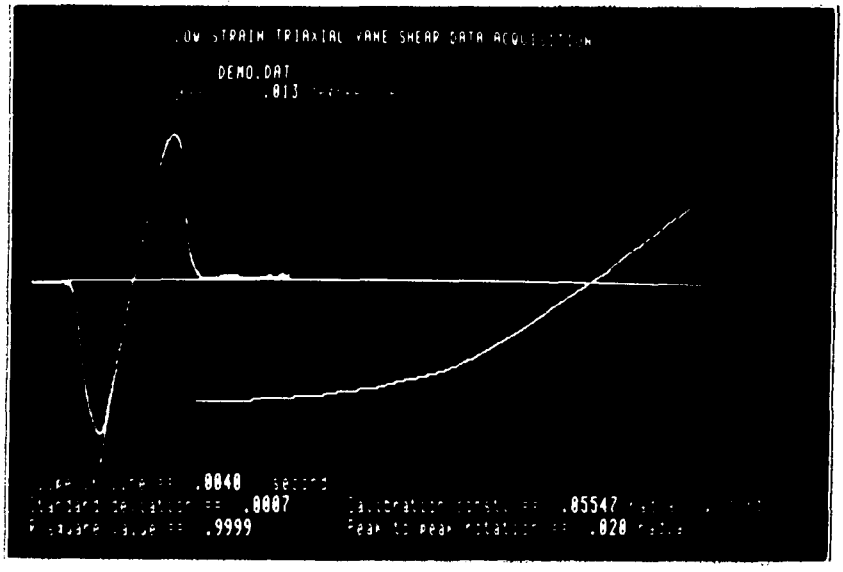

Fig. 3.15 OPCALIB - Acquisition of Data

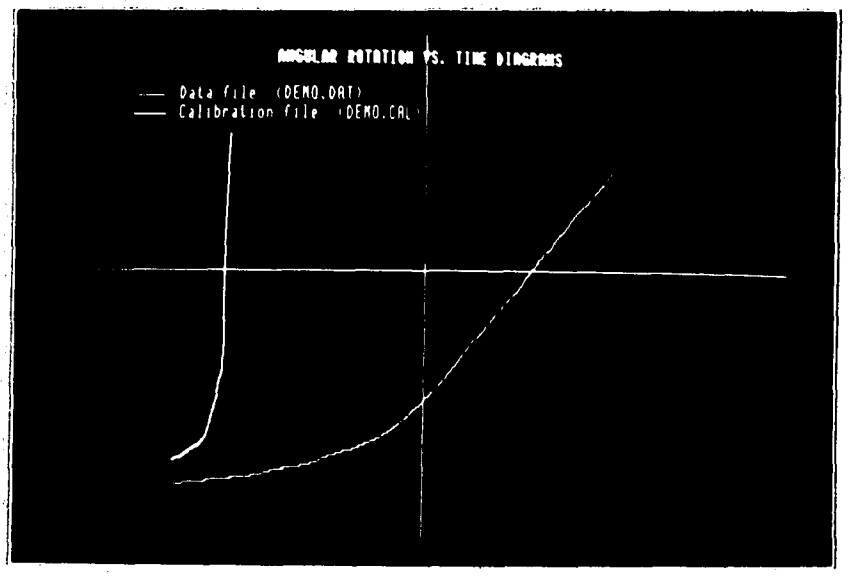

Fig. 3.16 OPAUX2 - Original Positions of DAT and CAL File Data

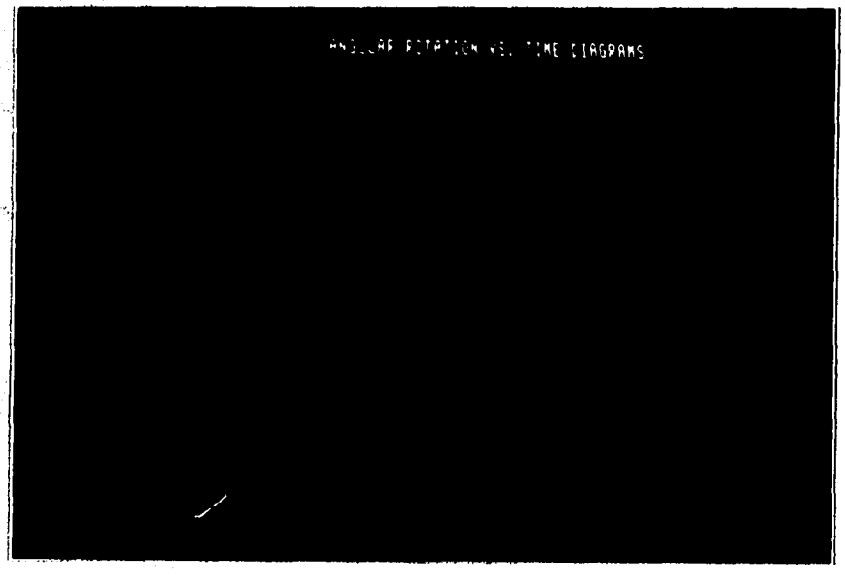

Fig. 3.17 OPAUX2 - Final Positions of DAT and CAL File Data

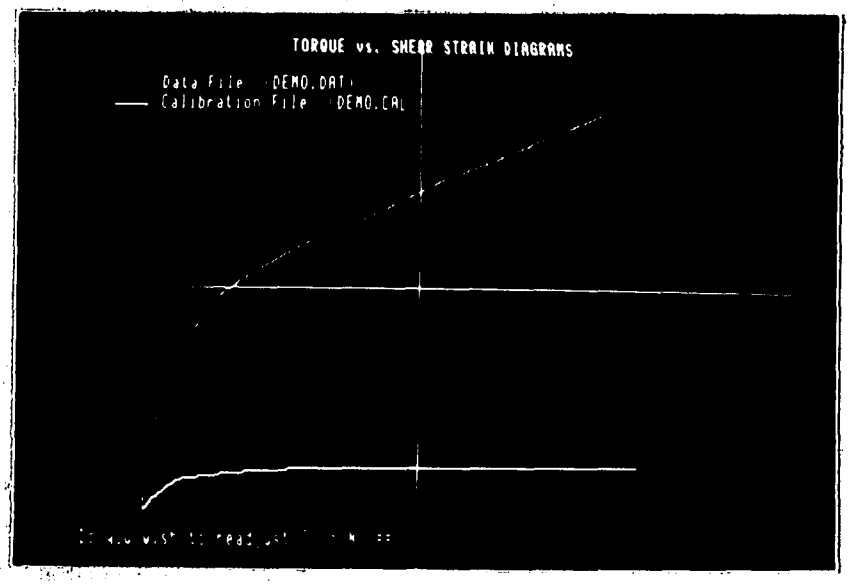

(a) Initial Position of Curves

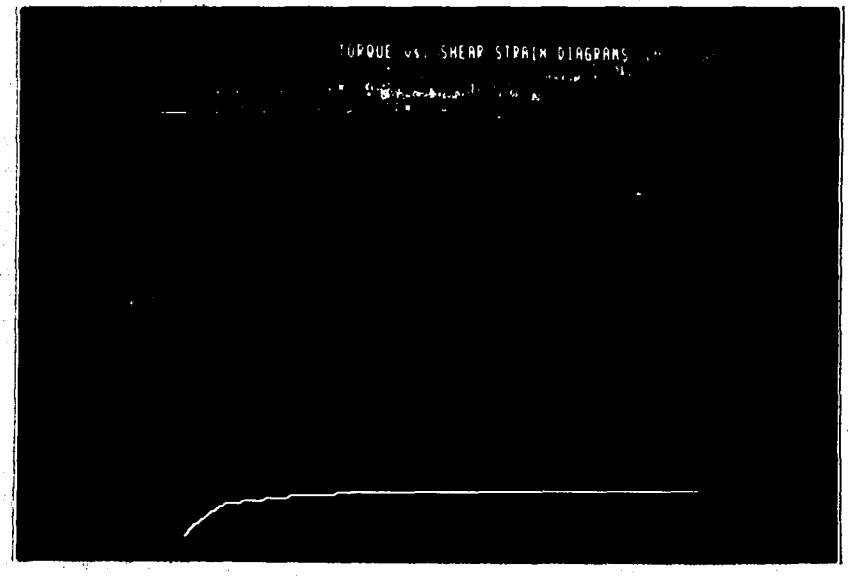

(b) Option of Curve Adjustment

Fig. 3.18 OPAUX3 - Superimposed Torque vs Shear Strain Data for DAT and CAL Files

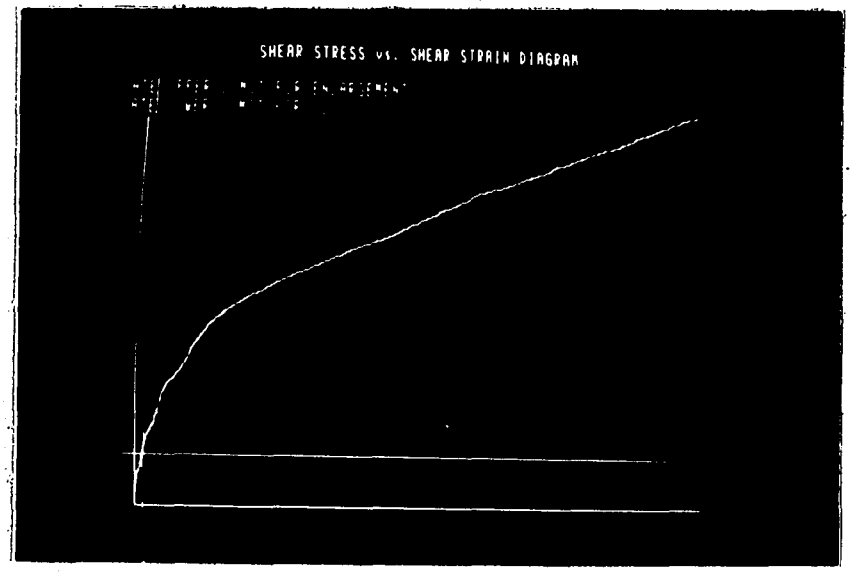

(a) Choosing an Upper Limit for Enlarged View of Low Strain Range

(b) Choosing a Lower Limit for Second Portion of Bilinear Representation

Fig. 3.19 OPAUX3 - Shear Stress-Strain Curve Corrected for Seal Friction

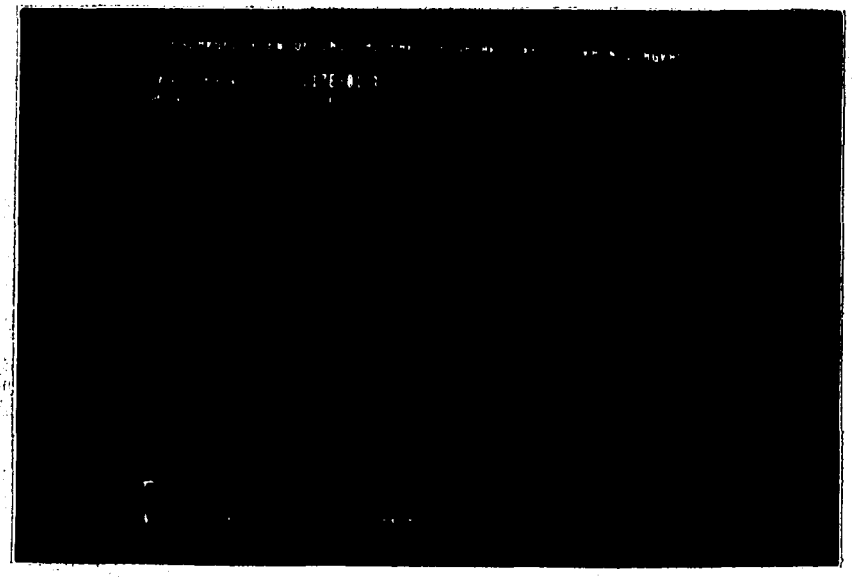

(a) Choosing a Lower Limit for Linear Regression Analysis

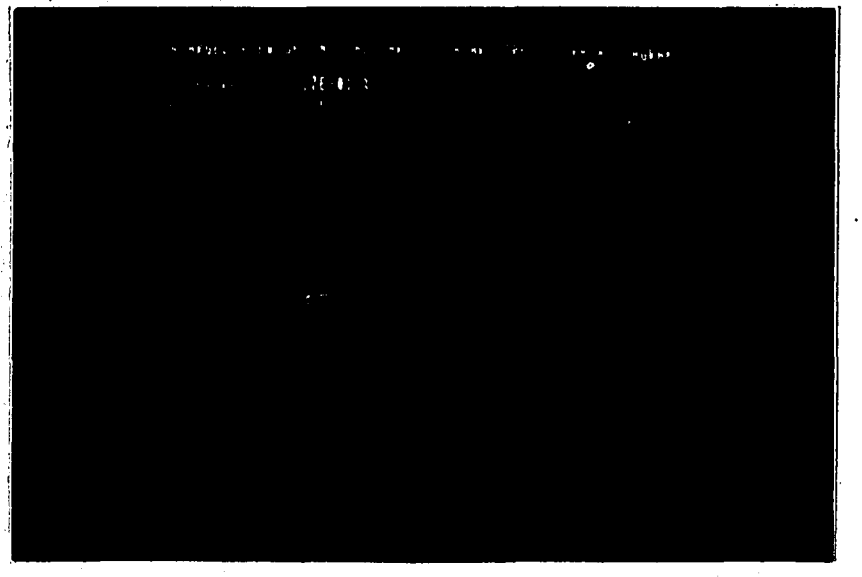

(b) Choosing an upper limit for Linear Regression Analysis

Fig. 3.20 OPAUX3 - Enlarged View of the Low Strain Range

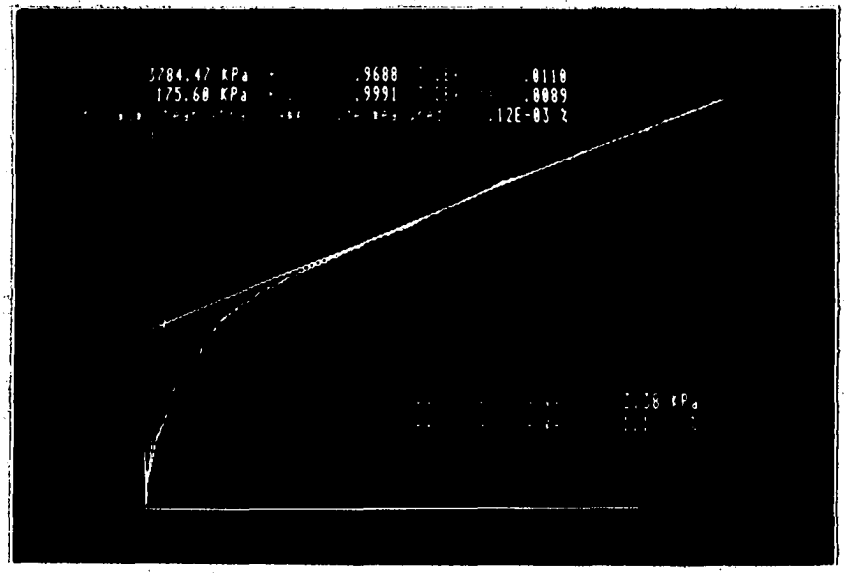

Fig. 3.21 OPAUX3 - Final Shear Stress-Strain Curve With Bilinear Representation

CHAPTER 4

DISCUSSION OF RESULTS

Analysis of both static and dynamic data was done using computer software for reasons of speed and maintaining consistency. Software included routines that read data from an input file, produce graphics and write results in an output file. Curve fitting procedures , linear regression routines and calculation of statistical parameters constituted several subroutines of the software.

4.1 PRESENTATION OF RESULTS

4.1.1 Specimen Index Data

Identification codes VT## and RT## are abbreviations for 'Vane Testing' and 'Resonant Column Testing', respectively. The first number in the identification code refers to confining pressure (e.g. 1 ==> 100 kPa), and the second number refers to test number.

The average water content and the average bulk density of all the specimens before testing were 63 %, 15.75 kN/m^3, respectively. The values of water content and bulk density for each specimen before and after testing were measured and recorded (Table 4.2). The computed value of dynamic shear modulus is directly proportional to the density of the specimen. Therefore erroneous or inconsistent measurement of the density would complicate moduli determination. In order to establish a consistency between the measured index

properties of both specimens, and compensate for differences in consolidation time and specimen size in two different tests, the following adjustment procedure was adopted. Using the formula :

$$-\frac{dV}{V_o} = \frac{w_f - w_i}{(1/Gs) + w_i} \qquad (7)$$

[where, $-dV/V_o$ = volume change, w_f and w_i = final and initial water contents, Gs = specific gravity (2.65)], volume change values were estimated for all specimens using initial and final water content values. Then, dV/Vo was correlated with measured bulk density, for both static and dynamic test specimens. Linear curves were fit to the data resulting in :

$$\text{Bulk density}]_{static} = 16.24 + 2.86 * dV/V_o \qquad (8)$$

$$\text{Bulk density}]_{dynamic} = 16.53 + 1.19 * dV/V_o \qquad (9)$$

Using the formulas above, new values of bulk density were derived. Measured values of dynamic and static maximum moduli were normalized with the corresponding density values. Fig. 4.1 illustrates the effect of this adjustment where the measured Gmax-s/Gmax-d is correlated with the adjusted Gmax-s/Gmax-d. The adjusted ratios are slightly higher than the measured, compensating for the effect of slightly higher final bulk density of the resonant column specimens measured after consolidation.

4.1.2 Static and Dynamic Test Results

The maximum static shear moduli values were determined using the data reduction and analysis program OPAUX3, as explained in Chapter 3. Table 4.3 summarizes the data extracted from OPAUX3 and the statistical parameters pertaining to linear regression analysis in determining the maximum moduli. Additional information obtained from OPAUX3 are minimum shear strain amplitude measured, extent of stress-strain data collected, and yield stress and strain values obtained from bilinear representation.

The maximum dynamic shear moduli values were estimated using data reduction program RESON. This program would yield maximum shear moduli estimated at 10^{-4} % or 10^{-5} % (depending on range of data) shear strain amplitude using a hyperbolic curve fitted to the data. Table 4.4 summarizes dynamic test results.

Figs. 4.2 through 4.24 illustrate shear moduli, G versus shear strain, γ variation for dynamic and static tests on duplicate specimens. The shear moduli values are secant moduli except for the estimated maximum value for both curves. Shear strain is represented on logarithmic scale. The data points on static curves were sampled automatically using a computer program that would match nearest shear strain values of static data to dynamic data. The points on the extension of the static curves were sampled at equal intervals. Hyperbolic curves were fit to

both dynamic and static data. These curves did not agree well with data above the shear strain amplitude of approximately 10^{-4}. Therefore curve fitting was terminated at shear strain 10^{-4} and approximate trend of data was followed to construct higher strain range of the curves.

The behaviour of the static and dynamic curves are observed to be very similar to the results of an earlier work done by Kavazanjian and Hadj-Hamou (34) (Fig. 2.14). At low strain amplitudes the dynamic and static stress-strain behavior is quite different for soft clays than the general assumption of coincidence. Due to degradation, the dynamic shear moduli reduces much faster than the static moduli above a certain threshold of shear strain amplitude. Thus the dynamic curve crosses over the static curve and continues reduction with respect to increasing shear strain amplitude with a much higher gradient than the static curve. It is not unrealistic to assume that this reduction would gradually level off and join the static curve at some higher shear strain amplitude. Lack of dynamic data at higher strain ranges (due to equipment limitation), inhibit verification of this assumption in this study. The cross over of the dynamic curve is more evident in normally consolidated specimens [VT-RT11 - VT-RT18]. The threshold shear strain amplitude where the cross over occurs seems to be between 10^{-5} and 10^{-4}.

For specimens tested under higher confining pressures but induced pore pressure ratios of 0.5 and 0.67, the

static curve shifts down significantly, whereas the dynamic curve tends to shift upward. The static moduli are substantially affected by the excess pore water pressures. The dynamic moduli, on the other hand, increase with increasing confining pressure, and are not affected as much by excess pore water pressures. However, the close values of Gmax-dynamic for pore pressure ratios of 0.5 and 0.67 show that at a higher pore pressure ratio the effect of confining stress increment diminish. The average values of Gmax for static and dynamic tests listed in Table 4.1 confirms these observations. For VT2-RT2 and VT3-RT3 series of tests, there is no apparent confirmation to assume that dynamic curve degrades faster than the static curve because static curve starts with significant reduction due to the effect of excess pore pressure. It is important to note that effective confining stress for all of the tests are the same, that is 100 kPa.

4.1.3 Correlation of Various Test Results

Determining the effects of existing excess pore water pressure on shear modulus of soft saturated clays was one of the important tasks of this study. The results from static and dynamic tests differed in this aspect also. Fig. 4.25 shows the variation of Gmax-static / Gmax-dynamic ratio with pore pressure ratio (u_r = u_{excess} / P_t). A hyperbolic curve was fit to the data through the mean points of the vertical moduli ratio ranges at 4 different u_r values (= 0.1, 0.5,

0.67, 1.0). Using the hyperbolic variation, Gmax-s/Gmax-d for the normally consolidated case (u_r=0.0) is estimated to be 0.85. The equation of the curve is given in the figure (Fig. 4.25). This finding is in agreement with other investigators' findings which show static shear stress-strain curve to lie below the first cycle (backbone) curve of cyclic loading (see Chapter 2).

Refering back to the G vs γ curves, it is observed that degradation in dynamic testing is evident above shear strain amplitudes of 10^{-5} %. Degradation of shear moduli during cyclic loading is known to result from dynamic pore pressure buildup, softening due to stress reversal, and internal breakup of soil matrix structure. Even at low strain cyclic loading, all of the factors above contribute to the slowly changing character of the soil. The same threshold of strain that determine degradation of stress-strain behaviour seem to apply for the effects of existing pore water pressures also.

An increase in the confining pressure in resonant column testing contributed to the increase in Gmax for 200 and 300 kPa total stress tests. However, the fact that there was essentially no increase from 200 kPa case to 300 kPa case indicated that the higher pore pressure ratio in the second case influenced the measurements. These findings pertaining to resonant column tests show that, the maximum dynamic shear modulus for soft clays is a strong function of

effective stress. [It is important to note that all of the specimens used in this study were consolidated under same effective stress and the excess pore water pressures were induced]. Dynamic moduli are influenced by total stress increase more than pore pressure increase below a threshold of shear strain amplitude, which is identified to be 10^{-5} for the specimens tested. It is only at high pore pressure ratios that measurable influence can be observed. These findings, however do not apply to strain dependent shear moduli due to fast degradation that starts at very low strains for soft clays.

Maximum static modulus, on the other hand, measured through slow monotonic loading is very sensitive to the state of excess pore water pressure for soft saturated clays.

Other parameters obtained from triaxial vane tests were the undrained shear strength, Su, and the undrained residual shear strength, Ru (see Table 4.5). Static maximum modulus values were normalized with the corresponding Su values. These ratios were also correlated with pore pressure ratios, and an hyperbolic curve was fit to data in the same manner as explained above. The data points, fitted curve, and the equation of the curve are given in Fig 4.26. The Gmax-s/Su at u_r=0.0 is approximated to be 112. This value is lower than the typical values cited in literature all of which were dynamic maximum shear modulus normalized by Su, a property determined through static tests.

Using the Su/P_p (P_p= effective preconsolidation pressure) vs PI relation of Skempton for normally consolidated soils, for PI of 30 and P_p value of 100 kPa, Su was estimated to be 22 kPa. Using another approach given by Anderson and Lukas (85), Su , approximated for consolidated undrained triaxial compression, was 27 kPa. An average value of 25 kPa was chosen. The average values of Su obtained from triaxial vane for confining pressures of 100, 200, and 300 kPa are 29, 36 and 36 kPa, respectively. The experimental value for the normally consolidated case (u_r = 0.0) is 16 % overestimated with respect to the empirical value of Su, 25 kPa. This is considered to be a small deviation and therefore the measured value is validated. The other two Su values displayed similar behaviour as the maximum dynamic shear moduli. They were not particularly influenced by the excess pore water pressures. This occurrence strongly suggests that due to low angular rotation rate of the vane there was some amount of localized pore water migration and partial drainage around the vane shear zone. Nevertheless, increase in Su was not substantial to suggest basic violation of the undrained conditions of the test. The invariance of Su with pore pressure ratio is illustrated in Fig. 4.27. It is normalized with Gmax-d for comparison with Fig.4.25.

Undrained residual shear strength, Ru was obtained by rotating the vane up to 90 degrees after maximum strength

was reached. Su and Ru are correlated in Fig 4.28. If the intercept parameter of the correlation equation is neglected, than slope of the straight line fitted to the data would directly represent Ru/Su ratio, which is 0.727. This value is higher than the value reported for San Fransisco bay mud of 0.42 (48). Good correlation of the data once again validates the repeatability of the testing procedure.

The yield stress and strain values obtained from the bilinear representation of the static stress-strain curves were used to assess two important correlations. Fig. 4.29 shows the variation of Gmax ratio with yield strain. Yield strain increases with decreasing moduli ratio. This occurrence confirms the highly nonlinear behaviour of soft clays. Variation of G with yield strain provides useful information that can be used in limit analysis and numerical analysis techniques. A theoretical curve was not fit to this data.

Yield stress was correlated with undrained shear strength as shown in Fig. 4.30. Data showed consistent behaviour. This variation is significant in the sense that useful information can be extracted for use in numerical analysis techniques. The scatter of data both in yield strain and yield stress correlations are due to the fact that determination of these factors involves the investigator interactively in program OPAUX3, consequently operator judgement or error becomes an inherent factor.

Nevertheless, larger number of data collection and increased expertise should certainly help to narrow down the band of scatter.

4.2 GENERAL DISCUSSION OF RESULTS

Degradation of soil shear moduli with cyclic loading is an important factor to consider when measuring low stress-strain properties of soft saturated clays using dynamic testing methods. Degradation starts at low shear strain amplitudes and interferes with determination of the "true" backbone curve in these soils. As illustrated in Figs. 4.2 - 4.9, for the normally consolidated duplicate specimens, the dynamic moduli reduction curve crosses over the static curve at a threshold strain amplitude, and continues reduction with a faster gradient. Using this information a schematic diagram illustrating static stress-strain behaviour and degraded dynamic stress-strain behavior with the superimposed hypothetical first cycle dynamic stress-strain curve (backbone curve) are produced in Fig. 4.31. Two shear strain locations γ_d, γ_c are identified on the diagram. Shear strain amplitude γ_d, marks the location where the distance between the static curve and the degraded dynamic curve is the longest before crossover point. It is the first threshold shear strain amplitude where deviation of the experimental dynamic curve from the theoretical backbone curve starts. Shear strain amplitude γ_c, is the second threshold value at which the degraded dynamic curve crosses

over and stays below the static curve thereafter. Tests of normally consolidated specimens (VT1-RT1) revealed γ_c value to lie between 10^{-5} and 10^{-4} .

The observations discussed above are important to investigators who are involved in low strain limit design problems in soft soils. In order to develop a comprehensive theory of low stress-strain behaviour of soft saturated clays both under cyclic loading and monotonic loading, one has to undertake an extensive experimentation program collecting a large number of quality data. In the absence of large number of data, modelling techniques work as well provided that realistic parameters are used. One such study conducted by Prevost (56) on soft saturated clays, reveals information (see Chapter 2), which further strengthens the main claim of this study, which is the need to assess low strain static shear stress-strain behaviour of soft clays to be able to define realistic design parameters. A schematic diagram of hypothetical first cyle dynamic curve , static curve and a typical hysteresis loop representing cycle $N=N_1$, at constant shear strain amplitude, γ_1, is shown in Fig 4.32. The experimental and numerical findings of Prevost study show that, the gradient at the tip of the hysteresis loop at any cycle is equal to the gradient (tangent modulus) on the static curve at the particular strain amplitude, γ_1. Therefore, in order to understand hysteresis behaviour of soft clays under controlled loading conditions, using a

low strain static curve would produce more realistic information than a degraded cyclic curve. Since soft saturated clays will exhibit degradation under cyclic loading even at the lowest shear strain amplitudes generally possible to measure, and influence shear stress-strain curve substantially, the best solution seems to utilize an alternative testing method. This study proposes and tests a method which produces good results by eliminating problems in association with cyclic loading.

Another outcome of the method discussed herein is that highly detailed data could be collected. The enlarged view of the initial portion of a typical shear stress-strain curve given in Fig. 3.19a illustrates this effect. The nonlinear nature of the relation is evident even within the low strain range of 10^{-5}. The fine detail in the stress-strain curve shown in Fig. 3.19a indicate micro structure changes occurring within soil matrix even at the low shear strains applied. The perturbation of the stress-strain curve may be attributed to stress relaxation or phase transformations. This observation suggests a new area of research on soil shear behaviour using the testing method proposed in this study.

The significant components of this study which makes it original as well as beneficial can be summarized as follows:

1. A semi-computer aided experiment was designed and implemented utilizing state-of-art instrumentation.

2. Data obtained using the new system showed significant improvement with respect to scope and detail when compared to data obtained through conventional testing methods.
3. Analysis of the results revealed important findings pertaining to low strain properties of soft saturated clays.
4. The system designed and tested herein can be used to research various concerns in low shear strain range and also with different soils, including cemented clays.

The results presented in this section should be reviewed with the provision that the testing method utilized to obtain these results was a new method in the respective area. Therefore, direct comparison of the low strain results to that of other static tests could not be made. However, correlations were made with respect to dynamic test data. Low stress-strain behaviour proves to be consistent with the anticipated and widely reported highly-nonlinear behaviour of soft clays. The accuracy of static data obtained using the new method is as satisfactory, if not better than, the accuracy of the dynamic data obtained using an established equipment and method (see Table 4.1). In the light of these observations, the new method of testing can safely be claimed to produce realistic, accurate and repeatable data. Moreover, with the elimination of the effects of cyclic

degradation due to dynamic pore pressure buildup, and stress reversal in all dynamic laboratory tests, this testing method proves to be a valuable research tool in lowstrain analysis of soft saturated clays and may as well become one for other types fine grained soils .

No. of Duplicate Specimens	Mean Effective Stress,kPa	Mean Total Stress,kPa	STATIC TESTS (VT SERIES) Average Gmax,kPa	Standard Deviation	Confidence Interval α=0.02	DYNAMIC TESTS (RT SERIES) Average Gmax,kPa	Standard Deviation	Confidence Interval α=0.02
8	100	100	2533	509	2533+360	3884	561	3884+396
10	100	200	1786	306	1786+194	5210	714	5210+450
5	100	300	898	213	898+244	5156	705	5156+630

Table 4.1 Statistical analysis of Gmax values for three sets of data

	STATIC TESTS (VT series)			DYNAMIC TESTS (RT series)		
	Water Content,%		Bulk Density	Water Content,%		Bulk Density
Test No	Initial	Final	kN/m³	Initial	Final	kN/m³
1-1	62.73	58.87	16.02	62.90	55.10	16.15
1-2	65.73	59.62	16.53	66.08	58.71	15.91
1-3	64.20	60.04	16.30	65.10	57.17	16.55
1-4	64.54	59.44	16.28	64.30	57.25	16.62
1-5	62.22	58.44	16.56	61.00	56.91	16.66
1-6	63.70	58.54	16.28	63.70	55.89	16.78
1-7	60.76	60.41	16.34	59.23	58.42	16.63
1-8	60.21	57.08	16.50	59.31	54.51	17.10
2-1	60.64	52.33	16.24	62.03	53.11	16.85
2-2	59.48	-	-	59.48	54.02	16.23
2-3	58.81	56.22	16.42	58.81	54.19	16.35
2-4	65.20	56.05	16.92	65.65	56.81	17.21
2-5	66.30	61.80	15.98	65.20	55.36	16.61
2-6	65.41	60.10	16.37	64.13	53.68	16.69
2-7	64.76	57.99	16.60	64.58	52.47	16.57
2-8	64.51	60.04	16.24	63.79	52.59	16.85
2-9	64.31	58.94	16.36	65.10	52.28	16.44
2-10	65.39	56.85	16.67	63.63	53.05	16.85
3-1	58.20	52.17	16.70	56.57	49.66	16.66
3-2	65.96	55.26	16.36	66.19	53.20	16.54
3-3	65.23	60.69	16.17	65.46	54.59	16.44
3-4	58.45	59.15	16.42	60.58	53.43	16.67
3-5	64.79	59.49	16.25	64.93	52.54	16.97

Table4.2 Index Properties of Static and Dynamic Test Specimens

Table 4.3 Low strain parameters estimated in triaxial vane tests, and statistical information pertaining to determination of Gmax from OPAUX3

Test No	Gmax kPa	Min.Strain Measured,%	γ_{yield} %	τ_{yield} kPa	Standard Deviation	Test of Fit (r^2)
VT11	2709	2.7E-4	5.3E-2	1.44	0.0087	0.8440
VT12	2887	4.7E-4	5.9E-2	1.71	0.0089	0.5270
VT13	2382	2.8E-4	3.8E-2	0.9	0.0120	0.9410
VT14	1965	2.7E-4	5.8E-2	1.15	0.0066	0.9035
VT15	2032	5.9E-4	308E-2	0.80	0.0190	0.8469
VT16	3581	3.8E-4	3.2E-2	1.15	0.0551	0.4990
VT17	2073	2.8E-4	1.0E-2	2.13	0.0937	0.5154
VT18	2635	3.5E-4	4.7E-2	1.25	0.0372	0.3865
VT21	1310	706E-4	1.8E-1	2.41	0.0290	0.8740
VT22	2171	5.1E-4	1.2E-1	2.65	0.0186	0.9138
VT23	1408	3.8E-4	2.7E-1	3.86	0.0164	0.8641
VT24	1488	1.1E-4	1.6E-1	2.86	0.0164	0.8641
VT25	1959	2.4E-4	7.5E-2	1.47	0.0106	0.9591
VT26	1891	2.9E-4	1.7E-1	3.22	0.0156	0.8857
VT27	1965	2.8E-4	1.1E-1	2.25	0.0052	0.9879
VT28	2274	2.7E-4	6.3E-2	1.44	0.0152	0.9259
VT29	1681	2.5E-4	1.9E-1	3.15	0.0055	0.9856
VT210	1713	3.5E-4	5.8E-2	1.68	0.0124	0.9595
VT31	763	3.1E-4	2.0E-1	1.58	0.0078	0.9951
VT32	800	5.2E-4	4.0E-1	3.30	0.0032	0.9986
VT33	1268	6.3E-4	1.1E-1	1.36	0.0149	0.9720
VT34	1146	5.4E-4	5.5E-2	0.67	0.0169	0.9338
VT35	514	2.5E-4	1.2E-1	0.66	0.0050	0.9787

Table 4.4 Maximum shear moduli obtained from dynamic tests and the statistical parameters pertaining to the hyperbolic line fit to the data

Test No	Gmax kPa	Min.Strain Measured,%	Standard Deviation	Test of Fit (r^2)
RT11	3102	6.5 E-4	0.775E-8	0.8896
RT12	3874	4.5 E-4	0.362E-8	0.1062
RT13	3998	8.3 E-4	0.205E-7	0.5415
RT14	3650	7.2 E-4	0.505E-8	0.3680
RT15	3131	7.6 E-4	0.402E-8	0.0011
RT16	4337	6.7 E-4	0.232E-8	0.2370
RT17	4083	5.5 E-4	0.185E-7	0.0052
RT18	3998	5.5 E-4	0.205E-7	0.5415
RT21	5928	6.5 E-4	0.476E-8	0.4325
RT22	5945	4.9 E-4	0.568E-8	0.0073
RT23	5643	7.2 E-4	0.243E-8	0.1231
RT24	6264	3.4 E-3	0.341E-8	0.2807
RT25	4814	6.4 E-4	0.379E-7	0.3350
RT25	4814	6.4 E-4	0.379E-7	0.3350
RT26	4758	5.8 E-4	0.547E-8	0.8187
RT27	4831	5.9 E-4	0.330E-8	0.0045
RT28	5402	4.9 E-3	0.175E-6	0.2365
RT29	4702	1.6 E-3	0.984E-7	0.2153
RT210	3812	4.1 E-4	0.238E-7	0.1544
RT31	5986	3.8 E-4	0.133E-6	0.4328
RT32	4702	9.7 E-4	0.154E-6	0.4195
RT33	5960	3.5 E-3	0.179E-7	0.5127
RT34	4911	4.1 E-4	0.880E-8	0.4380
RT35	4218	5.6 E-4	0.450E-8	0.4594

Table 4.5 The undrained shear strength (=Su) and undrained residual shear strength (=Ru) values obtained from triaxial vane tests

Test No	Su (kPa)	Ru (kPa)
VT11	28.30	24.47
VT12	25.03	20.80
VT13	29.75	24.80
VT14	23.59	19.93
VT15	31.31	25.57
VT16	34.02	26.48
VT17	32.46	25.60
VT18	28.07	20.20
VT21	-	-
VT22	-	-
VT23	42.09	33.36
VT24	46.27	33.10
VT25	27.72	20.88
VT26	24.50	21.36
VT27	34.69	27.37
VT28	35.26	25.34
VT29	36.69	28.71
VT210	39.77	26.77
VT31	-	-
VT32	-	-
VT33	30.45	29.18
VT34	34.56	31.23
VT35	42.23	34.76

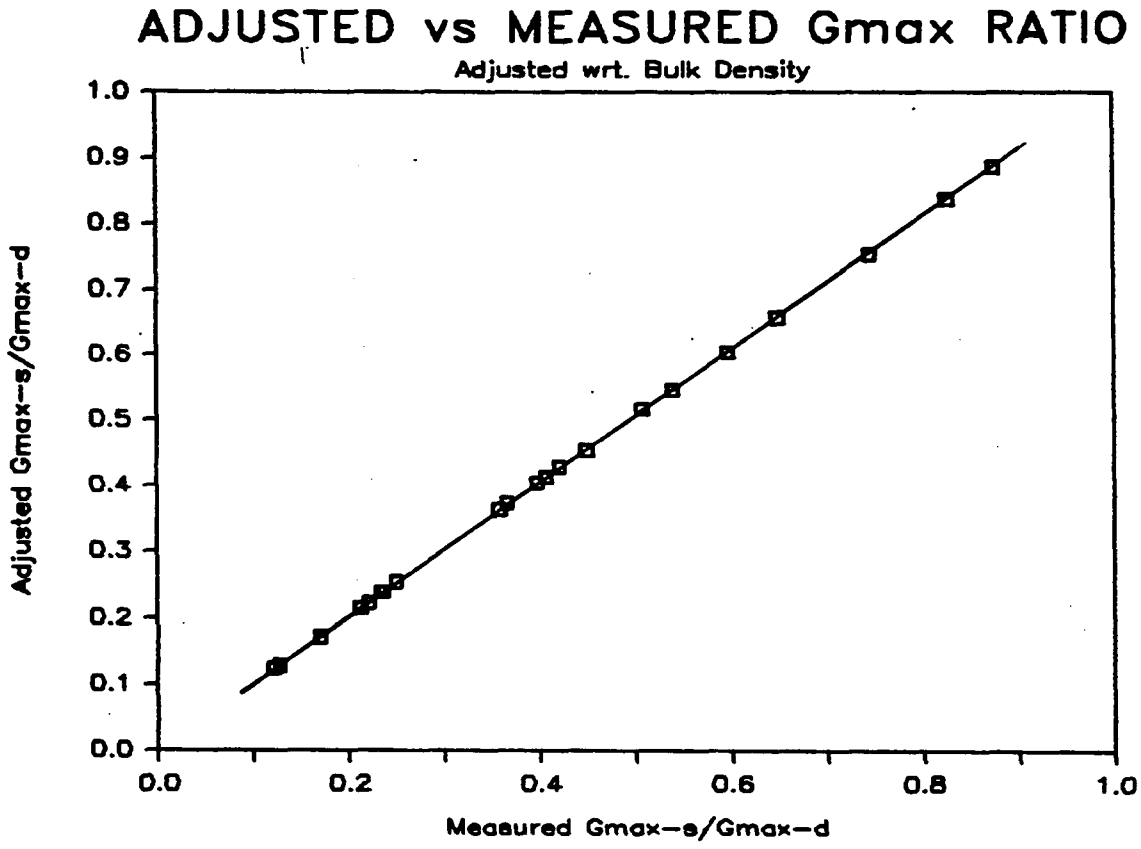

Fig. 4.1 Adjusted versus measured Gmax-s/Gmax-d ratios

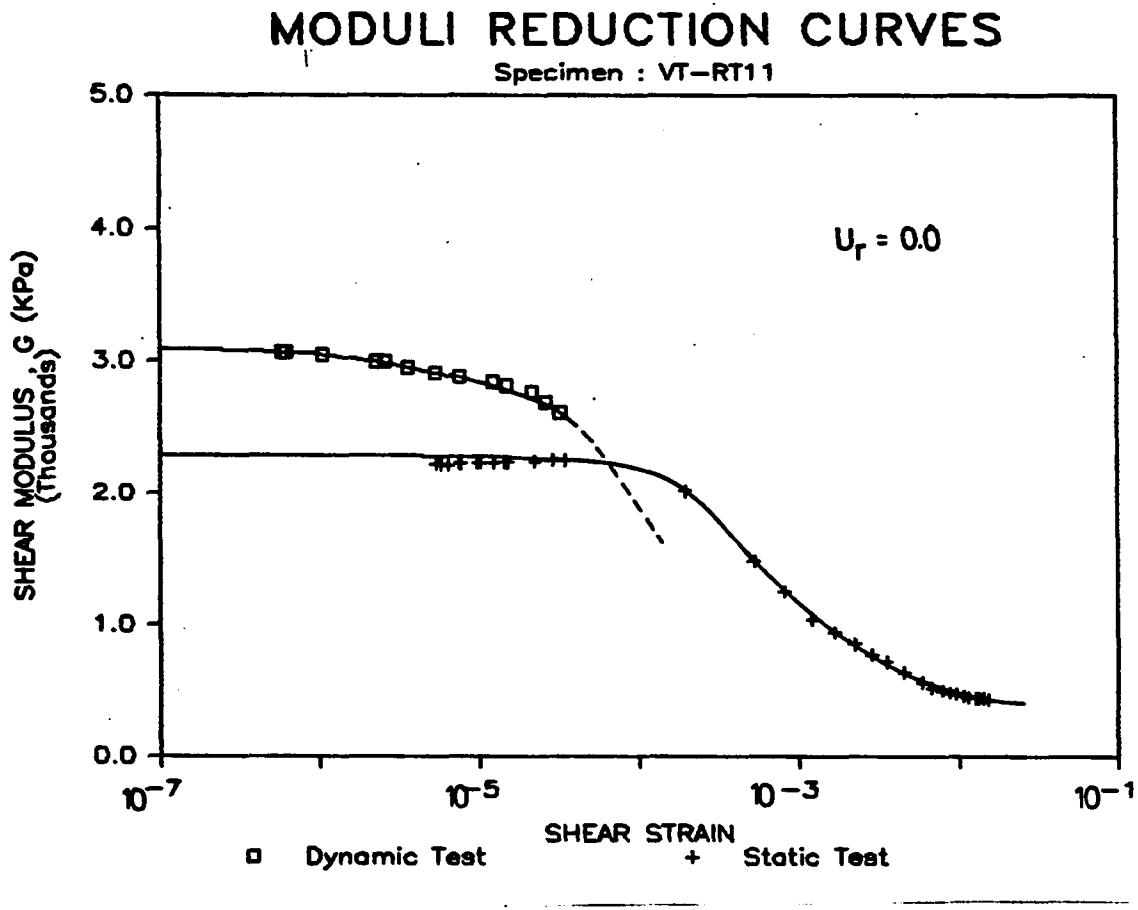

Fig. 4.2 Dynamic and static moduli reduction curves compared VT-RT11

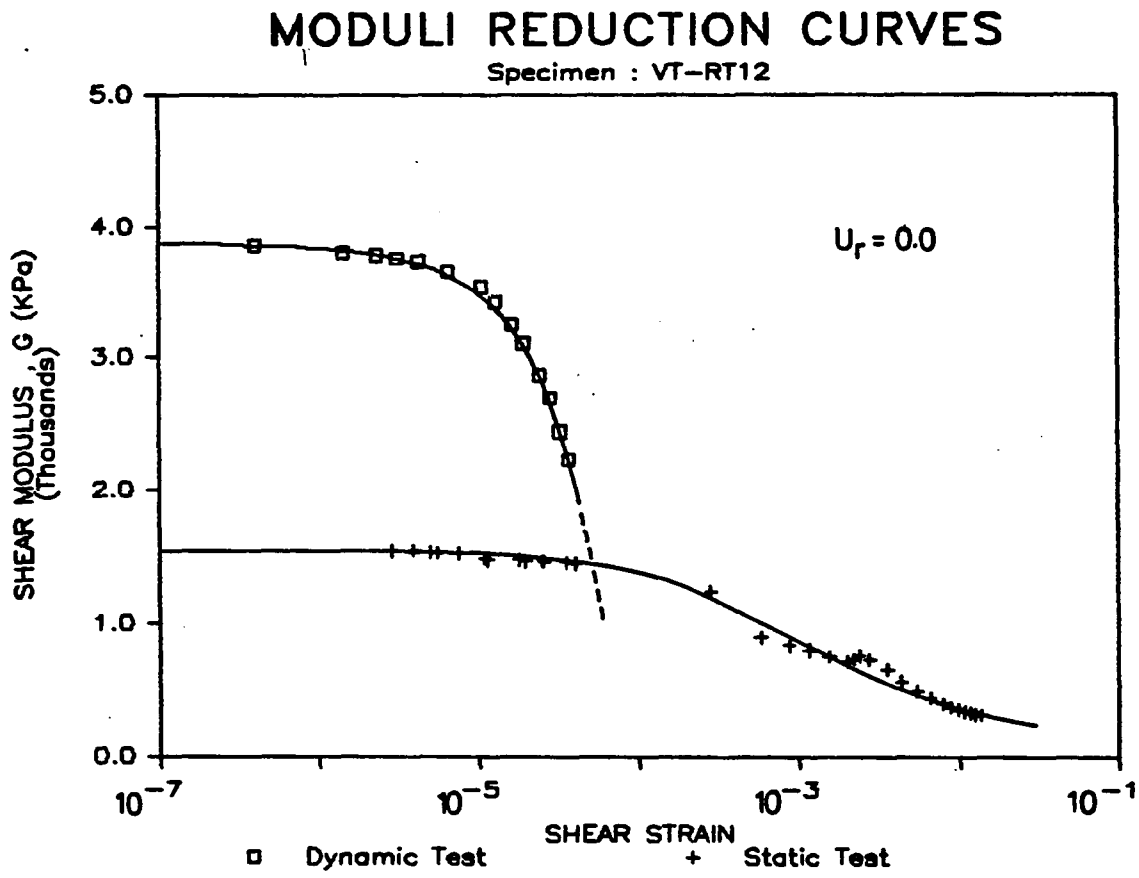

Fig. 4.3 Dynamic and static moduli reduction curves compared VT-RT12

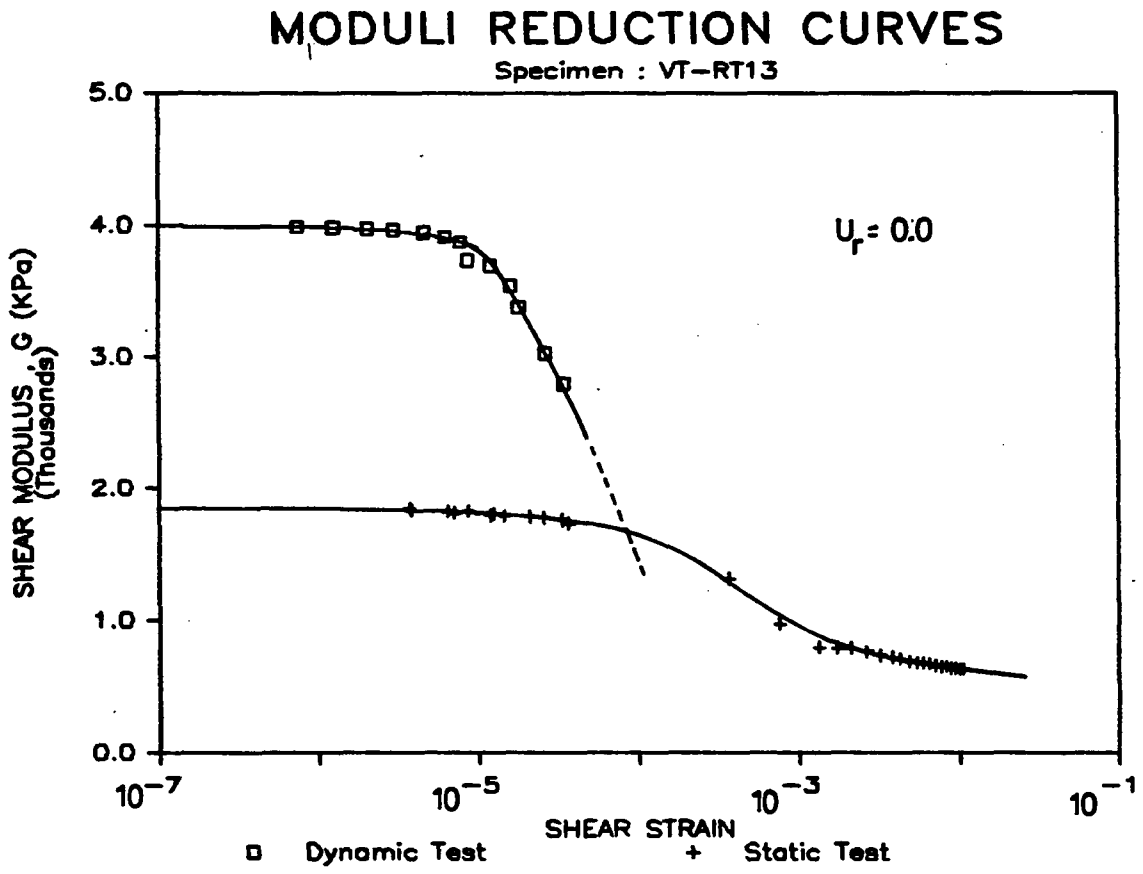

Fig. 4.4 Dynamic and static moduli reduction curves compared VT-RT13

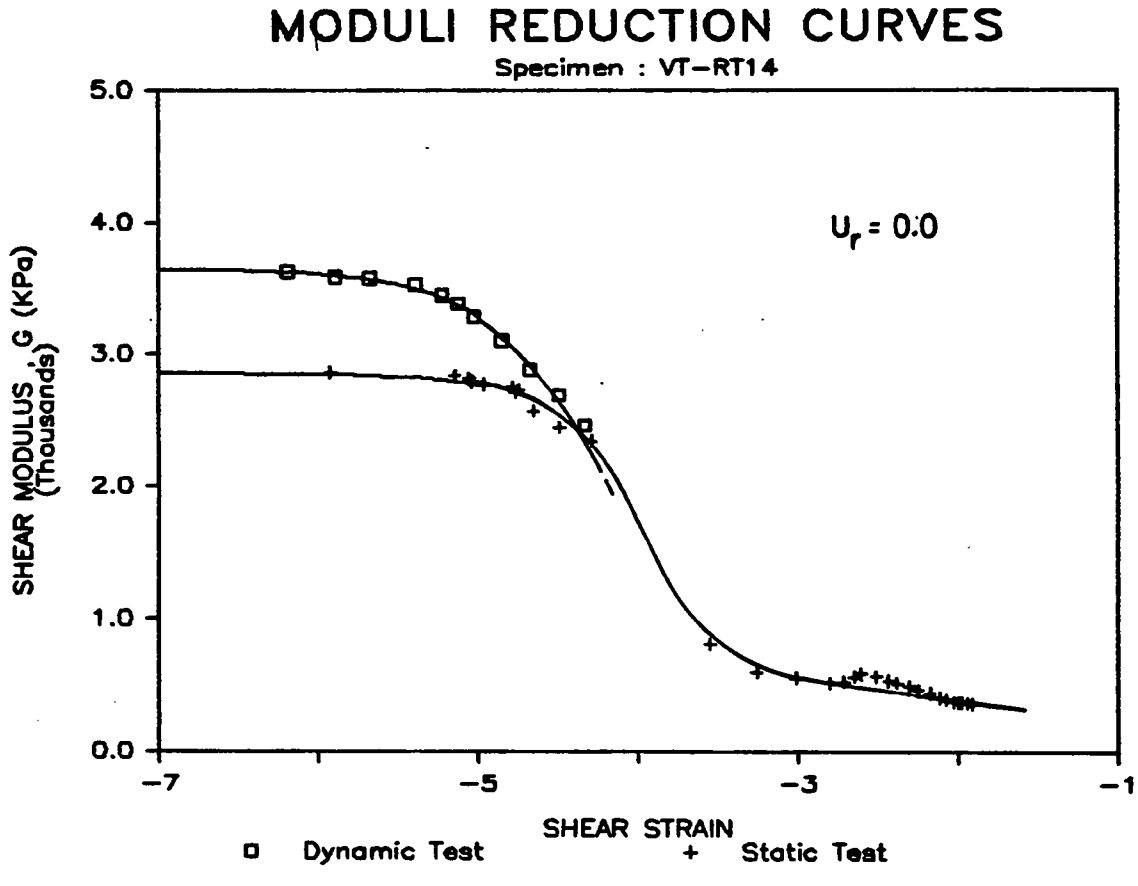

Fig. 4.5 Dynamic and static moduli reduction curves compared VT-RT14

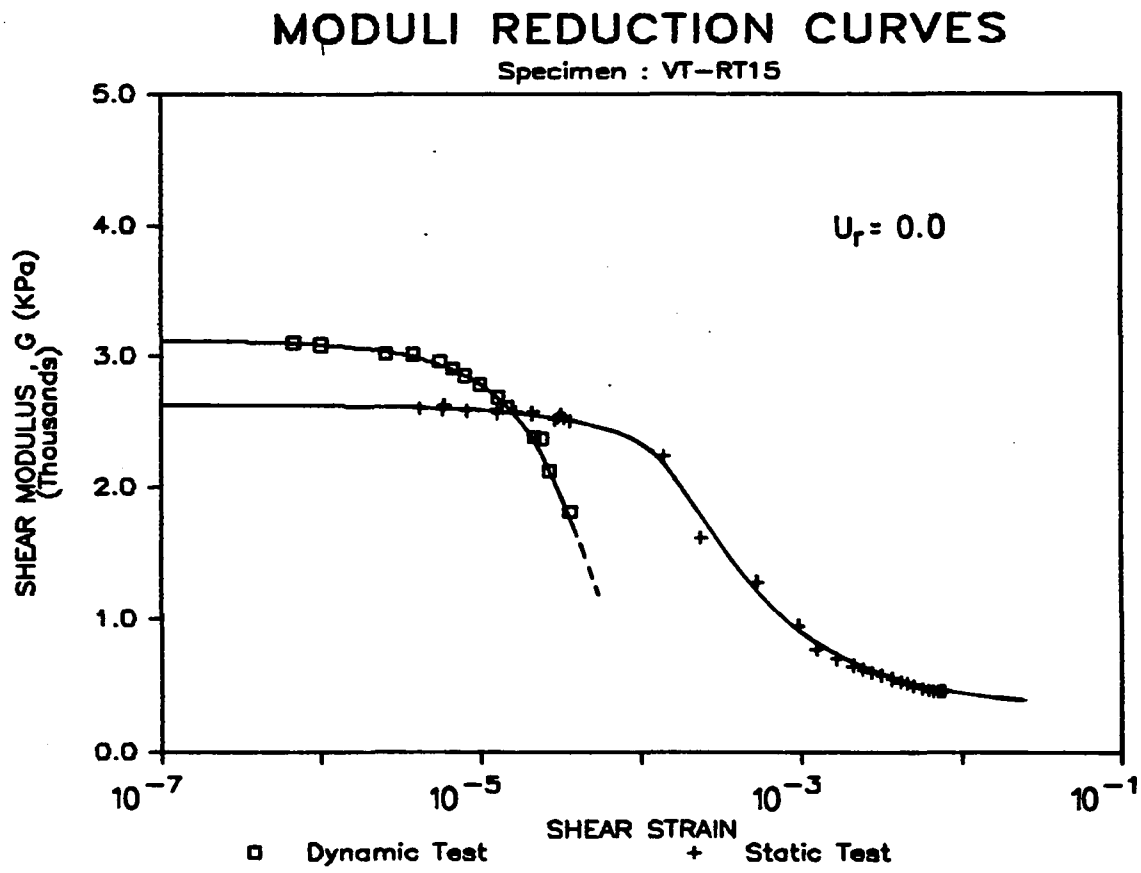

Fig. 4.6 Dynamic and static moduli reduction curves compared VT-RT15

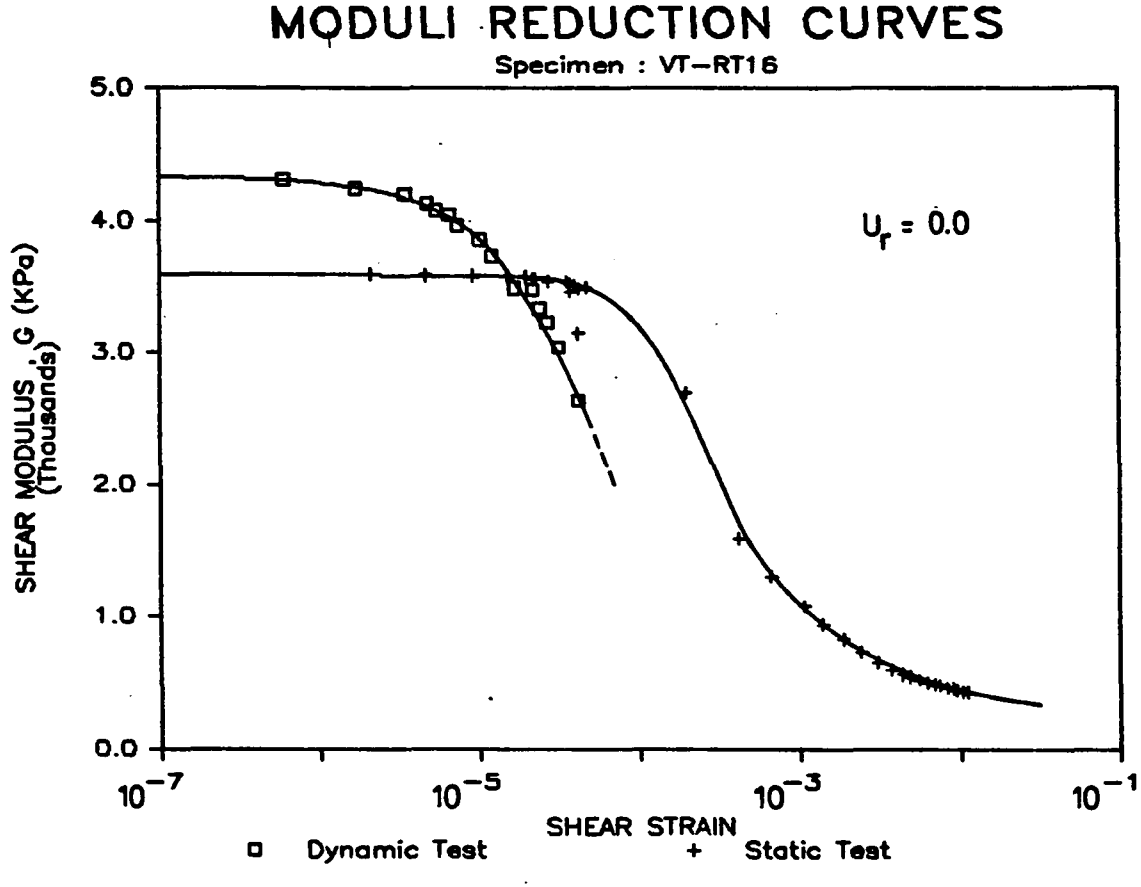

Fig. 4.7 Dynamic and static moduli reduction curves compared VT-RT16

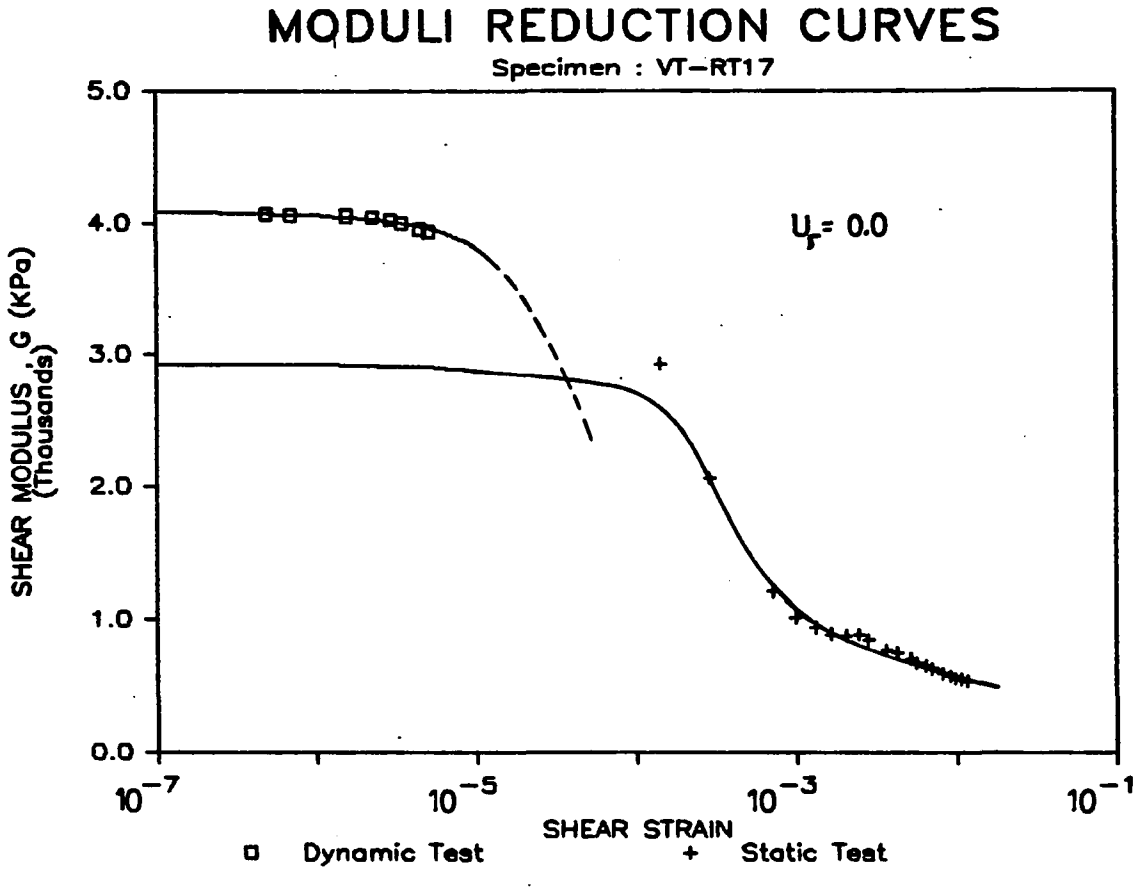

Fig. 4.8 Dynamic and static moduli reduction curves compared VT-RT17

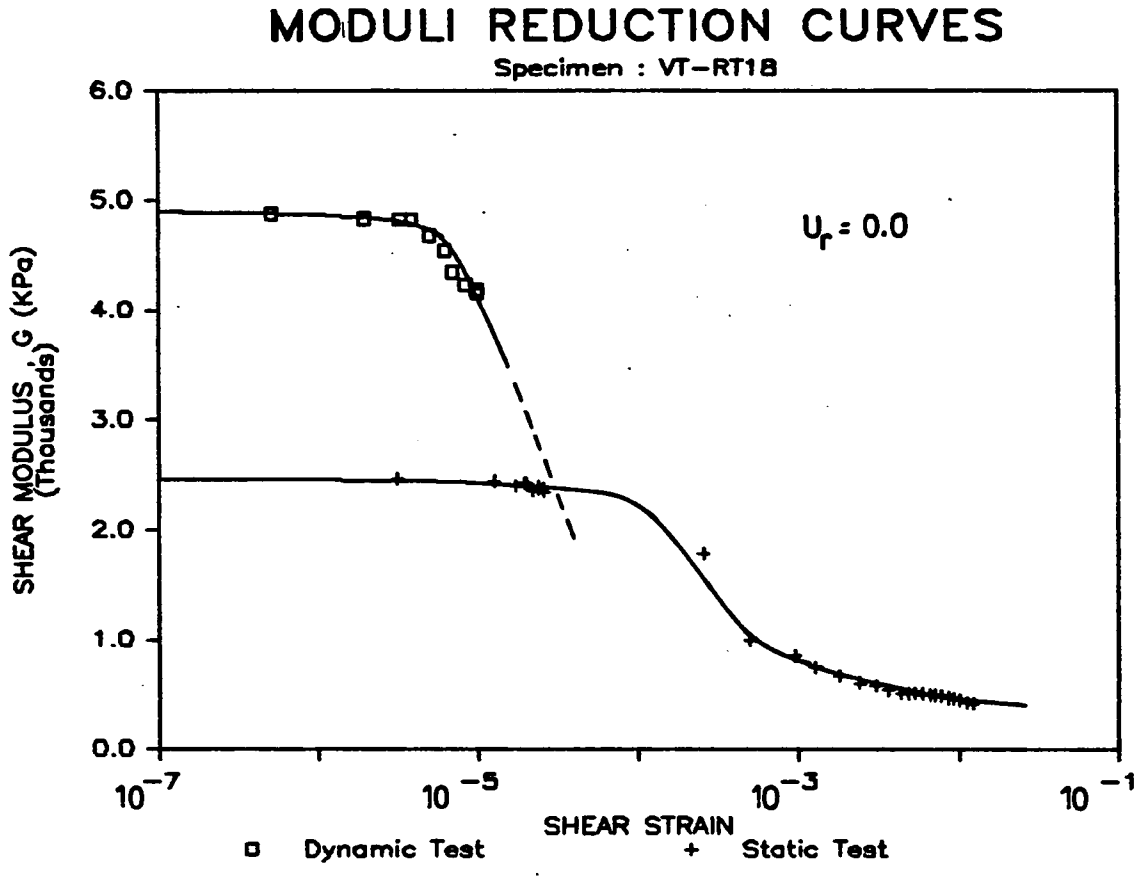

Fig. 4.9 Dynamic and static moduli reduction curves compared VT-RT18

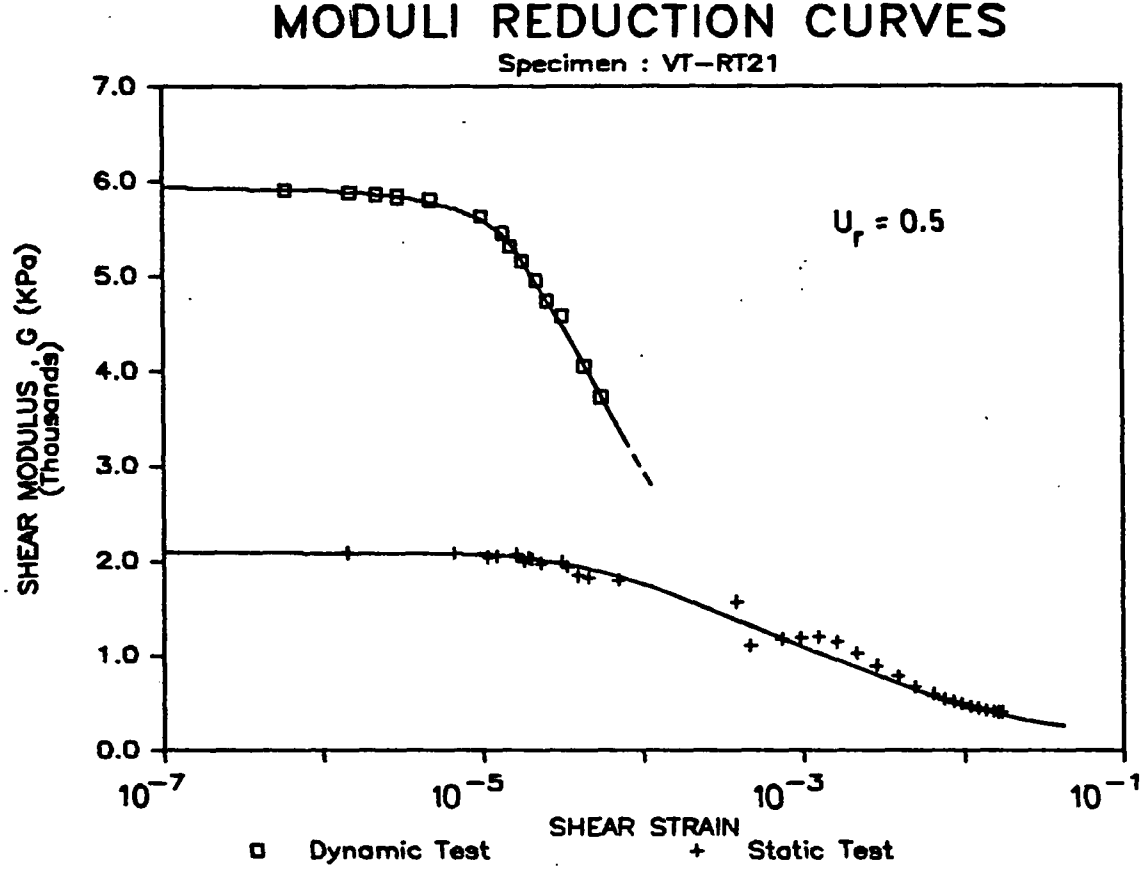

Fig. 4.10 Dynamic and static moduli reduction curves compared VT-RT21

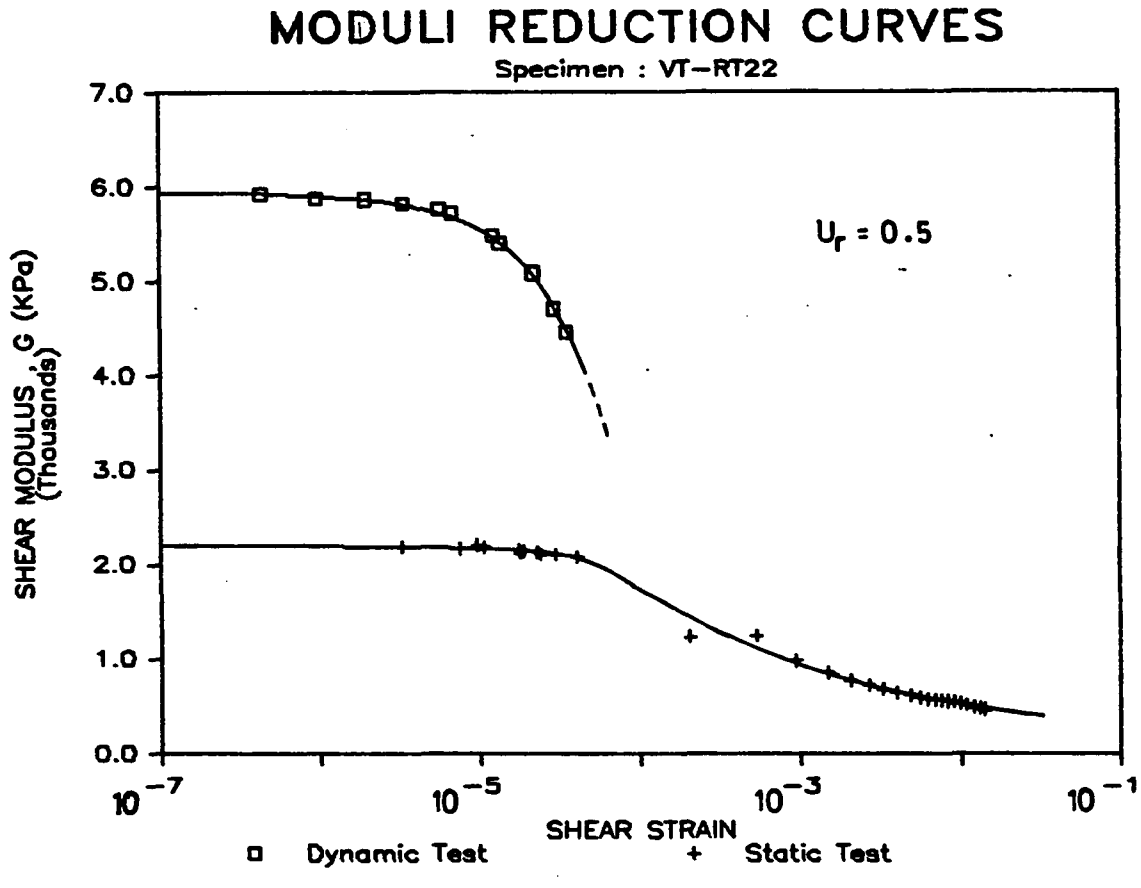

Fig. 4.11 Dynamic and static moduli reduction curves compared VT-RT22

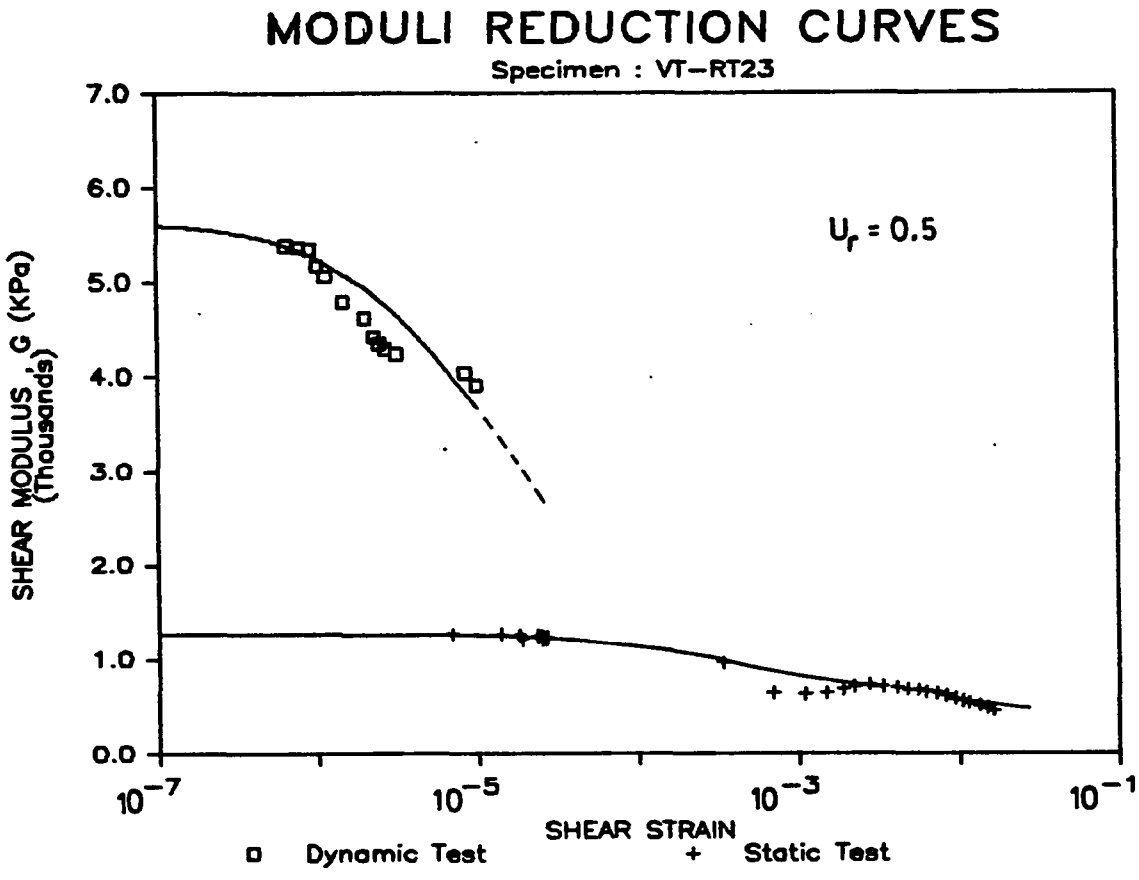

Fig. 4.12 Dynamic and static moduli reduction curves compared VT-RT23

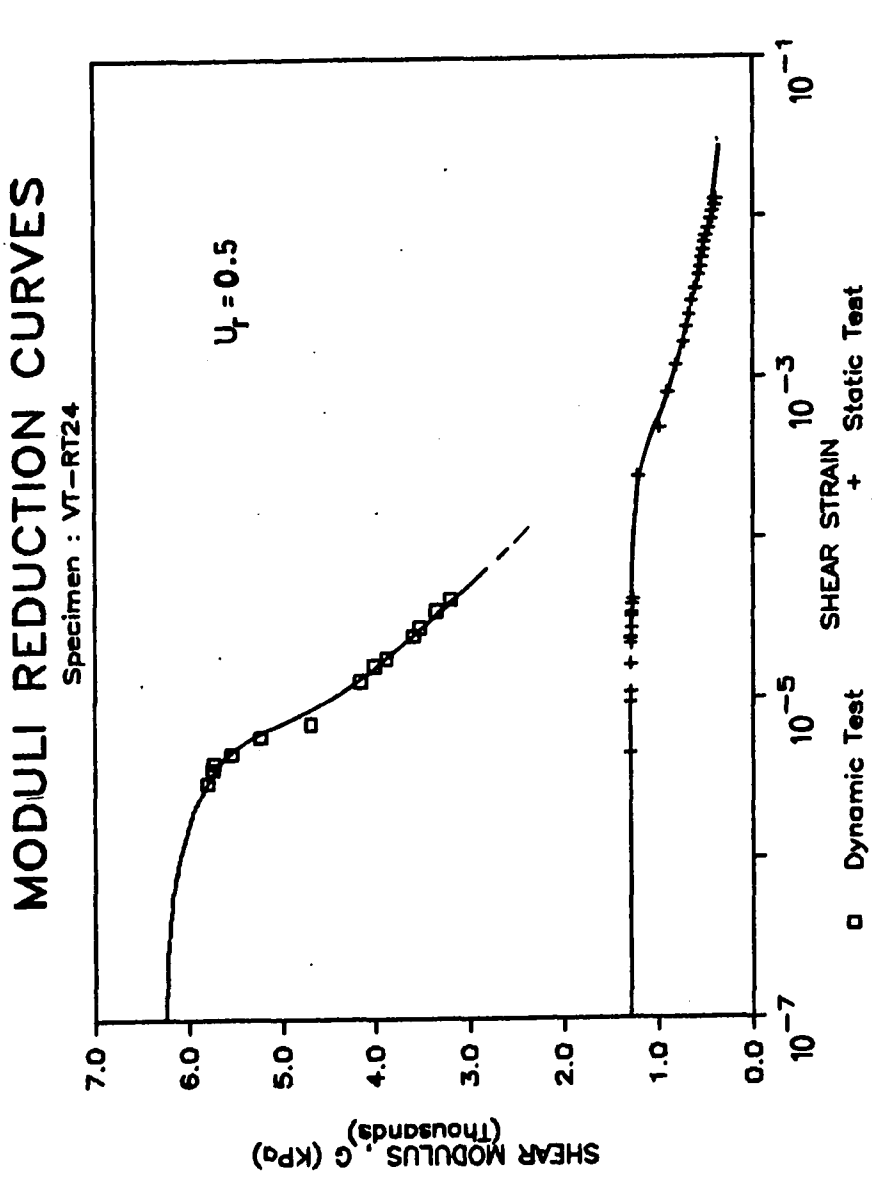

Fig. 4.13 Dynamic and static moduli reduction curves compared VT-RT24

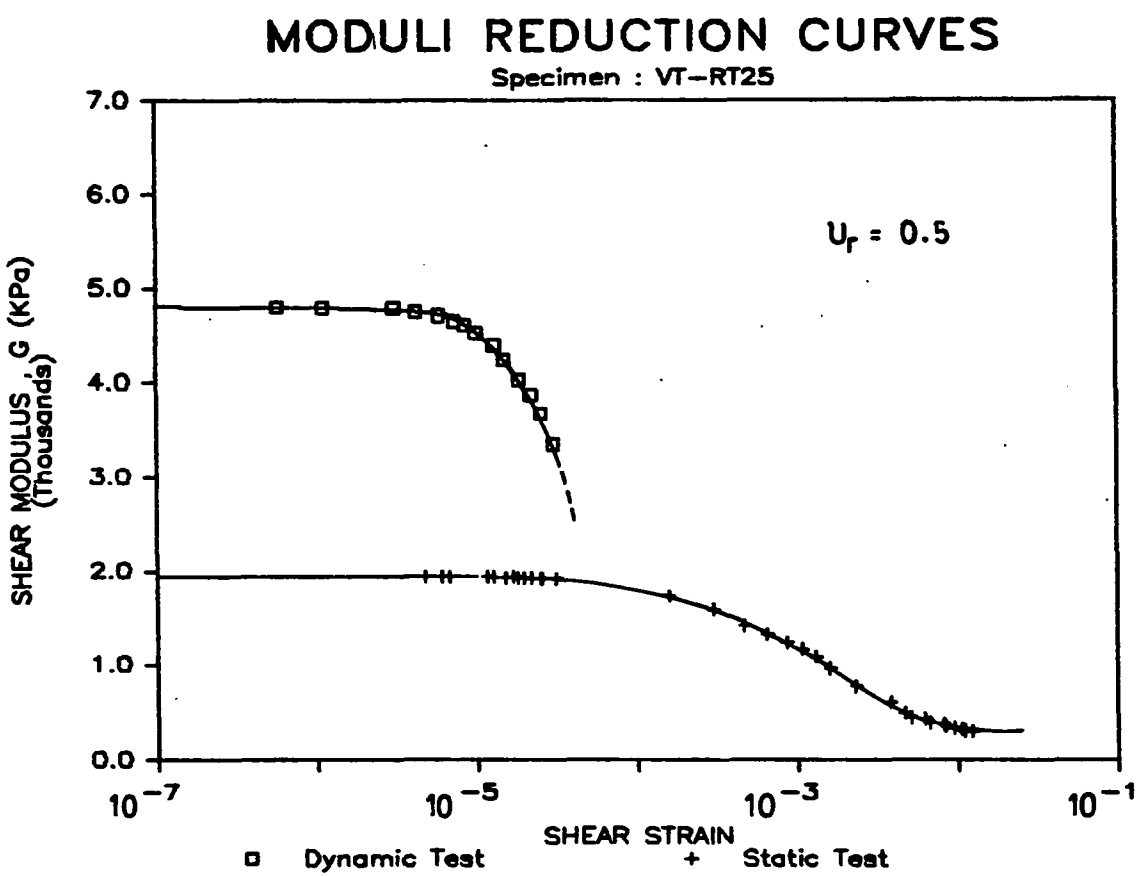

Fig. 4.14 Dynamic and static moduli reduction curves compared VT-RT25

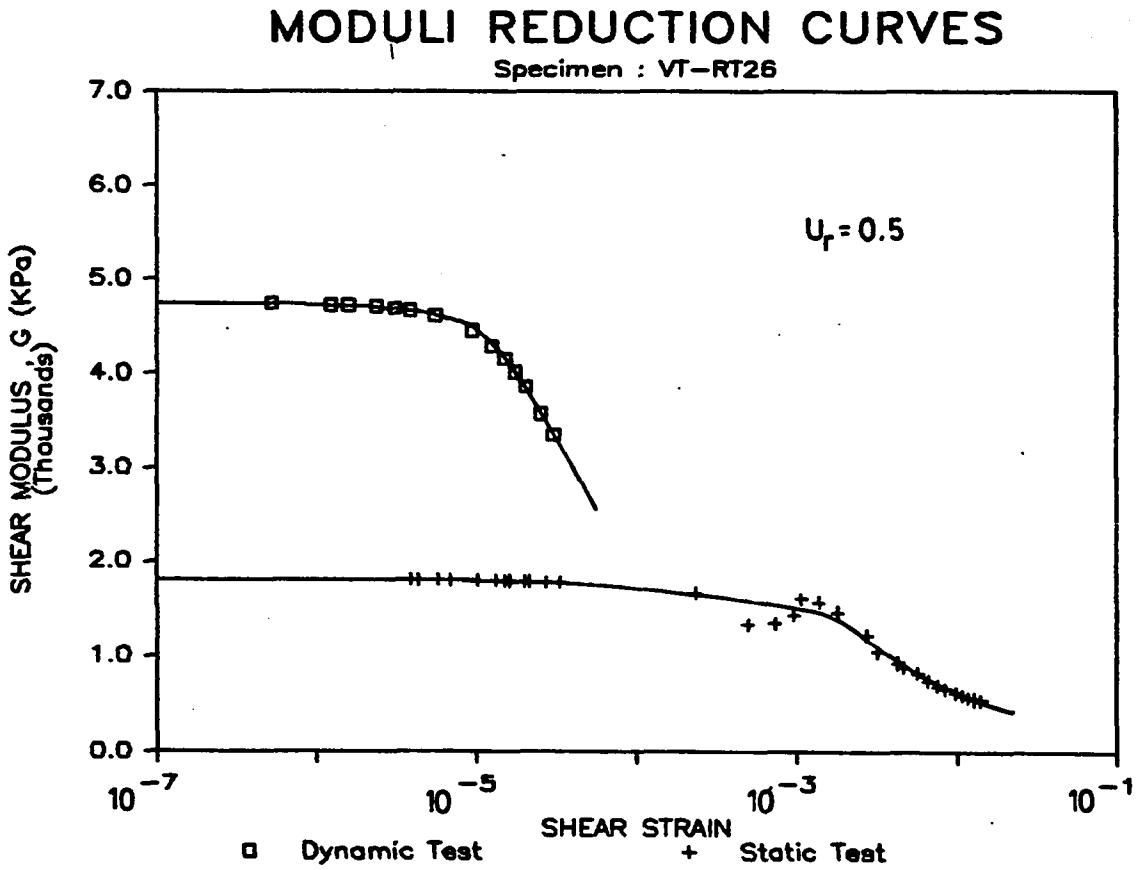

Fig. 4.15 Dynamic and static moduli reduction curves compared VT-RT26

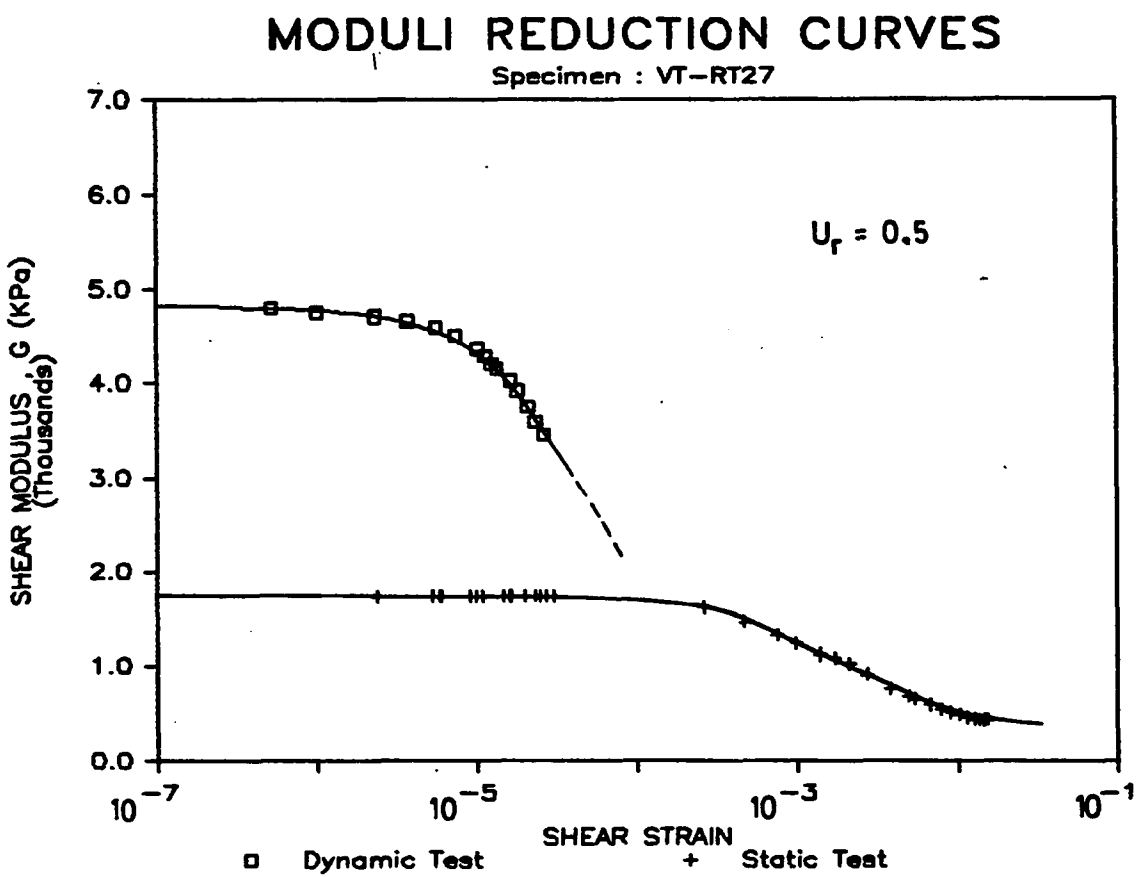

Fig. 4.16 Dynamic and static moduli reduction curves compared VT-RT27

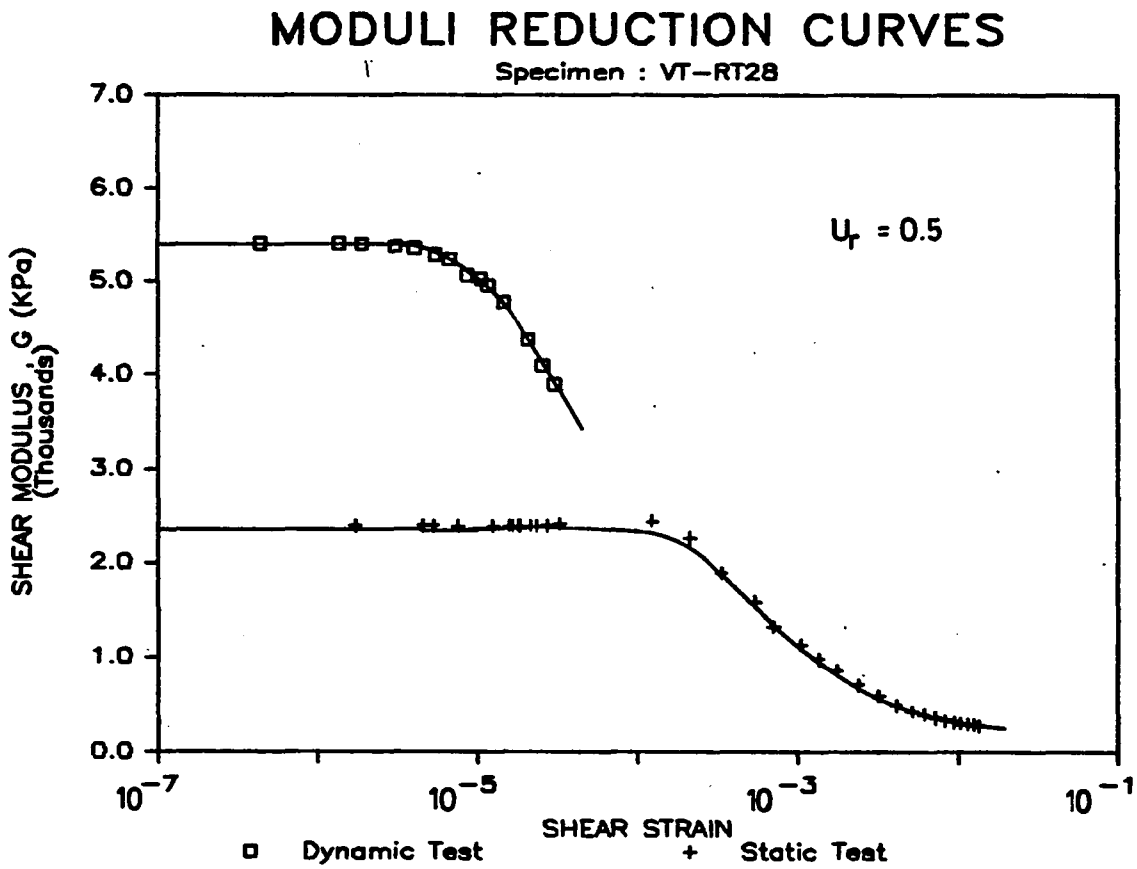

Fig. 4.17 Dynamic and static moduli reduction curves compared VT-RT28

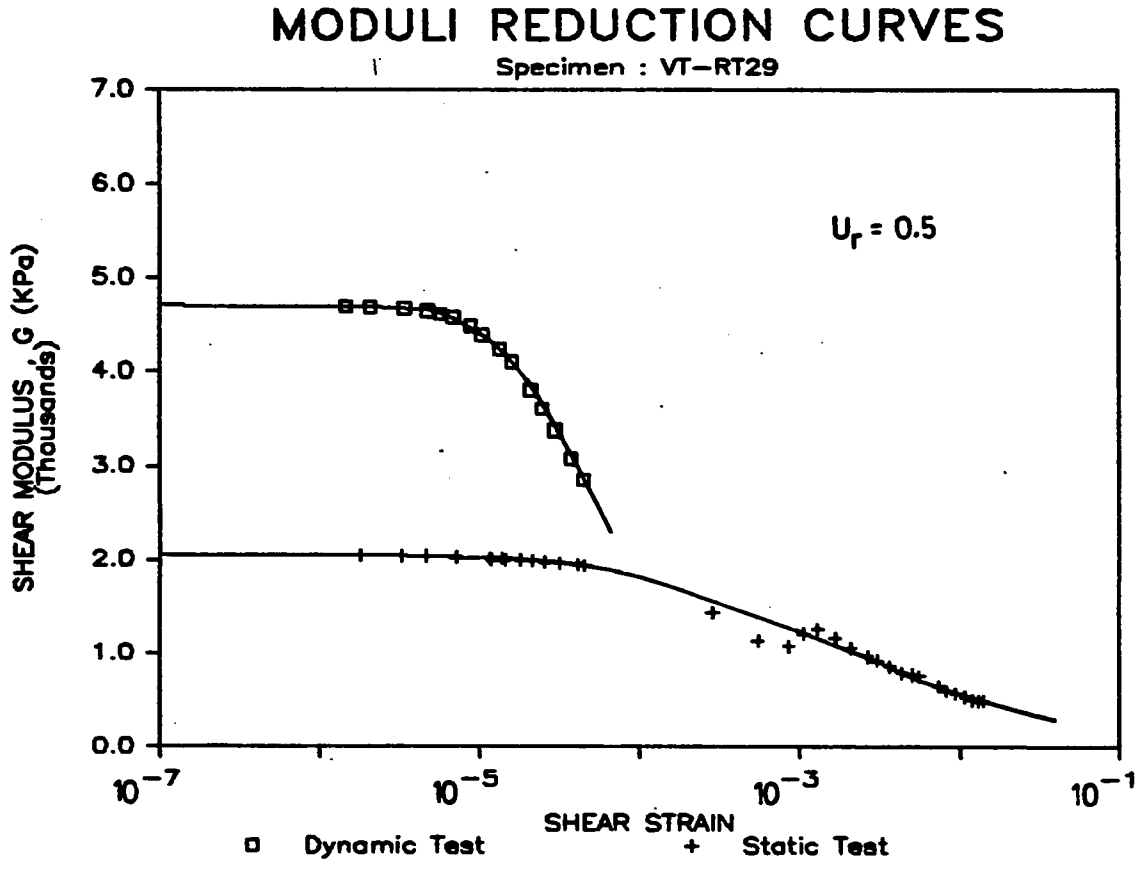

Fig. 4.18 Dynamic and static moduli reduction curves compared VT-RT29

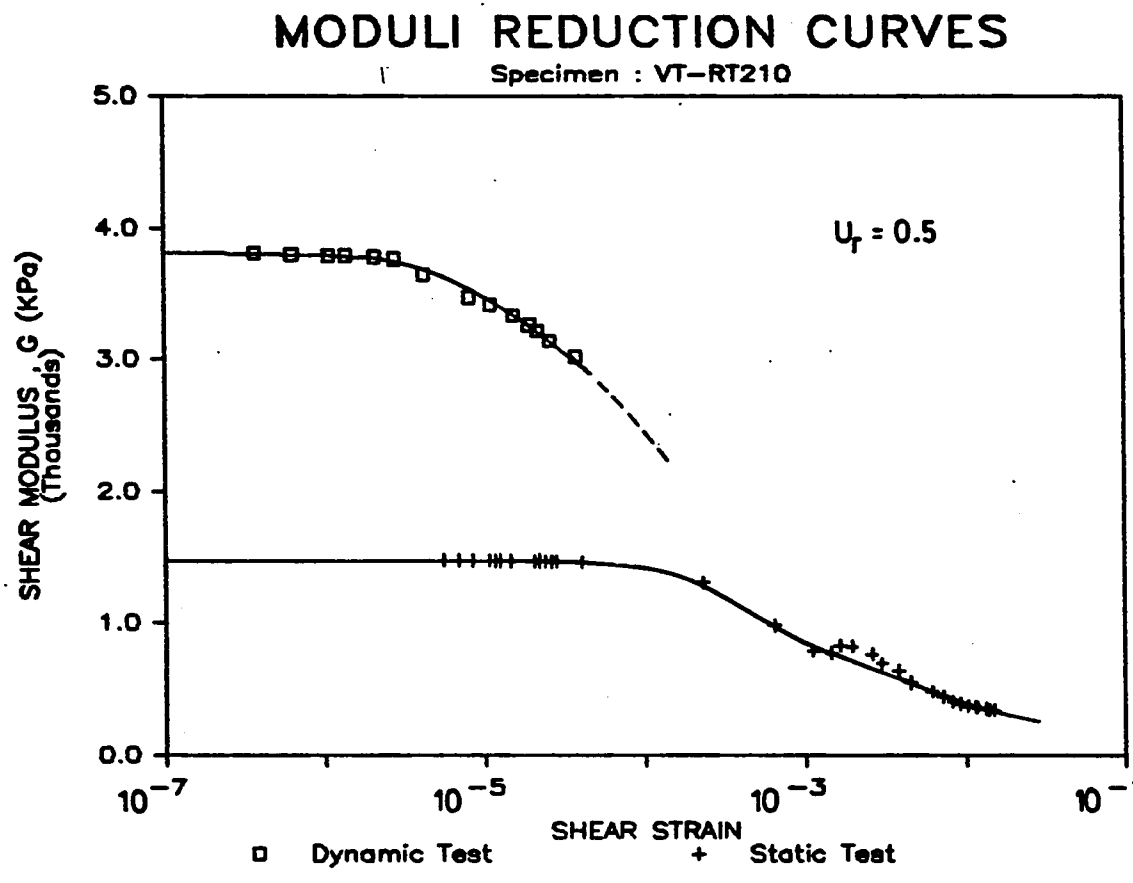

Fig. 4.19 Dynamic and static moduli reduction curves compared VT-RT210

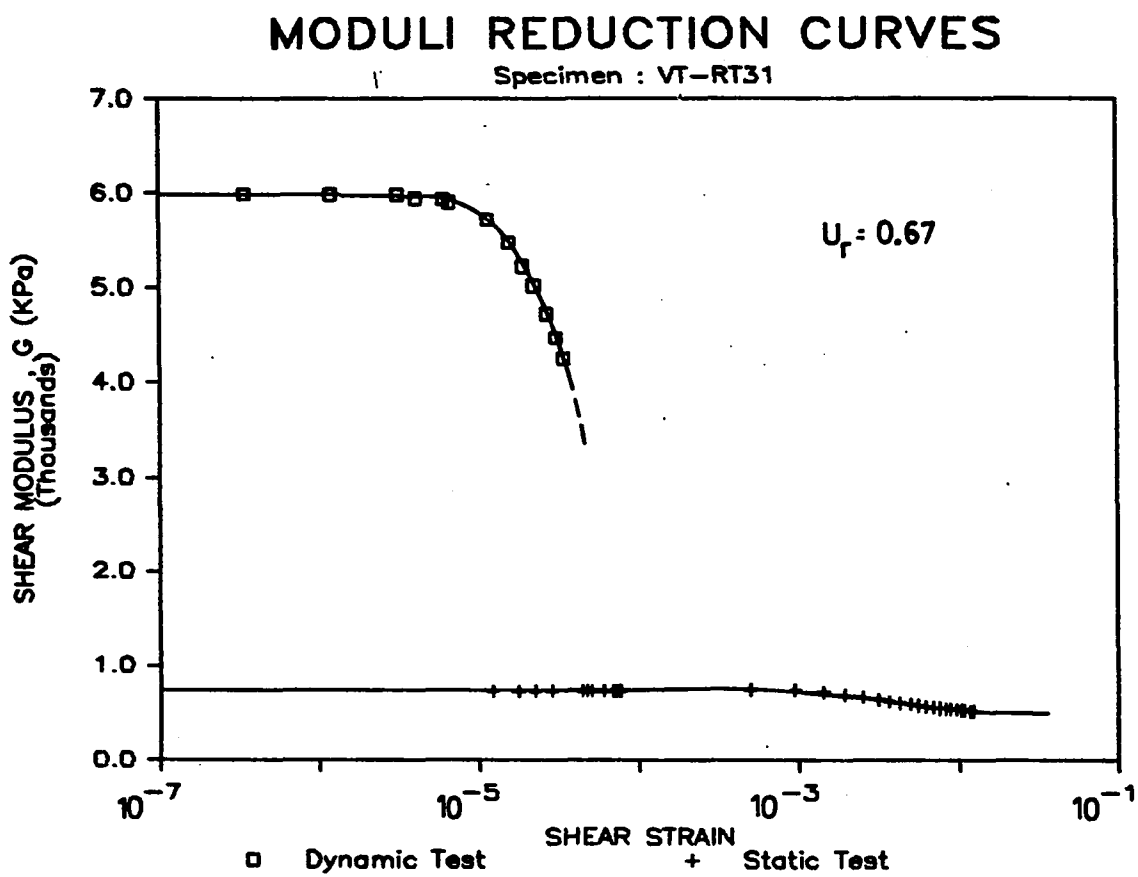

Fig. 4.20 Dynamic and static moduli reduction curves compared VT-RT31

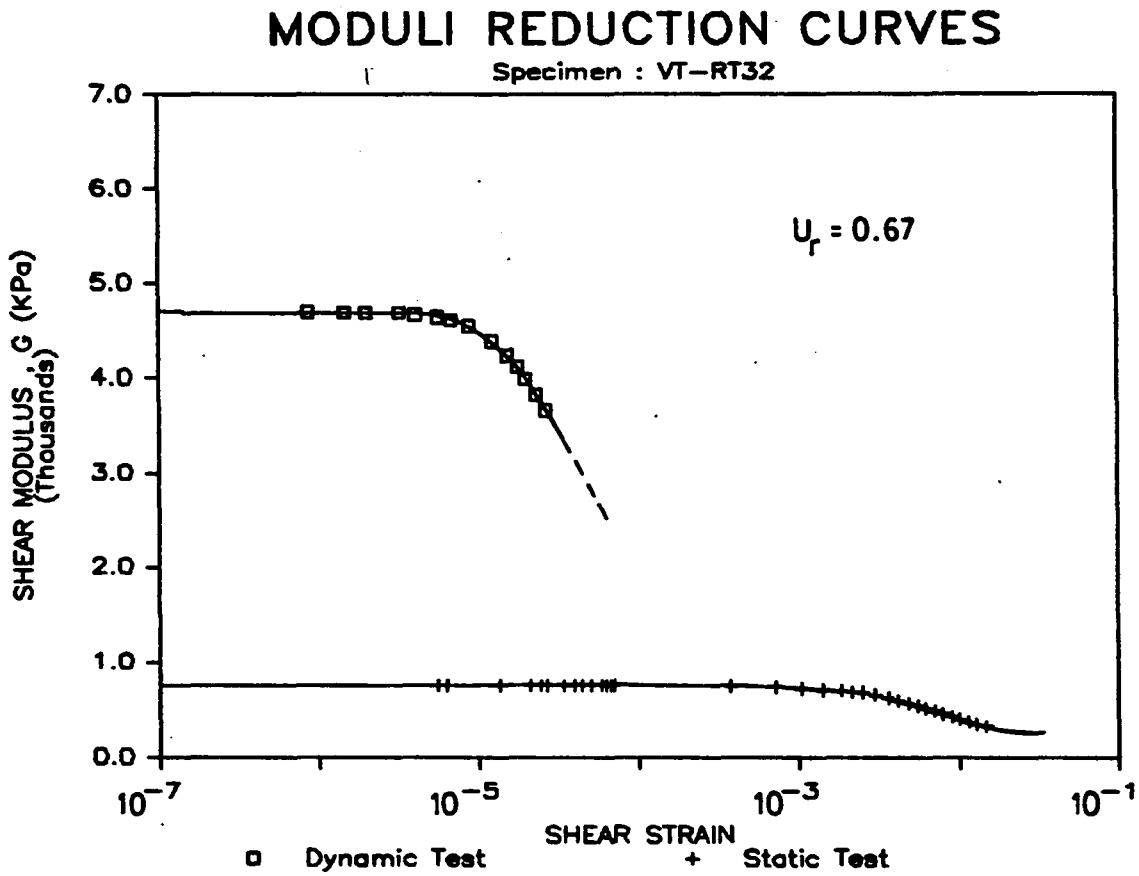

Fig. 4.21 Dynamic and static moduli reduction curves compared VT-RT32

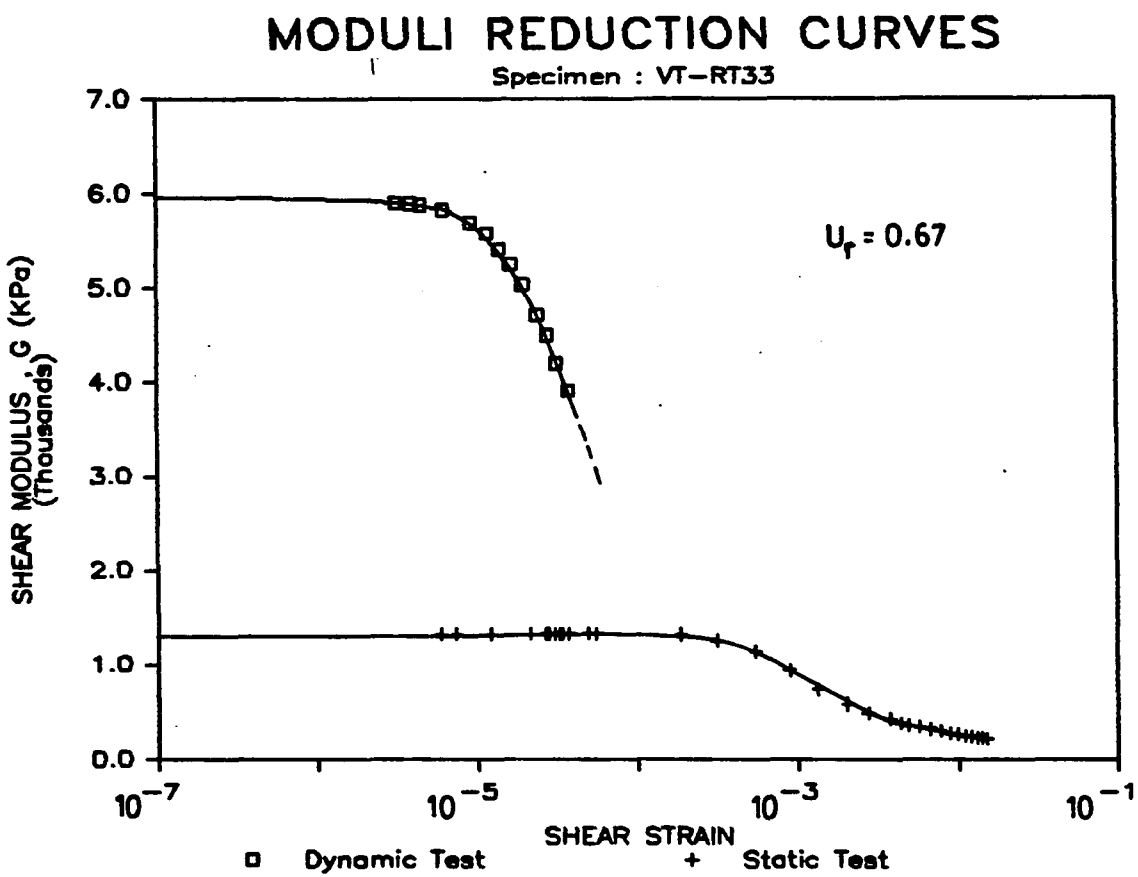

Fig. 4.22 Dynamic and static moduli reduction curves compared VT-RT33

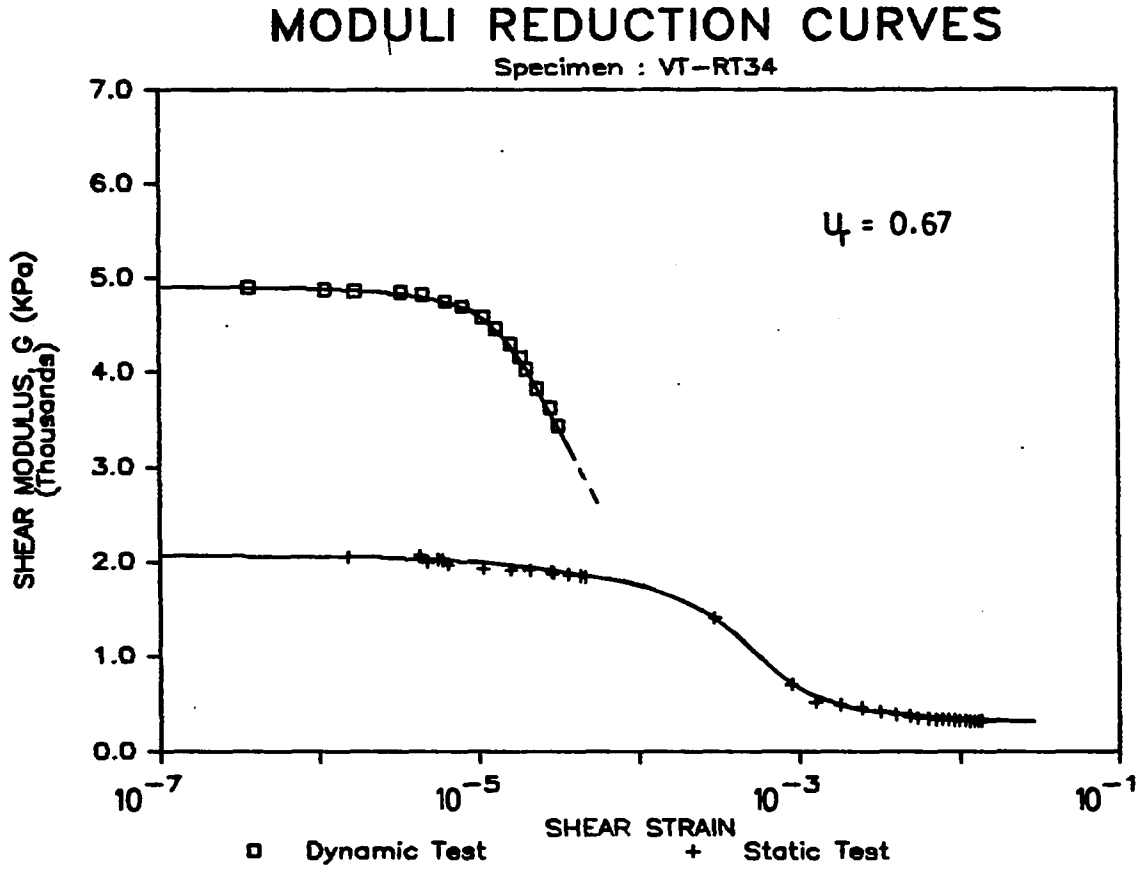

Fig. 4.23 Dynamic and static moduli reduction curves compared VT-RT34

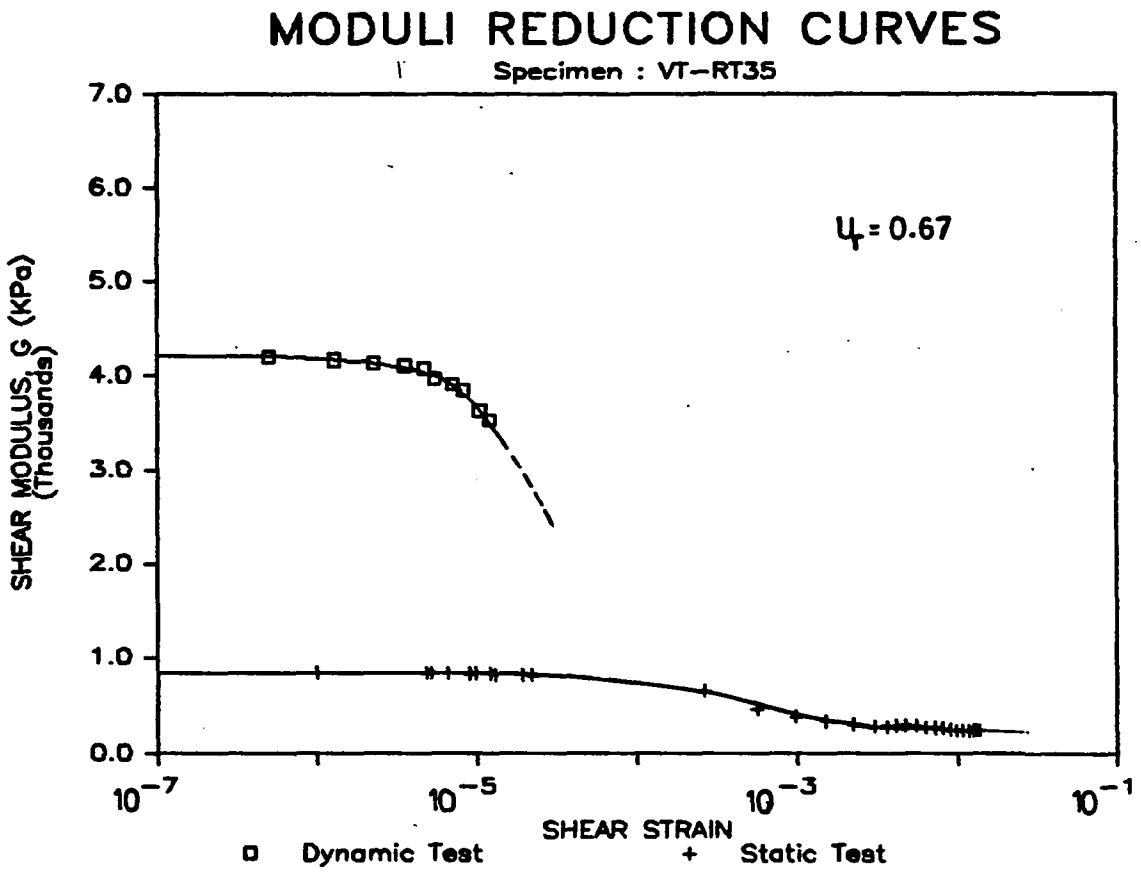

Fig. 4.24 Dynamic and static moduli reduction curves compared VT-RT35

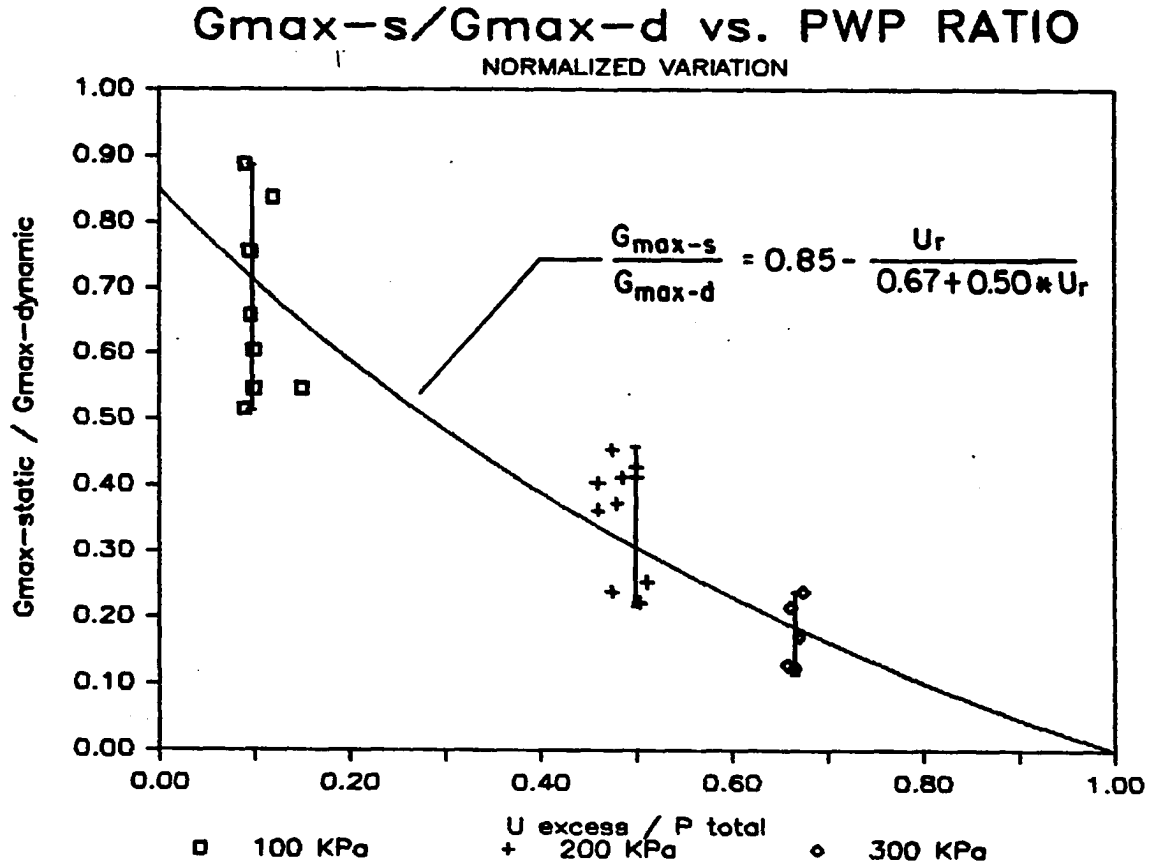

Fig. 4.25 Variation of Gmax-static/Gmax-dynamic with excess pore water pressure ratio

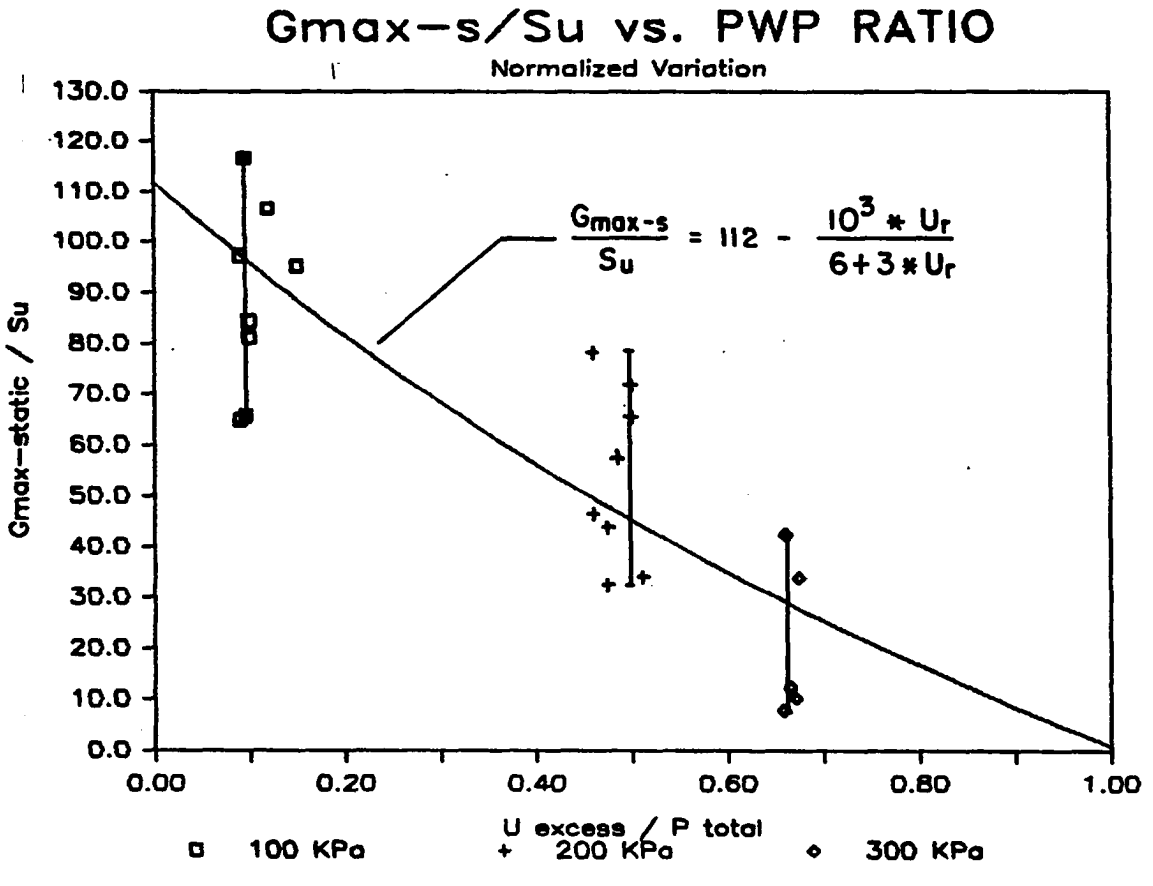

Fig. 4.26 Variation of Gmax-static/Su with excess pore water pressure ratio

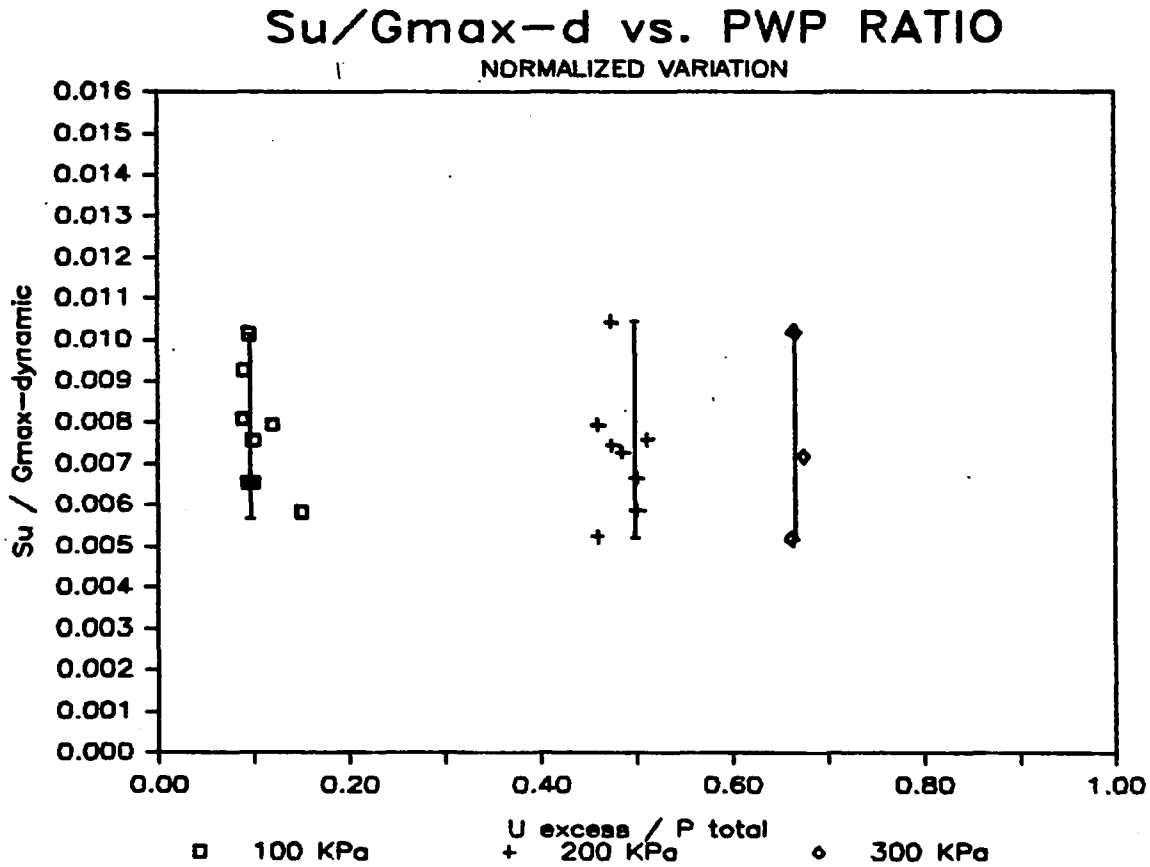

Fig. 4.27 Variation of Su/Gmax-dynamic with excess pore water pressure ratio

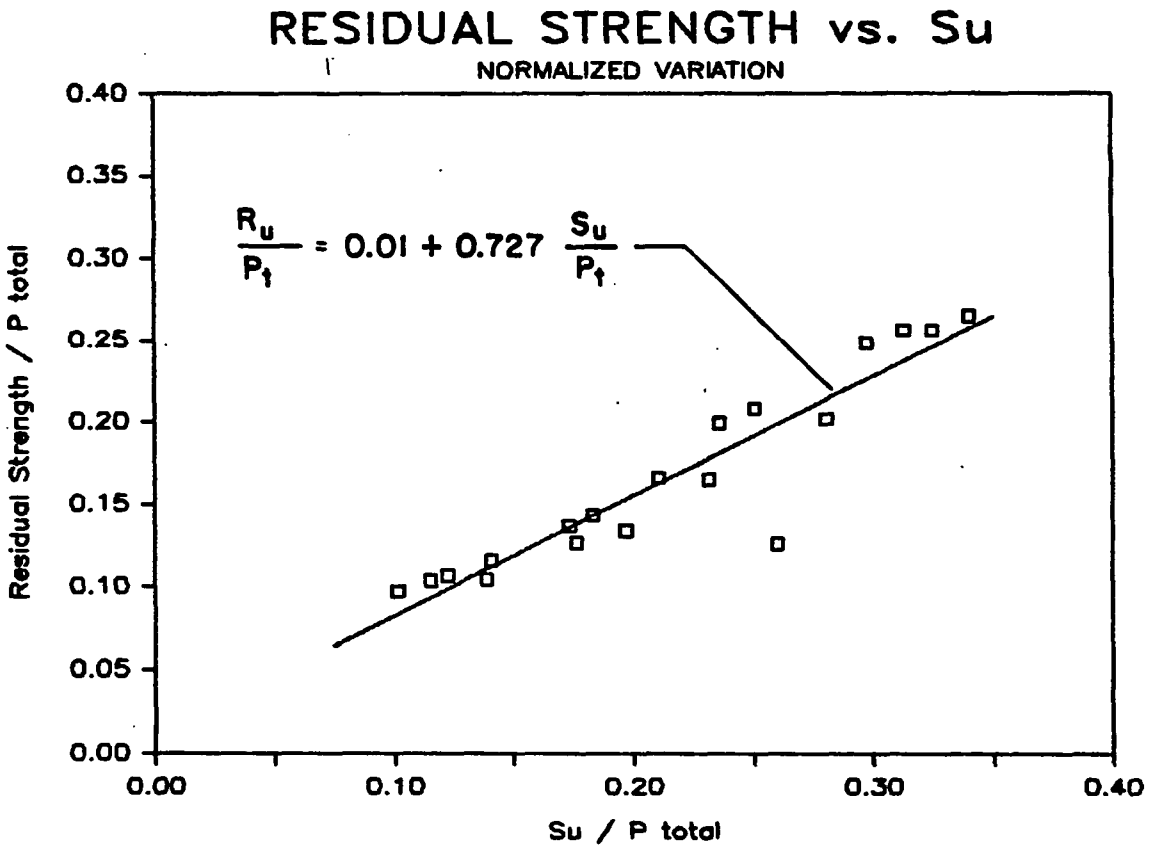

Fig. 4.28 Variation of undrained residual shear strength (Ru) with undrained shear strength (Su)

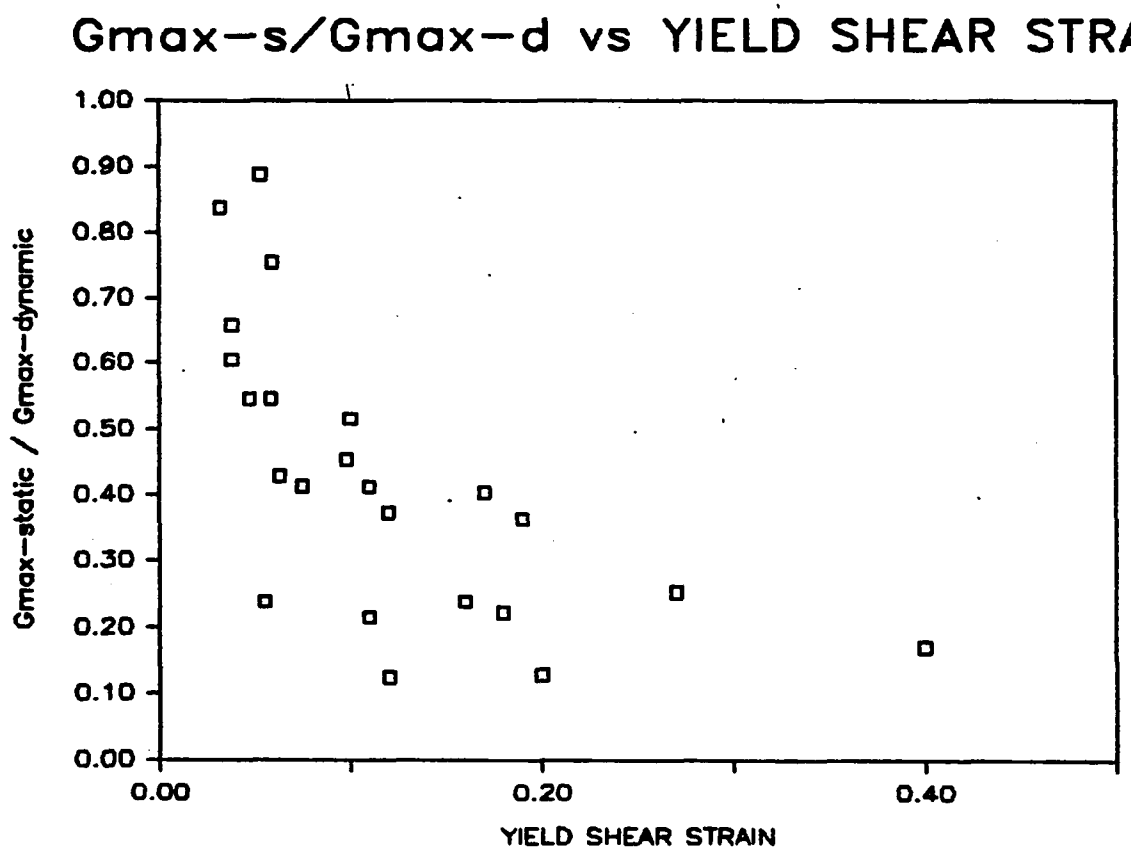

Fig. 4.29 Variation of Gmax-static/Gmax-dynamic with yield shear strain

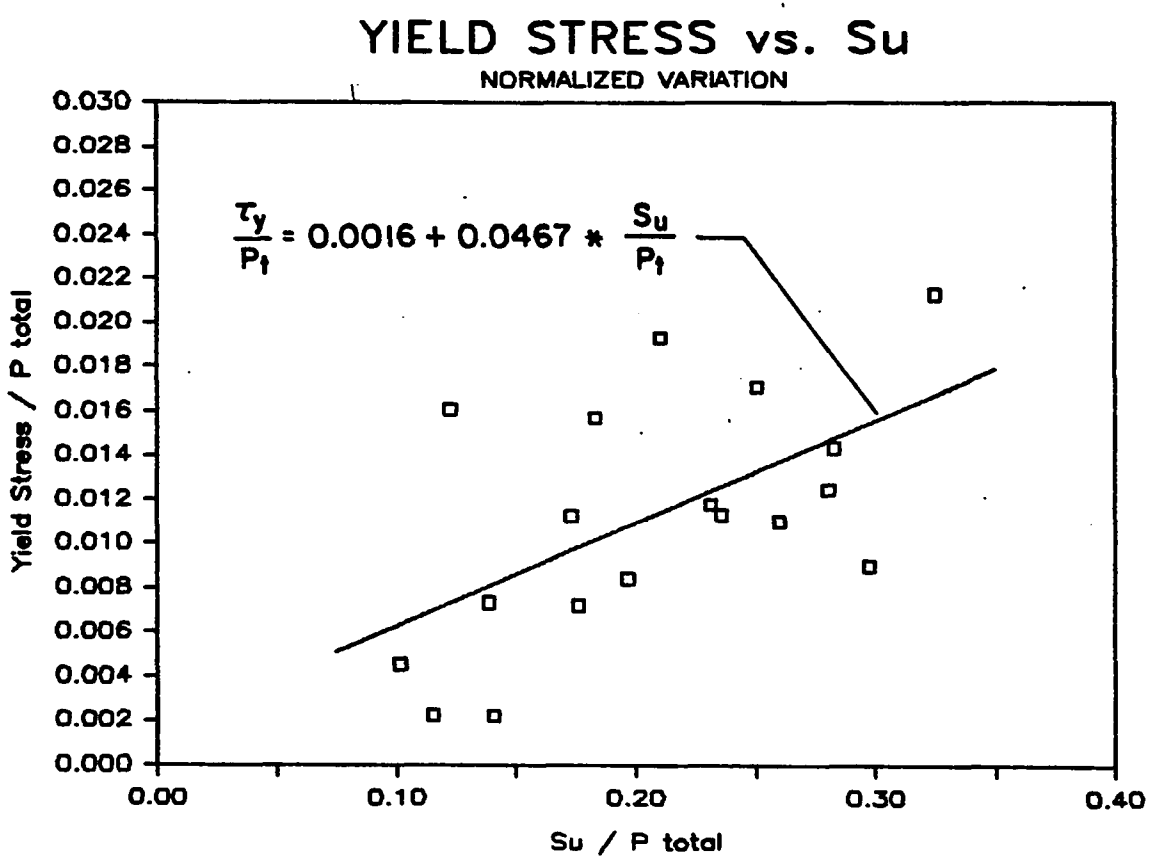

Fig. 4.30 Variation of yield stress with undrained shear strength

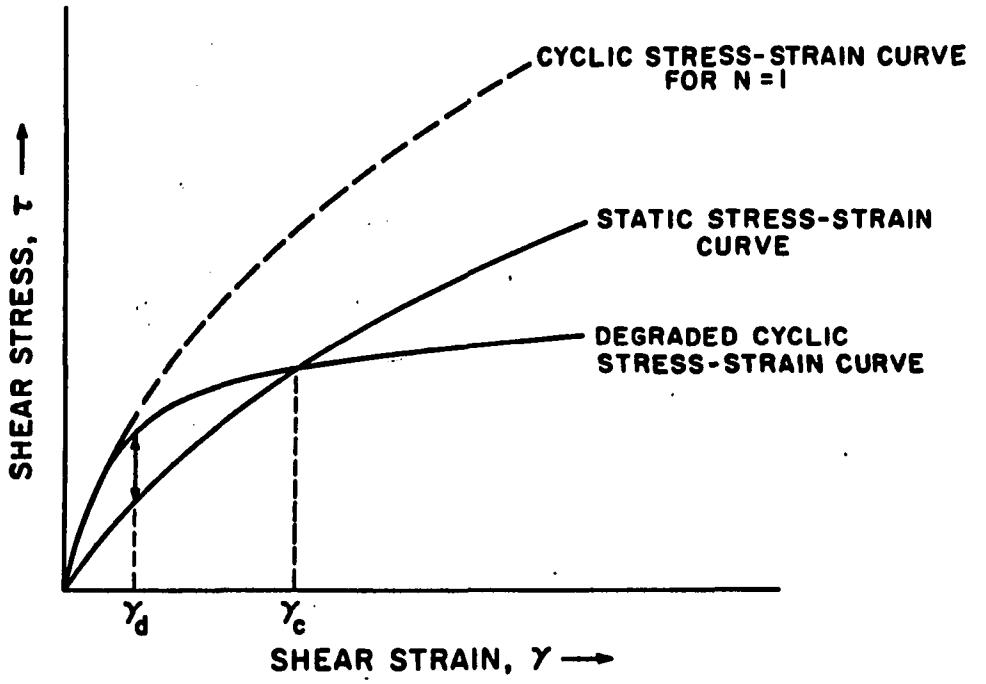

Fig. 4.31 Hypothetical representation of dynamic and static shear stress-strain curves

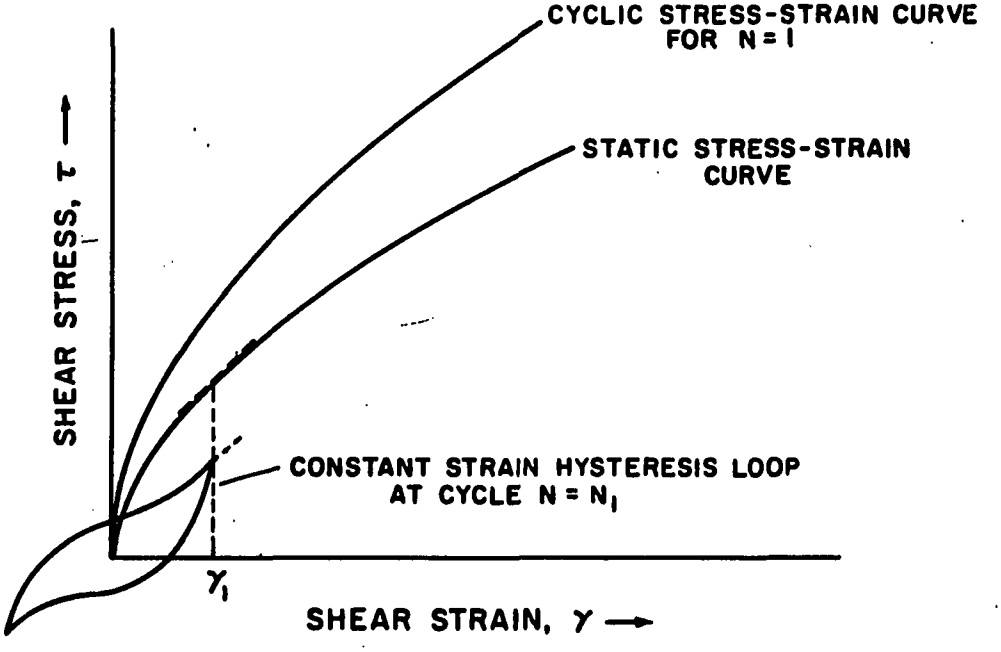

Fig. 4.32 Hypothetical representation of the relation between static shear stress-strain curve and constant strain hysteresis loop at cycle $N=N_1$

CHAPTER 5

CONCLUSIONS AND RECOMMENDATIONS

A new method was designed and implemented to measure low strain shear properties of soft saturated clays. The method basically consisted of an unconventional use of triaxial vane device and fully computerized data acquisition. The results obtained through this method were compared and correlated with the result obtained through an established dynamic testing method, namely resonant column. Conclusions made pertaining to this study are listed below:

5.1 ABOUT EXPERIMENTAL METHOD

1. A semi-computer aided research tool was developed and implemented. The system is flexible and lends itself to be modified for different applications, e.g. axial or other types of torsional shear loading. Variety of fine grained soil types other than soft clays can be tested. One good example is cemented clays.

2. Scope of obtainable data covers a wide range from 10^{-4} % resolution to 20% (or larger) shear strain amplitudes. Accuracy of data is comparable with the accuracy delivered by more established methods of testing. In comparison with resonant column data, lower standard deviations are observed. Precision is high corresponding to approximately 1500 data points sampled within 1% shear strain range. More realistic low strain shear parameters can be obtained for soft saturated clays.

5.2 ABOUT RESULTS

1. The dynamic and static shear moduli, G versus shear strain, γ variation reveals detailed information at low strain ranges which is valuable for numerical analysis methods, and basic understanding of soft saturated clay behaviour at these strain amplitudes. Degradation of dynamic shear moduli is found to be a major complicating factor in assessing low strain properties of soft clays using dynamic testing methods. The information obtained from the static testing in this study was used to identify important parameters of a theoretical model complying with the findings of other researchers.

2. Effects of total and effective stresses and existing excess pore water pressures on the measurement of dynamic and static maximum moduli are compared. For normally consolidated material the ratio of maximum static modulus to dynamic modulus is estimated to be Ø.85 (= Gmax-s/Gmax-d).

3. Effects of total and effective stresses and existing excess pore pressures on the measurement of Gmax/Su ratio are investigated. For normally consolidated material Gmax/Su ratio was estimated to be 112.

4. Yield parameters (γ_y, τ_y), with respect to bilinear modelling of the low strain range of the stress-strain curve are estimated and some correlations made. It is recommended that further research is needed on this subject area to achieve less scatter in data.

5. The system can successfully be utilized to assess

large strain properties also. An example of which was given by measuring and correlating the undrained shear strength and the undrained residual shear strength.

5.3 GENERAL CONCLUSIONS AND RECOMMENDATIONS

1. Dynamic testing of soft saturated clays can produce misleading results with respect to existing pore pressures below a certain threshold amplitude of shear strain. Substantial influence of degradation above a threshold of shear strain will result in unrealistic prediction of cyclic stress-strain behaviour. Frequency of loading applied in most dynamic testing methods will not properly simulate actual loading conditions in some applications. In order to eliminate the complicating factors cited above, a new low shear strain amplitude testing method is proposed.

2. The new method, designed and implemented, proves to be an improvement over the existing techniques of low strain shear testing of soft saturated clays.

3. The new method can also be utilized in other areas of research including vane testing mechanism; detailed analysis of low strain nonlinearity of soft soils and low strain properties of less understood materials such as cemented soils.

4. The data acquisition technique described in this study is a new tool to obtain better quality data and can easily be adopted to other testing methods with some modifications.

REFERENCES

1. Aas,G. "A Study of the Effect of Vane Shape and Rate of Strain on the Measured Values of In-Situ Shear Strength of Clay," Sixth ICSMFE, Montreal, 1965, Proceedings, Vol. 1, pp. 141-145.

2. Anderson, T.C and Lukas, R.G., "Preconsolidation Pressure Predicted Using Su/P' Ratio," Laboratory Shear Strength of Soil, ASTM STP 740, American Society for Testing and Materials, 1981, pp. 502-515.

3. Arango, I., Moriwaki, Y. and Brown, F., "In-Situ and Laboratory Shear Velocity and Modulus," Specialty Conference on Earthquake Engineering and Soil Dynamics, Pasedena, CA, June, 1978, Vol. 1, pp. 198-122.

4. Arman, A., Poplin, J.K. and Ahmad, N., "Study of the Vane Shear," Specialty Conference on In-Situ Measurement of Soil Properties, ASCE, Raleigh, 1975, Proceedings, Vol. 1, pp. 93-120.

5. Athanasopoulos, G.A. and Richart,Jr F.E., "Correlation Between Go and Tmax For Kaolinite Clay," Journal of the Geotechnical Engineering Division, ASCE, Vol. 109, No. 5, May, 1983, pp. 719-723.

6. Au, W.C. and Chae, Y.S.," Dynamic Shear Modulus of Treated Expansive Soils," Journal of the Geotechnical Engineering Division, ASCE, Vol. 106, No. 3, March, 1980, pp. 255-273.

7. Azzouz, A.S. and Baligh, M.M., "Corrected Field Vane Strength For Embankment Design," Journal of the Geotechnical Engineering Division, ASCE, Vol. 109, No. 5, May, 1983, pp. 730-734.

8. Bea, R.G. and Arnold, P.,"Movements and Forces Developed by Wave Induced Slides in Soft Clays," Fifth Annual Offshore Technology Conference, OTC 1899, April 29 - May 20, 1973.

9. Bea, R.G, Bernard, H.A., Arnold, P. and Doyle, E.H.,"Soil Movements and Forces Developed by Wave Induced Slides in the Mississippi Delta," Journal of Petroleum Technology, April 1975, pp. 500-514.

10. Bea, R.G.,Wright,S.G., Sircar,P. and Niedoroda, A.L., "Wave Induced Slides in South Pass Block 70, Mississippi Delta," Journal of the Geotechnical Engineering Division, ASCE, Vol. 109, No. 4, April, 1983, pp. 619-644.

11. Bishop, A.W. and Henkel, D.J. The Measurement of Soil Properties in the Triaxial Test, Edward Arnold Publishers, London, 1957.

12. Bjerrum L., "Enbankments on Soft Ground - State of the Art Report," Specialty Conference on Performance of Earth and Earth-Supported Structures, ASCE, Lafayette, IN, 1972, Proceedings, Vol. II, pp. 1-54.

13. Bjerrum, L., "Problems of Soil Mechanics and Construction on Soft Clay," Eight ICSMFE, Moscow, 1973, Proceedings, Vol. 3, pp. 111-159.

14. Blight, G.E., "A Note on Field Vane Testing of Silty Soils," Canadian Geotechnical Journal, 1968, Vol. 5, No. 3, pp. 142-149.

15. Cadling, L. and Odenstad, S., "The Vane Borer," Royal Sweedish Geotechnical Institute, Proceedings, No. 2, 1950.

16. Cargill, W.K.,"Prediction of Consolidation of Very Soft Soil," Journal of the Geotechnical Engineering Division, ASCE, Vol. 110, No.6, June, 1984, pp.775-795.

17. Carlson, L., "Determination of the In-Situ of the Shear Strength of Undisturbed Clay by Means of a Rotating Auger," Second ICSMFE, Rotterdam, 1948, Proceedings, Vol. 1, pp. 265-270.

18. Chae, Y.S, Au, W.C. and Chiang, Y.C., "Determination of Dynamic Shear Modulus of Soils From Static Strength," International Conference on Recent Advances in Geotechnical Earthquake Engineering and Soil Dynamics, University of Missouri, Rolla, Mo, April 26-May 3, 1981, Proceedings, pp. 33-38.

19. D'Appolonia, D.J. and Poulos, H.G., "Initial Settlement of Structure on Clay," Journal of the Soil Mechanics and Foundation Division, ASCE, Vol. 97, SM10, 1971, pp. 1359-1376.

20. Donald, I.B., Jordan, D.O., Parker, I.J. and Toh, C.T., "The Vane Test - A Critical Appraisal," Ninth ICSMFE, Tokyo, 1967, Vol. 1, pp. 81-88.

21. Ducker, D.C, Gibson R.E., and Henkel, D.J., "Soil Mechanics and Work Hardening Theories of Plasticity," Transactions, ASCE, 1957, Vol. 24, pp. 338-346.

22. Dyvik, R., Zimmie, T.F. and Schimelfenyg, P., "Cyclic Simple Shear Behaviour of Fine Grained Soils," Norwegian Geotechnical Institute, Publication No. 149, 1983, 6p.

23. Eden, W.J. and Law, K.T., "Comparison of Undrained Shear Strength Results Obtained by Different Test Methods in Soft Clays," Canadian Geotechnical Journal, 1980, Vol. 17, pp.369-381.

24. Finn, W.D.L., Siddharthan, R. and Martin, R.G., "Response of Seafloor to Ocean Waves," Journal of the Geotechnical Engineering Division, ASCE, Vol. 109, No. 4, April, 1983, pp. 556-572.

25. Flaate, K., "Factors Influencing the Results of Vane Test," Canadian Geotechnical Journal, 1966, Vol. 3, No. 1, pp. 18-31.

26. Hadj-Hamou, T.A., "Determination of the Dynamic Material Properties From Static Tests," thesis presented to Stanford University, in i981, in partial fulfillment of the requirements for the degree of Engineer.

27. Hara, A., Ohta, T., Niwa, M., Tanaka, S. and Banno, T., "Shear Modulus and Shear Strength of Cohesive Soils," Soils and Foundations, JSSMFE, Vol. 14, No. 3, September, 1974, pp. 1-12.

28. Hardin, B.O. and Drnevich, V.P., "Shear Modulus and Damping in Soils: I. Measurements and Parameter Effects, II. Design Equations and Curve," Technical Report UKY 27-70-CE 2 and 3, College of Engineering, University of Kentucky, Lexington, Kentucky, 1970.

29. Hardin, B.O., "State of the Art Paper," Specialty Conference on Earthquake and Soil Dynamics, ASCE, Pasedena, June 1978, Proceedings.

30. Idriss, I.M., Dobry, R., and Singh R.D., "Nonlinear Behaviour of Soft Clays During Cyclic Loading," Journal of the Geotechnical Engineering Division, ASCE, GT12, December, 1978, pp. 1427-1447.

31. Idriss, I.M., Moriwaki, Y., Wright, S.G., Doyle, E.H., and Ladd, R.S., "Behaviour of Normally Consolidated Clay Under Simulated Earthquake and Ocean Wave Loading," International Symposium on Soils Under Cyclic and Transient Loading, Swansea, January, 1980, Proceedings, pp. 437-445.

32. Isenhower, W.M. and Stokoe II, K.H., "Strain-Rate Dependent Shear Modulus of San Fransisco Bay Mud," International Conference on Recent Advances in Geotechnical Earthquake Engineering and Soil Dynamics, University of Missouri, Rolla, Mo, April 26-May 3, 1981, Proceedings, pp. 597-602.

33. Ishihara, K. and Yasuda, S., "Cyclic Strengths of Undisturbed Cohesive Soils of Western Tokyo," International Symposium on Soils Under Cyclic and Transient Loading, Swansea, January, 1980, Proceedings, pp.57-66.

34. Kavazanjian,Jr. E., and Hadj-Hamou, T.A., "Estimating Dynamic Properties From Static Tests," International Conference on Recent Advances in Geotechnical Earthquake Engineering and Soil Dynamics, University of Missouri, Rolla, Mo, April 26-May 3, 1981, Proceedings, pp.1-6.

35. Kenney, T.C. and Landva, A., "Vane Triaxial Apparatus," Sixth ICSMFE, Montreal, 1965, Proceedings, Vol. 1, pp.269-272.

36. Kimura, T. and Saitoh, K., "Effect of Disturbance Due to Insertion on Vane Shear Strength of Normally Consolidated Cohesive Soils," Soils and Foundations, JSSMFE, June 1983, Vol. 23, No. 2, pp. 113-124.

37. Ko, Hon-Yim and Sture, S.,"State of the Art:Data Reduction and Application for Analytical Modeling," Laboratory Shear Strength of Soil, ASTM STP 740, American Society for Testing and Materials, 1981, pp. 329-386.

38. Kondner, R.L., "Hyperbolic Stress-Strain Response for Cohesive Soils," Journal of the Soil Mechanics and Foundation Division, ASCE, Vol. 89, SM1, February, 1963, pp. 115-143.

39. Koutsoftas, D.C. and Fischer, J.A., "Dynamic Properties of Two Marine Clays," Journal of the Geotechnical Engineering Division, ASCE, Vol. 106, No. 6, June,1980, pp. 645-657.

40. Lade, P.W. and Duncan, J.M.,"Elastoplastic Stress Strain Theory For Cohesionless Soil," American Society of Civil Engineers, Proceedings, Vol. 101, No. GT10, pp. 1037-1053.

41. Lade, P.V.,Presentation of Predictions at NSF/NSERC Symposium on Constitutive Equations For Soils, McGill University, Montreal, 1980.

42. La Rocelle P., Roy, M. and Tavenas, F., "Field Measurements of Cohesion in Champlain Clays," Eight ICSMFE, Moscow, 1973, Proceedings, Vol. 1-1, pp. 229-236.

43. Larkin, T.J. and Donovan, N.C., "Sensitivity of Computed Nonlinear Effective Stress Soil Response to Shear Modulus Relationships," Second U.S. National Conference on Earthquake Engineering, August 22-24,1979, Stanford University, Stanford, CA, Proceedings, pp. 573-582.

44. Law, K.T.,"Triaxial Vane Tests on Soft Marine Clay," Canadian Geotechnical Journal, Vol. 16, No. 1, Feb., 1979, pp.11-18.

45. Lee, K.L. and Focht, J.A., "Liquefaction Potential at Ekofisk Tank in North Sea," Journal of the Geotechnical Engineering Division, ASCE, No. GT1, January, 1975, pp. 1-18.

46. Lunne, T., Eide, O. and De Ruiter, J., "Correlations Between Cone Resistance and Vane Shear Strength in Some Scandinavian Soft to Medium Stiff Clays," Canadian Geotechnical Journal, 1976, Vol 13., No. 1, pp.1-12

47. Matsui, T. and Abe, N., "Shear Mechanism of Vane Test in Soft Clays," Soils and Foundations, JSSMFE, December, 1981, Vol. 21, No. 4, pp. 69-80.

48. Meimon, Y. and Hicher, P.Y., "Mechanical Behaviour of Clays Under Cyclic Loading," International Symposium on Soils Under Cyclic and Transient Loading, Swansea, January, 1980, Proceedings, pp. 77-88.

49. Menzies, B.K. and Merrifield, C.M., "Measurements of Shear Stress Distribution on the Edges of a Shear Vane Blade," Geotechnique, 1980, Vol. 30, No. 3, pp. 314-318.

50. Mitchell, R.J., Tsui, K.K. and Sangrey, D.A.,"Failure of Submarine Slopes Under Wave Action," Thirteenth Coastal Engineering Conference, Vancouver, 1972, Proceedings, Vol. II pp. 1515-1542.

51. Monney, N.T., "An Analysis of the Vane Shear Test at Varying Rates of Shear," Deep Sea Sediments: Physical and Mechanical Properties, A.L. Inderlitzen, ed., Plenum Press, New York, 1974, pp. 151-167.

52. Pamukcu, Sibel,"Dynamic Analysis of Sediments of Gulf of Mexico and Numerical Simulation of Mud Flows," thesis presented to Louisiana State University, Baton Rouge, LA, in 1981, in partial fulfillment of the requirements for the degree of Master of Science.

53. Pamukcu, S., Poplin, J.K., Suhayda, J.N. and Tumay, M.T., "Dynamic Sediment Properties, Mississippi Delta," Conference on Geotechnical Practice in Offshore Engineering, ASCE, University of Texas, Austin, TX, April 27-29, 1983, Proceedings, pp. 111-132.

54. Pamukcu, S. and Suhayda, J.N., "Dynamic Properties and Critical State Parameters, Mississippi Delta," ASCE Annual Convention in Houston,TX, October 17-21,1983, Proceedings of Session No. 52: Evaluation of Seafloor Soil Properties Under Cyclic Loads.

55. Pamukcu, S. and Suhayda, J.N., "Evaluation of Shear Modulus for Soft Marine Clays, Mississippi Delta," Strength Testing of Marine Sediments: Laboratory and In-Situ Measurements, ASTM STP 883, American Society for Testing and Materials, Philadelphia, pp. 352-362.

56. Prevost, J.H., "Mathematical Modelling of Monotonic and Cyclic Undrained Clay Behaviour," International Journal for Numerical and Analytical Methods in Geotechnical Engineering, 1977, Vol. 1, No. 2, pp. 195-216.

57. Prevost, J.H. and Hoeg, K.,"Effective Stress Strain Strength Model For Soils," American Society of Civil Engineers, Proceedings, Vol. 101, No. GT3, pp. 259-278.

58. Prevost, J.H. and Hoeg, K., "Mathematical Model for Static and Cyclic Undrained Clay Behaviour: Part 1 and 2," Norwegian Geotechnical Institute, Report 52412, 1975.

59. Prior,D.B., and Suhayda, J.H.,"Application of Infinite Slope Analysis to Subaqueous Sediment Instability, Mississippi Delta," Engineering Geology, No. 14, 1979, pp. 1-10.

60. Pyles, M.R."Vane Shear Data on Undrained Residual Strength," Journal of the Geotechnical Engineering Division, ASCE, Vol. 110, No. 5, April 1984, pp. 543-547.

61. Rahman, M.S., Seed, H.B., and Booker, J.R.,"Pore Pressure Development Under Offshore Gravity Structures," Journal of the Geotechnical Engineering Division, ASCE, No. GT12, December, 1977, pp. 1419-1435.

62. Roscoe, K.H. and Schofield, A.N.,"Mechanical Behaviour of an Idealized 'Wet Clay'," European Conference on Soil Mechanics and Foundation Engineering, 3, Wiesbaden, 1963,Proceedings, Vol.1, pp. 47-54.

63. Roscoe,K.H., Schofield, A.N., and Thurairajah A., "Yielding of Clays in States Wetter Than Critical," Geotechnique, Vol. 13, No. 3, pp. 211-240.

64. Schapery, R.A., Riggins, M., and Dunlap, W.A., "Movement of Marine Clay Sediments During Cyclic Loading," A Report from Mechanics and Materials Research Center, Texas Engineering Experiment Station, Texas A&M University, TX, September, 1976.

65. Schofield, A. and Wroth, P.,Critical State Soil Mechanics, New York, McGraw-Hill, 1968, 310 p.

66. Schmertmann, J.H., "Measurement of In-Situ Shear Strength," Specialty Conference on In-Situ Measurement of Soil Properties, ASCE, Raliegh, 1975, Proceedings, Vol. 2, pp. 57-138.

67. Seed, H.B. and Chan, C.K., "Clay Strength Under Earthquake Loading Conditions," Proceedings, ASCE, SM2, 1966, pp. 53-78.

68. Seed, H.B. and Idriss, I.M., "Soil Moduli and Damping Factors for Dynamic Response Analysis," College of Engineering, University of California, Berkeley, CA, Report No. EERC 70-10, December, 1970.

69. Seed, H.B. and Rahman, M.S.,"Analysis for Wave Induced Liquefaction in Relation to Ocean Floor Stability," Report No. UCB/TE-77/02, Department of Civil Engineering, Institute of Transportation and Traffic Engineering, University of California, Berkeley, May 1977.

70. Sharifounnasab, M. and Ullrich, C.R., "Rate of Shear Effects on Vane Shear Strength," Journal of the Geotechnical Engineering Division, ASCE, Vol. 111, No. 1, January, 1985, pp. 135-139.

71. Shibata, T. "On the Shear Strength of Normally Consolidated Clay," JSCE, 1967, Proceedings, No. 138, pp. 39-48 (in Japanese).

72. Shibata, T. and Tagawa, S., "Vane Shear Strength of Clays," Annuals, Disaster Prevention Research Institute, Kyoto University, No. 11B, pp. 537-548 (in Japanese).

73. Silver, M.L., "Load,Deformation and Strength Behavior of Soils Under Dynamic Loadings," International Conference on Recent Advances in Geotechnical Earthquake Engineering and Soil Dynamics, April 26-May 3, 1981, Saint Louis, Rolla,Mo, Proceedings, pp. 873-895.

74. Silver, M.L. and Park, T.K., "Dynamic Triaxial and Simple Shear Behaviour of Sand," Journal of the Geotechnical Engineering Division, ASCE, Volume 101, GT6, June, 1975, pp. 513-529.

75. Sterling, G.H. and Stohbeck, E.E.,"The Failure of the South Pass 70 "B" Platform in Hurricane Camille," Fifth Annual Offshore Technology Conference, OTC 1898, April 29 - May 2, 1973.

76. Stevenson, H.S., "Vane Shear Determination of the Viscoelastic Shear Modulus of Submarine Sediments," thesis presented to Texas A&M University, in 1973, in partial fulfillment of the requirements for Master of Science degree.

77. Suhayda, J.N., and Prior, D.B.,"Explanation of Submarine Landslide Morphology by Stability Analysis and Rheological Models," Tenth Annual Offshore Technology Conference, OTC 3171, May 8-11, 1978.

78. Tokheim, O.,"Deformation Behaviour of Soils In Terms of Soil Moduli," Norwegian Geotechnical Institute, Publication No. 152, 1984, 18 p.

79. Torstenson, B.A., "Time-dependent Effects in Field Vane Tests," International Symposium on Soft Clay, Bangkok, 1977, Proceedings, pp. 387-397.

80. Tsai, Chan-Feng, Lam,I. and Martin, I.M.,"Seismic Response of Cohesive Marine Soils," Journal of the Geotechnical Engineering Division, ASCE, GT9, September, 1980, pp. 997-1012.

81. Wiesel, C.E., "Some Factors Influencing In-Situ Vane Test Results," Eight ICSMFE, Moscow, 1973, Vol. 1-2, pp.475-479.

82. Wilson, N.E., "Laboratory Vane Shear Tests and the Influence of Pore-Water Stresses," Laboratory Shear Testing of Soils, ASTM STP No. 361, American Society for Testing and Materials, pp. 377-385.

83. Wilson, S.D. and Dietrich, R.J., "Effect of Consolidation Pressure on Elastic and Strength Properties of Clay," ASCE Research Conference on Shear Strength of Cohesive Soils, Boulder, Colorado, 1960, pp. 419-435.

APPENDIX A

SPECIFICATIONS OF SOME DATA ACQUISITION EQUIPMENT AND BAL-SEAL

ELECTRONIC AUTOCOLLIMATOR
Model 1000-135

Manufacturer : United Detector Technology (UDT)
3939 Landmark Street
Culver City, CA 90230
(213) 204-2250

Specifications

Beam Diameter	.....	45 mm
Overall Length, including lens	.....	180 mm
Angular coverage	.....	0.074 rad
Angular resolution (with OP-EYE 4)	.....	0.5 arc sec.
Linearity in angular coverage		
central 25 %	.....	0.5-5 %
central 75 %	.....	5-20 %
LED input current,DC	.....	100 mA
LED wavelength	.....	880 nm
Temperature coefficient drift	.....	0.4 arc sec./^{o}F
OP-EYE gain required for optimum operation	.....	200K
Sensitivity falloff with distance	.....	0.7%/inch

OPTICAL POSITION INDICATOR
Model OP-EYE-4

Manufacturer: United Detector Technology (UDT)

Specifications

Programmable gain	.....	1,10,100,500
A/D resolution	.....	16-bit
Frequency response of A/D	.....	2.5 kHz (625 Hz for each dual axis detector)
Interface	.....	RS-232C (9600 Baud) and IEE-488 ports on rear panel

BAL-SEAL
Series R304A-(.125) SP-23

Manufacturer: Bal-Seal Eng. Co.
620 W.Warner Ave.
Santa Ana, California 92707
(714) 557 5192

Specifications

Material	Teflon
ID (cm)	0.125 +/- 0.005
OD flange (cm)	0.434 +/- 0.010
Maximum pressure (kg/cm^2)	10
Maximum clearance (mm)	0.13
Wire diameter (cm)	0.011

APPENDIX B

COMPUTER PROGRAMS

OPCALIB.FOR

OPAUX1.FOR

OPAUX2.FOR

OPAUX3.FOR

RESON.FOR

```
C*************************************************************
C                                                            *
C     OPCALIB.FOR                                            *
C                                                            *
C     THIS IS AN INTERACTIVE FORTRAN GRAPHICS PROGRAM        *
C     TO CALIBRATE, COLLECT AND STORE ANGULAR ROTATION       *
C     DATA VIA AUTOCOLLIMATOR AND OP-EYE                     *
C                                                            *
C                  By  SIBEL PAMUKCU                         *
C                                                            *
C           Latest Revision : February 1986                  *
C                                                            *
C*************************************************************
C
C
      COMMON/POS/X(3500),Z(3500)
      COMMON/GRAPH/IX(3500),IZ(3500)
      COMMON KK,NDATA,CR,R
      INTEGER*2 IX,IZ,NUM,KK,LL,NDATA,NUMB,I,J,K,ICOL
      INTEGER*2 INZEN,N(6),DATA(6),IMIN,IMAX,IFLAG,NBEG,IIZ
      INTEGER*2 IST,IFN,RFAC,NI,N3,NTOT,N5,N6,N6P1
      INTEGER*2 KEY,INKEY,IIX,IMP1
      CHARACTER*1 CK,CR,R,GAIN
      CHARACTER*10 DATF
      CALL CLS
      WRITE(*,5)
5     FORMAT(' ENTER DATA FILE NAME ==> ',\)
      READ(*,'(A10)') DATF
      WRITE(*,6)
6     FORMAT(' ENTER MOTOR SPEED REDUCTION (%) ==> ',\)
      READ(*,'(I4)') RFAC
C
      OPEN(8,FILE=DATF,STATUS='NEW',FORM='BINARY')
      WRITE(*,10)
10    FORMAT(' TURN ON OPEYE AND HIT RETURN ',\)
      READ(*,'(A1)') CK
20    NUM=INZEN(NUM)
      IF(NUM.NE.42) GO TO 20
C
C     INITIALIZE OPEYE (M1,S4,C4)
C
      CR=CHAR(13)
      R=CHAR(82)
      CK=CHAR(77)
      CALL OUTZEN(CK)
      CK=CHAR(49)
      CALL OUTZEN(CK)
      CK=CHAR(83)
      CALL OUTZEN(CK)
      CK=CHAR(52)
      CALL OUTZEN(CK)
      CK=CHAR(67)
```

```
      CALL OUTZEN(CK)
      CK=CHAR(52)
      CALL OUTZEN(CK)
      CALL OUTZEN(CR)
30    NUM=INZEN(NUM)
      IF(NUM.NE.42) GO TO 30
      GAIN=CHAR(50)
      CK=CHAR(71)
      CALL OUTZEN(CK)
      CALL OUTZEN(GAIN)
      CALL OUTZEN(CR)
40    NUM=INZEN(NUM)
      IF(NUM.NE.42) GO TO 40
C
      CALFAC=0.25
      IF(RFAC.GT.50) CALFAC=2.0
      IF(RFAC.LE.50) CALFAC=1.0
      IF(RFAC.LE.40) CALFAC=0.75
      IF(RFAC.LE.30) CALFAC=0.5
      IF(RFAC.LE.20) CALFAC=0.25
      XMAX=0.0
      XMIN=0.0
      IFLAG=1
      NDATA=1
      ICOL=6
      CALL CLS
      CALL LINE(0,112,620,112,3,-1)
      KK=0
      ZDUM=RDTIME(0)
      CALL ASSEM
      X1=ABS(X(NDATA))
      X(NDATA)=X(NDATA)-X1
      IX(1)=112
      IZ(1)=NINT(CALFAC*Z(NDATA))
C
C     INITIALIZATION COMPLETE
C
1010  NDATA=NDATA+1
      KK=0
C
      CALL ASSEM
C
C     STEPS BRANCH FROM HERE
C
      X(NDATA)=X(NDATA)-X1
      IF(IFLAG.EQ.2) GO TO 1050
      IF(IFLAG.EQ.3) GO TO 1500
C     **************
C     IFLAG IS 1
C     **************
      IF(X(NDATA).LT.XMIN) THEN
        XMIN=X(NDATA)
        IMIN=NDATA
```

```
      ENDIF
      IF(X(NDATA).GT.XMAX) THEN
        XMAX=X(NDATA)
        IMAX=NDATA
      ENDIF
      KEY=INKEY()
      IF(KEY.NE.13) GO TO 1500
      WRITE(*,201)
      READ(*,'(A1)') CK
      IST=IMIN+(IMAX-IMIN)/4
      IFN=IMIN+3*(IMAX-IMIN)/4
      CALL FIT(Z,X,IST,IFN,A,B,RS,SIG)
      DO 220 I=IMIN,IMAX
      X(I)=A+B*Z(I)
220   CONTINUE
      IMP1=IMIN+1
      IX(IMIN)=112-NINT(350*X(IMIN))
      DO 225 I=IMP1,IMAX
      IX(I)=112-NINT(350*X(I))
      CALL LINE(IZ(I-1),IX(I-1),IZ(I),IX(I),1,-1)
225   CONTINUE
      BCAL=(RFAC*1.009997-7.629231)*0.001
      RAD=(BCAL*3.141592654)/(B*180.)
      WRITE(*,226) XMAX,XMIN,B,RS,SIG*100,RAD
226   FORMAT(' XMAX=> ',F8.5,'  XMIN=> ',F8.5,'  B=> ',F10.8,
     &'  RS=> ',F6.4,'  SIG=> ',F6.3,'%',/,
     &' CALIBRATION CONSTANT =>',G15.8,' RADIANS/UNIT READING')
      CALL COLOR(2,-1)
      IZ(NDATA)=NINT(CALFAC*Z(NDATA))
      IX(NDATA)=112-NINT(350*X(NDATA))
      IFLAG=2
      ICOL=4
      WRITE(*,202)
      READ(*,'(A1)') CK
      BASE=Z(NDATA)
      ZDUM=RDTIME(0)
      GO TO 1010
C     ***************
C     IFLAG IS 2
C     ***************
1050  CONTINUE
      KEY=INKEY()
      IF(KEY.NE.13) GO TO 1500
      ZD=Z(NDATA)
201   FORMAT(' TURN OFF VANE !! HIT RETURN ',\)
202   FORMAT(' REVERSE VANE , HIT RETURN ',\)
      CALL COLOR(7,-1)
      WRITE(*,230)
230   FORMAT(' SET READY FOR STEP 3 - ADJUST BEGINNING POSITION',\)
C
C     ************************************************
      IIZ=NINT(CALFAC*(BASE-ZD))
      DO 99 LL=1,10
```

```
      READ(*,'(A1)') CK
      KK=0
      XBEG=X(NDATA)-X1
      IIX=112-NINT(350*XBEG)
      CALL PSET(IIZ,IIX,2)
99    CONTINUE
C     ************************************************
C
      NDATA=1
      ZBEG=BASE-ZD
      X(NDATA)=XBEG
      IX(NDATA)=112-NINT(350*XBEG)
      IZ(NDATA)=NINT(CALFAC*ZBEG)
      IFLAG=3
      ICOL=1
      WRITE(*,202)
      READ(*,'(A1)') CK
      ZDUM=RDTIME(0)
      Z(NDATA)=ZDUM
      GO TO 1010
C     ***********
C     FLAG IS 3
C     ***********
C
1500  CONTINUE
      IX(NDATA)=112-NINT(350*X(NDATA))
      IF(IFLAG.EQ.1) THEN
      IZ(NDATA)=NINT(CALFAC*Z(NDATA))
      IF(NDATA.EQ.1) GO TO 1010
      ENDIF
      IF(IFLAG.EQ.2) THEN
      IZ(NDATA)=NINT(CALFAC*(BASE-Z(NDATA)))
      ENDIF
      IF(IFLAG.EQ.3) THEN
      IF(NDATA.EQ.3250) GO TO 2000
      IF(Z(NDATA).LE.Z(NDATA-1)) GO TO 2000
      KEY=INKEY()
      IF(KEY.EQ.13) GO TO 2000
      IZ(NDATA)=NINT(CALFAC*(ZBEG+Z(NDATA)))
      IF(IZ(NDATA).GT.620) GO TO 3000
      ENDIF
      CALL LINE(IZ(NDATA-1),IX(NDATA-1),IZ(NDATA),IX(NDATA),ICOL,-1)
      GO TO 1010
3000  CONTINUE
      N5=NDATA-1
      N6=NDATA
      IZ(NDATA)=IZ(NDATA)-620
3100  NDATA=NDATA+1
      KEY=INKEY()
      IF(KEY.EQ.13) GO TO 2000
      KK=0
      CALL ASSEM
      IF(NDATA.EQ.3250) GO TO 2000
```

```
      IF(Z(NDATA).LE.Z(NDATA-1)) GO TO 2000
      X(NDATA)=X(NDATA)-X1
      IX(NDATA)=112-NINT(350*X(NDATA))
      IZ(NDATA)=NINT(CALFAC*(ZBEG+Z(NDATA)))-620
      CALL LINE(IZ(NDATA-1),IX(NDATA-1),IZ(NDATA),IX(NDATA),ICOL,-1)
      GO TO 3100
2000  CONTINUE
      WRITE(*,201)
      READ(*,'(A1)') CK
      NTOT=NDATA-1
C
      WRITE(8) RFAC,NTOT
      WRITE(8) A,B
      WRITE(8) ZBEG,XMAX,X1
      WRITE(8) (I,X(I),Z(I),I=1,NTOT)
      CALL CLS
      CALL LINE(0,112,620,112,3,-1)
      N3=NTOT
      IF(N5.NE.0) N3=N5
      DO 119 I=2,N3
      CALL LINE(IZ(I-1),IX(I-1),IZ(I),IX(I),2,-1)
119   CONTINUE
      IF(N6.NE.0) THEN
        N6P1=N6+1
        DO 129 I=N6P1,NTOT
        CALL LINE(IZ(I-1),IX(I-1),IZ(I),IX(I),2,-1)
129     CONTINUE
      ENDIF
      WRITE(*,240)
240   FORMAT(' *** HARD COPY *** ',\)
      READ(*,'(A1)') CK
      STOP
      END
C
C     **********
C
      SUBROUTINE ASSEM
      COMMON/POS/X(3500),Z(3500)
      COMMON KK,NDATA,CR,R
      CHARACTER*1 CR,R
      INTEGER*2 NUM,KK,NDATA,INZEN,I,J,K,NUMB
      INTEGER*2 N(6),DATA(6)
      CALL OUTZEN(R)
      CALL OUTZEN(CR)
      Z(NDATA)=RDTIME(1)
C
1000  KK=KK+1
      DO 50 J=1,12
50    NUM=INZEN(NUM)
60    NUM=INZEN(NUM)
      IF(NUM.NE.116) GO TO 60
      NUM=INZEN(NUM)
      NUM=INZEN(NUM)
```

```
      I=1
      N(I)=INZEN(NUM)-48
70    I=I+1
      N(I)=INZEN(NUM)-48
      IF(N(I).NE.-35) GO TO 70
      J=I-1
      NUMB=0
      I=0
      K=1
80    NUMB=NUMB+N(J-I)*K
      I=I+1
      K=K*10
      IF(I.LT.J) GO TO 80
C
C     NUMB IS THE NUMBER
C
      DATA(KK)=NUMB
      IF(KK.EQ.4) GO TO 90
      GO TO 1000
90    CONTINUE
C
C     FIND *
C
92    NUM=INZEN(NUM)
      IF(NUM.NE.42) GO TO 92
      X1=DATA(1)
      X2=DATA(2)
      X(NDATA)=(X1-X2)/(X1+X2+0.0001)
      RETURN
      END
C
      SUBROUTINE FIT(XX,ZZ,NB,NE,A,B,RS,SIG)
      DIMENSION XX(1),ZZ(1)
      INTEGER*2  NB,NE,I,NT
C
C     A IS THE INTERCEPT, B IS THE SLOPE OF A STRAIGHT LINE FIT
C
      XS=0.0
      ZS=0.0
      XZS=0.0
      XXS=0.0
      ZZS=0.0
      NT=NE-NB+1
      DO 100 I=NB,NE
      XS=XS+XX(I)
      ZS=ZS+ZZ(I)
      XZS=XZS+(XX(I)*ZZ(I))
      XXS=XXS+(XX(I)*XX(I))
      ZZS=ZZS+(ZZ(I)*ZZ(I))
100   CONTINUE
      A=((XZS*XS)-(ZS*XXS))/((XS*XS)-(NT*XXS))
      B=((ZS*XS)-(NT*XZS))/((XS*XS)-(NT*XXS))
      SSTO=ZZS-(ZS*ZS)/NT
```

```
      SSE=0.0
      DO 200 I=NB,NE
      ZHAT=A+B*XX(I)
      ZDIF=ZZ(I)-ZHAT
      SSE=SSE+(ZDIF*ZDIF)
200   CONTINUE
      RS=1-(SSE/SSTO)
      SIG=SQRT(SSE/(NT-2))
      RETURN
      END
```

```
C*************************************************************
C                                                            *
C      OPAUX1.FOR                                            *
C                                                            *
C      THIS IS AN INTERACTIVE GRAPHICS PROGRAM TO FILTER     *
C      DAT AND CAL FILES USING RUNNING MEAN METHOD           *
C                                                            *
C                  By SIBEL PAMUKCU                          *
C                                                            *
C            Latest revision : February 1986                 *
C                                                            *
C     STEP NO 1 ********************                         *
C                                                            *
C*************************************************************
C
C
      COMMON/POS/X(3500),Z(3500)
      COMMON/GRAPH/IX(3500),IZ(3500)
      COMMON/AUX/XS(3500),IXS(3500)
      INTEGER*2 IX,IZ,IXS,NDUM(20),ISM(20)
      INTEGER*2 I,J,K,L,NL,NB,NDP1,ND
      INTEGER*2 RFAC,IFLAG,NLAST
      CHARACTER*10 DATIN
      CHARACTER*1 CK
      CALL CLS
      WRITE(*,5)
5     FORMAT(' ENTER INPUT DATA FILE NAME ==> ',\)
      READ(*,'(A10)') DATIN
      OPEN(8,FILE=DATIN,STATUS='OLD',FORM='BINARY')
      IFLAG=1
500   CONTINUE
      WRITE(*,10) DATIN
10    FORMAT(' READING ',A10,'FILE ... PLEASE WAIT ')
      READ(8) RFAC,NLAST
      READ(8) A,B
      READ(8) ZBEG,XMAX,X1
      READ(8) (ND,X(I),Z(I),I=1,NLAST)
      CLOSE(8,STATUS='KEEP')
C
      CALL COLOR(2,-1)
      WRITE(*,35)
35    FORMAT(' PROCESSING... WAIT ',\)
      XNM=X(1)
      DO 40 I=1,NLAST
      IF(X(I).LE.XNM) XNM=X(I)
40    CONTINUE
      XDIF=X(NLAST)-XNM
      ZDIF=Z(NLAST)-Z(1)
      DO 45 I=1,NLAST
      IZ(I)=1+NINT(620*(Z(I)-Z(1))/ZDIF)
      IX(I)=220-NINT(220*(X(I)-XNM)/XDIF)
45    CONTINUE
```

```
50    CALL CLS
      DO 55 I=2,NLAST
      CALL LINE(IZ(I-1),IX(I-1),IZ(I),IX(I),4,-1)
55    CONTINUE
      DO 56 I=50,NLAST,50
      CALL PSET(IZ(I),IX(I),7)
56    CONTINUE
C
      CALL COLOR(7,-1)
      WRITE(*,58) NLAST
58    FORMAT(' TOTAL # OF DATA POINTS ARE ==> ',I5)
      WRITE(*,59)
59    FORMAT(' DOTS ARE LOCATED AT EVERY 50TH POINT ')
      WRITE(*,60)
60    FORMAT(' ENTER NUMBER OF RUNNING MEAN FACTOR CHANGES ==> ',\)
      READ(*,65) NL
65    FORMAT(I5)
      IF(NL.EQ.0) STOP
      WRITE(*,67)
67    FORMAT(' ENTER RMF AND CORRESPONDING DATA POINT (2I5)')
      I=0
68    I=I+1
      WRITE(*,71) I
      READ(*,69) ISM(I),NDUM(I)
      IF(I.EQ.NL) GO TO 72
      GO TO 68
71    FORMAT(I2,\)
69    FORMAT(2I5)
72    CONTINUE
      WRITE(*,35)
C
C     SMOOTH DATA USING ISM(I) POINT RUNNING MEAN
C
      K=0
70    K=K+1
      IF(K.EQ.1) THEN
        NB=1
        ELSE
        NB=NDUM(K-1)+1
      ENDIF
      DO 80 I=NB,NDUM(K)
      XTEMP=0.0
      J=0
75    XTEMP=XTEMP+X(I+J)
      J=J+1
      IF((I+J).GT.NLAST) ISM(K)=J
      IF(J.LT.ISM(K)) GO TO 75
      XS(I)=XTEMP/ISM(K)
80    CONTINUE
      IF(K.EQ.NL) THEN
       GO TO 85
       ELSE
       GO TO 70
```

```
      ENDIF
85    CONTINUE
      NDP1=NDUM(NL)+1
      IF(NDP1.EQ.NLAST) THEN
        XS(NLAST)=X(I)
        GO TO 100
      ENDIF
      IF(NDP1.GT.NLAST) GO TO 100
      DO 90 I=NDP1,NLAST
90    XS(I)=X(I)
100   CONTINUE
C
C     DRAW SMOOTH CURVE OVER THE ORIGINAL
C
      DO 95 I=1,NLAST
      IXS(I)=220-NINT(220*(XS(I)-XNM)/XDIF)
95    CONTINUE
      DO 96 I=2,NLAST
      CALL LINE(IZ(I-1),IXS(I-1),IZ(I),IXS(I),1,-1)
96    CONTINUE
      WRITE(*,110)
110   FORMAT(' ENTER "Y" TO RETRY ==> ',\)
      READ(*,'(A1)') CK
      IF(CK.EQ.'Y') GO TO 50
300   CONTINUE
      OPEN(8,FILE=DATIN,STATUS='OLD',FORM='BINARY')
      WRITE(8) RFAC,NLAST
      WRITE(8) A,B
      WRITE(8) ZBEG,XMAX,X1
      WRITE(8) (I,XS(I),Z(I),I=1,NLAST)
      CLOSE(8,STATUS='KEEP')
      IF(IFLAG.EQ.1) THEN
        CALL CLS
        WRITE(*,111)
111     FORMAT(' DO YOU WISH TO PROCESS ANOTHER FILE ? (Y/N) ==> ',\)
        READ(*,'(A1)') CK
        IF(CK.EQ.'Y') THEN
          WRITE(*,120)
120       FORMAT( ' ENTER NEW FILE NAME ==> ',\)
          READ(*,'(A10)') DATIN
          OPEN(8,FILE=DATIN,STATUS='OLD',FORM='BINARY')
          IFLAG=2
          GO TO 500
        ENDIF
      ENDIF
      STOP
      END
```

```
C*************************************************************
C                                                            *
C     OPAUX2.FOR                                             *
C                                                            *
C     THIS IS AN INTERACTIVE GRAPHICS PROGRAM TO             *
C     RELOCATE AND ADJUST DAT AND CAL CURVES                 *
C                                                            *
C                    By SIBEL PAMUKCU                        *
C                                                            *
C           Latest revision : February 1986                  *
C                                                            *
C     STEP NO 2 ********************                         *
C                                                            *
C*************************************************************
C
C
      COMMON/POS/X(3500),Y(3500)
      COMMON/CAL/XCAL(3500),YCAL(3500)
      COMMON/PLOT1/JX(3500),JY(3500)
      COMMON/PLOT2/IXC(3500),IYC(3500)
      INTEGER*2 I,J,JX,JY,NUM,NX,NY,IXC,IYC,IIX,IIY
      INTEGER*2 NT1,M,NL3,NT2,RFAC1,RFAC2,JIX,JIY,NXDIF,NYDIF
      CHARACTER*10 DATIN,DATCAL,DATOUT
      CHARACTER*1 CK
C
      CALL CLS
      WRITE(*,10)
10    FORMAT(' ENTER INPUT FILE NAME ==> ',\)
      READ(*,20) DATIN
20    FORMAT(A10)
      WRITE(*,30)
30    FORMAT(' ENTER CAL FILE NAME ==> ',\)
      READ(*,20) DATCAL
      WRITE(*,40)
40    FORMAT(' ENTER OUTPUT FILE NAME ==> ',\)
      READ(*,20) DATOUT
C
      OPEN(8,FILE=DATIN,STATUS='OLD',FORM='BINARY')
      WRITE(*,45) DATIN
45    FORMAT(' READING ',A10,'FILE... PLEASE WAIT ')
      READ(8) RFAC1,NT1
      READ(8) A1,B1
      READ(8) ZBEG,X1,X2
      READ(8) (I,X(I),Y(I),I=1,NT1)
      CLOSE(8,STATUS='KEEP')
      OPEN(8,FILE=DATCAL,STATUS='OLD',FORM='BINARY')
      WRITE(*,45) DATCAL
      READ(8) RFAC2,NT2
      READ(8) A2,B2
      READ(8) ZBEG,X1,X2
      READ(8) (I,XCAL(I),YCAL(I),I=1,NT2)
      CLOSE(8,STATUS='KEEP')
```

```
      CALL COLOR(2,-1)
      WRITE(*,48)
48    FORMAT(' PROCESSING ... WAIT ')
      CALL COLOR(7,-1)
C
C
      DO 200 I=2,NT1
      Y(I)=Y(I)-((X(I)-X(1))/B1)
      IF(Y(I).LT.Y(I-1)) Y(I)=Y(I-1)
200   CONTINUE
      DO 210 I=2,NT2
      YCAL(I)=YCAL(I)-((XCAL(I)-XCAL(1))/B2)
      IF(YCAL(I).LT.YCAL(I-1)) YCAL(I)=YCAL(I-1)
210   CONTINUE
      Y1=Y(1)
      YC1=YCAL(1)
      DO 300 I=1,NT1
      Y(I)=Y(I)-Y1
300   CONTINUE
      DO 310 I=1,NT2
      YCAL(I)=YCAL(I)-YC1
310   CONTINUE
C
C
      XMIN=X(1)
      YMIN=Y(1)
      XMAX=X(1)
      YMAX=Y(1)
      DO 50 I=1,NT1
      IF(Y(I).LT.YMIN) YMIN=Y(I)
      IF(X(I).LT.XMIN) XMIN=X(I)
      IF(Y(I).GT.YMAX) YMAX=Y(I)
      IF(X(I).GT.XMAX) XMAX=X(I)
50    CONTINUE
      DO 60 I=1,NT2
      IF(YCAL(I).LT.YMIN) YMIN=YCAL(I)
      IF(XCAL(I).LT.XMIN) XMIN=XCAL(I)
      IF(YCAL(I).GT.YMAX) YMAX=YCAL(I)
      XG=XMAX-XMIN
      YG=YMAX-YMIN
      CALL CLS
C
C     PLOTTING HERE
C
      CALL DRAW(Y,X,1,NT1,6,YG,XG,YMIN,XMIN,JX,JY)
      CALL DRAW(YCAL,XCAL,1,NT2,7,YG,XG,YMIN,XMIN,IXC,IYC)
      IIX=IXC(1)
      IIY=IYC(1)
      JIX=JX(1)
      JIY=JY(1)
C
90    CALL ZLOCOO(NX,NY,NUM)
      IF(NUM.EQ.69) GO TO 100
```

```
      IF(NUM.EQ.85.OR.NUM.EQ.68) THEN
        CALL VSHIFT(NY,NUM,NT1,NT2)
        CALL CLS
        DO 70 I=2,NT2
70      CALL LINE(IXC(I-1),IYC(I-1),IXC(I),IYC(I),7,-1)
        DO 75 I=2,NT1
        CALL LINE(JX(I-1),JY(I-1),JX(I),JY(I),4,-1)
75      CONTINUE
      ENDIF
        IF(NUM.EQ.76.OR.NUM.EQ.82) THEN
        CALL HSHIFT(NX,NUM,NT1,NT2)
        CALL CLS
        DO 80 I=2,NT2
80      CALL LINE(IXC(I-1),IYC(I-1),IXC(I),IYC(I),7,-1)
        DO 85 I=2,NT1
        CALL LINE(JX(I-1),JY(I-1),JX(I),JY(I),4,-1)
85      CONTINUE
      ENDIF
      GO TO 90
100   CONTINUE
      WRITE(*,48)
      NXDIF= JX(1)-JIX
      NYDIF= JY(1)-JIY
      YDIF=NXDIF*YG/400.
      XDIF=NYDIF*XG/150.
      DO 110 I=1,NT1
      X(I)=X(I)-XDIF
      Y(I)=Y(I)+YDIF
110   CONTINUE
      NXDIF=IXC(1)-IIX
      NYDIF=IYC(1)-IIY
      YDIF=NXDIF*YG/400.
      XDIF=NYDIF*XG/150.
      DO 111 I=1,NT2
      XCAL(I)=XCAL(I)-XDIF
      YCAL(I)=YCAL(I)+YDIF
111   CONTINUE
C
C
      OPEN(8,FILE=DATOUT,STATUS='NEW',FORM='BINARY')
      WRITE(8) RFAC1,RFAC2,NT1,NT2
      WRITE(8) A1,B1,A2,B2
      WRITE(8) (I,X(I),Y(I),I=1,NT1)
      WRITE(8) (I,XCAL(I),YCAL(I),I=1,NT2)
      CLOSE(8,STATUS='KEEP')
      STOP
      END
C
C     ********************************************************
C
      SUBROUTINE DRAW(XX,YY,NB,NE,ICOL,XSL,YSL,XM,YM,JX,JY)
      DIMENSION XX(1),YY(1),JX(1),JY(1)
      INTEGER*2 I,NB,NE,ICOL,JX,JY,NBP1
```

```
      NBP1=NB+1
      JX(NB)=75+NINT(400*(XX(NB)-XM)/XSL)
      JY(NB)=200-NINT(150*(YY(NB)-YM)/YSL)
      DO 100 I=NBP1,NE
      JX(I)=75+NINT(400*(XX(I)-XM)/XSL)
      JY(I)=200-NINT(150*(YY(I)-YM)/YSL)
      CALL LINE(JX(I-1),JY(I-1),JX(I),JY(I),ICOL,-1)
100   CONTINUE
      RETURN
      END
C
      SUBROUTINE VSHIFT(NY,NUM,NT1,NT2)
      COMMON/PLOT1/JX(3500),JY(3500)
      COMMON/PLOT2/IXC(3500),IYC(3500)
      INTEGER*2 NUM,NY,NDUM,MX,MY,I,NDIF,NT1,NT2
      INTEGER*2 JX,JY,IXC,IYC
C
      CALL ZLOCOO(MX,MY,NDUM)
      NDIF=IABS(NY-MY)
      IF(NUM.EQ.85) NDIF=-NDIF
      IF(NDUM.EQ.67) GO TO 150
      DO 100 I=1,NT1
      JY(I)=JY(I)+NDIF
100   CONTINUE
      GO TO 300
150   CONTINUE
      DO 200 I=1,NT2
      IYC(I)=IYC(I)+NDIF
200   CONTINUE
300   CONTINUE
      RETURN
      END
C
      SUBROUTINE HSHIFT(NX,NUM,NT1,NT2)
      COMMON/PLOT1/JX(3500),JY(3500)
      COMMON/PLOT2/IXC(3500),IYC(3500)
      INTEGER*2 NUM,NX,NDUM,MX,MY,I,NDIF,NT1,NT2
      INTEGER*2 JX,JY,IXC,IYC
C
      CALL ZLOCOO(MX,MY,NDUM)
      NDIF=IABS(NX-MX)
      IF(NUM.EQ.76) NDIF=-NDIF
      IF(NDUM.EQ.67) GO TO 150
      DO 100 I=1,NT1
      JX(I)=JX(I)+NDIF
100   CONTINUE
      GO TO 300
150   CONTINUE
      DO 200 I=1,NT2
      IXC(I)=IXC(I)+NDIF
200   CONTINUE
300   CONTINUE
      RETURN
```

```
C*************************************************************
C                                                            *
C     OPAUX3.FOR                                             *
C                                                            *
C     THIS IS AN INTERACTIVE GRAPHPICS PROGRAM TO            *
C     ANALYZE ANGULAR ROTATION DATA AND FIND FINAL           *
C     STRESS-STRAIN CURVE                                    *
C                                                            *
C                  By SIBEL PAMUKCU                          *
C                                                            *
C           Latest revision : February 1986                  *
C                                                            *
C     STEP NO 3  ******************                        *
C                                                            *
C*************************************************************
C
C
      COMMON/POS/X(3500),Z(3500)
      COMMON/CAL/XCAL(1500),ZCAL(1500)
      COMMON/NEW/XNEW(3000),ZNEW(3000)
      COMMON/GRAPH/IX(3500),IZ(3500)
      COMMON/AUX1/ANG(20),TOR(20),INFN(200),NP(3,10)
      COMMON/AUX2/KK(1200),NN(1200)
      INTEGER*2 IX,IZ,KK,I,J,K,L,LL,N,ICR,INS,NL,NLP,NF
      INTEGER*2 NT1,NT2,NL33,INFN,NDIV,NX,NY,IASC,NTEMP
      INTEGER*2 N1,N2,N3,N4,N5,NS,IP11,IP12,IP21,IP22
      INTEGER*2 NDUM,ND1,ND2,NC2,NW,NFIN,NN,LC,NSET,NP
      INTEGER*2 RFAC1,RFAC2,NT21,NUM,NAR,NAC,IMIN,NC1
      INTEGER*2 NXDIF,NZDIF,JIZ,JIX,N11,NFLAG,NP1,NP2,NP3
      CHARACTER*10 DATIN,DATOUT,DATSP
      CHARACTER*1 CK
      DATA PI,SHEAR/3.141592654,96.163/
C
C
C     READ IN USER SUPPLIED DATA
C
C
      CALL CLS
      WRITE(*,5)
5     FORMAT(' ENTER INPUT DATA FILE NAME ==> ',\)
      READ(*,'(A10)') DATIN
      WRITE(*,10)
10    FORMAT(' ENTER OUTPUT DATA FILE NAME ==> ',\)
```

```
      READ(*,'(A10)') DATOUT
      WRITE(*,20)
20    FORMAT(' ENTER SPRING CAL FILE NAME ==> ',\)
      READ(*,'(A10)') DATSP
      OPEN(8,FILE=DATIN,STATUS='OLD',FORM='BINARY')
C
C     READ IN FILTERED DATA AND CALIBRATION
C
      WRITE(*,30) DATIN
30    FORMAT(' READING ',A10,'FILE ... PLEASE WAIT ')
      READ(8) RFAC1,RFAC2,NT1,NT2
      READ(8) A1,B1,A2,B2
      READ(8) (I,X(I),Z(I),I=1,NT1)
      READ(8) (I,XCAL(I),ZCAL(I),I=1,NT2)
      CLOSE(8,STATUS='KEEP')
      OPEN(9,FILE=DATSP,STATUS='OLD')
      READ(9,40) DATSP,INS
      READ(9,50) (ANG(I),TOR(I),I=1,INS)
40    FORMAT(A10,I5)
50    FORMAT(2F10.4)
      CLOSE(9,STATUS='KEEP')
      CALL COLOR(2,-1)
      WRITE(*,55)
55    FORMAT(' PROCESSING... WAIT...')
C
C
C     USING VANE ROTATION SPEED DATA,AND DATA COLLECTION SPEED
C     DATA CALCULATE UNPROCESSED STRESS-STRAIN CURVES FOR THE SAMPLE
C     AND FOR THE SEALS
C
      X1=X(1)
      XC1=XCAL(1)
      Z1=Z(1)
      ZC1=ZCAL(1)
      BCAL1=(RFAC1*1.009997-7.629231)*0.001
      BCAL2=(RFAC2*1.009997-7.629231)*0.001
      RAD1=(BCAL1*PI)/(B1*180.)
      RAD2=(BCAL2*PI)/(B2*180.)
```

```
C
C
C     RAD IS RADIANS OF ROTATION PER UNIT DATA
C
C     DRAW CALIBRATION CURVE AND SAMPLE CURVE AND DETERMINE
C
C     CUT-OFF POINTS FOR FRICTION ELIMINATION FROM THE SAMPLE DATA
C
C
      XCM=0.0
      XNM=0.0
      ZZ=ZC1
      XX=XC1
      ONERAD=180./PI
      IF(Z1.LT.ZC1) ZZ=Z1
      IF(X1.LT.XC1) XX=X1
      X(1)=(X(1)-XX)*RAD1
      Z(1)=BCAL1*(Z(1)-ZZ)-(X(1)*ONERAD)
      DO 60 I=2,NT1
      X(I)=(X(I)-XX)*RAD1
      Z(I)=BCAL1*(Z(I)-ZZ)-(X(I)*ONERAD)
      IF(Z(I).LT.Z(I-1)) Z(I)=Z(I-1)
      IF(X(I).LT.XNM) XNM=X(I)
60    CONTINUE
      XCAL(1)=(XCAL(1)-XX)*RAD2
      ZCAL(1)=BCAL2*(ZCAL(1)-ZZ)-(XCAL(1)*ONERAD)
      DO 70 I=2,NT2
      XCAL(I)=(XCAL(I)-XX)*RAD2
      ZCAL(I)=BCAL2*(ZCAL(I)-ZZ)-(XCAL(I)*ONERAD)
      IF(ZCAL(I).LT.ZCAL(I-1)) ZCAL(I)=ZCAL(I-1)
      IF(XCAL(I).LT.XCM) XCM=XCAL(I)
70    CONTINUE
      ZNM=Z(1)
```

```
      IF(ZCAL(1).LT.ZNM) ZNM=ZCAL(I)
      DO 72 I=1,NT1
      Z(I)=Z(I)-ZNM
72    CONTINUE
      DO 73 I=1,NT2
      ZCAL(I)=ZCAL(I)-ZNM
73    CONTINUE
      XMIN=XNM
      IF(XCM.LT.XNM) XMIN=XCM
      XMAX=X(NT1)
      IF(XCAL(NT2).GT.X(NT1)) XMAX=XCAL(NT2)
      XG=XMAX-XMIN
      ZG=Z(NT1)-ZNM
C
C     READJUST EITHER CURVE FOR COINCIDENCE
C
90    CALL CLS
      CALL DRAW(XCAL,ZCAL,1,NT2,7,XG,ZG)
      CALL DRAW(X,Z,1,NT1,6,XG,ZG)
C
C     ****************************************
C
91    NFLAG=0
      CALL COLOR(7,-1)
      WRITE(*,92)
92    FORMAT(' DO YOU WISH TO READJUST ? (Y/N) ==> ',\)
      READ(*,'(A1)') CK
      IF(CK.EQ.'Y') THEN
        NFLAG=1
        JIX=IX(1)
        JIZ=IZ(1)
94      CALL ZLOCOO(NX,NY,IASC)
        IF(IASC.EQ.69) GO TO 99
        IF(IASC.EQ.85.OR.IASC.EQ.68) THEN
          DO 95 I=1,NT1
          CALL PRESET(IX(I),IZ(I),-1)
95        CONTINUE
          CALL VSHIFT(NY,IASC,NT1)
          DO 96 I=2,NT1
          CALL LINE(IX(I-1),IZ(I-1),IX(I),IZ(I),4,-1)
96        CONTINUE
        ENDIF
        IF(IASC.EQ.76.OR.IASC.EQ.82) THEN
          DO 97 I=1,NT1
          CALL PRESET(IX(I),IZ(I),-1)
97        CONTINUE
          CALL HSHIFT(NX,IASC,NT1)
          DO 98 I=2,NT1
          CALL LINE(IX(I-1),IZ(I-1),IX(I),IZ(I),4,-1)
98        CONTINUE
        ENDIF
        GO TO 94
99      CONTINUE
```

```
      WRITE(*,55)
      NXDIF=IX(1)-JIX
      NZDIF=IZ(1)-JIZ
      ZDIF=NZDIF*ZG/180.
      XDIF=NXDIF*XG/520.
      ZM=0.0
      XM=0.0
      DO 102 I=1,NT1
      X(I)=X(I)+XDIF
      Z(I)=Z(I)-ZDIF
      IF(X(I).LT.XM) XM=X(I)
      IF(Z(I).LT.ZM) ZM=Z(I)
102   CONTINUE
      IF(ZM.LT.0.0) THEN
        DO 105 I=1,NT1
        Z(I)=Z(I)-ZM
105     CONTINUE
        DO 106 I=1,NT2
        ZCAL(I)=ZCAL(I)-ZM
106     CONTINUE
      ENDIF
      IF(XM.LT.0.0) THEN
        DO 107 I=1,NT1
        X(I)=X(I)-XM
107     CONTINUE
        DO 108 I=1,NT2
        XCAL(I)=XCAL(I)-XM
108     CONTINUE
      ENDIF
      CALL CLS
      CALL ADJUST(NT1,NT2)
      CALL DRAW(XCAL,ZCAL,1,NT2,7,XG,ZG)
      CALL DRAW(X,Z,1,NT1,6,XG,ZG)
      GO TO 91
    ENDIF
C
C   ******************************************************
C
    IF(NFLAG.EQ.0) THEN
      CALL ADJUST(NT1,NT2)
    ENDIF
    WRITE(*,100)
100 FORMAT(' ENTER LOWER AND UPPER CUT-OFF POINTS')
    CALL ZLOCV(NF)
    ND1=NF
    CALL ZLOCV(NF)
    ND2=NF
    WRITE(*,80)
80  FORMAT(' MORE PROCESSING... PLEASE WAIT...')
    ZDIR=Z(ND1)
    CALL FINDER(ZCAL,ZDIR,ND1,1,NT2,NC1)
    ZDIR=Z(ND2)
    CALL FINDER(ZCAL,ZDIR,ND2,1,NT2,NC2)
```

```
C
C     CALCULATE CALIBRATION CURVE ADJUSTMENT NUMBER OF POINTS
C     CALCULATE THE ACTUAL STRESS-STRAIN CURVEOF THE SAMPLE
C     BY ELIMINATING FRICTION EFFECTS
C
      I=ND1-1
      J=NC1-1
      K=0
130   I=I+1
      J=J+1
      K=K+1
      XNEW(K)=X(I)
      IF(I.EQ.ND2) GO TO 140
      GO TO 130
140   CONTINUE
      NW=K
C
      I=ND2+1
      J=NC2
      L=1
      LC=1
      KK(L)=NW
      NN(LC)=NC2
      ICR=ND1-1
150   J=J+1
      IF(J.GT.NT2) GO TO 160
      CALL SUB(I,J,L,LC,KK,NN,ICR,NT1,ND2,NT2)
      GO TO 150
160   CONTINUE
      NAR=L
      NAC=LC
      NFIN=KK(NAR)
      CALL CLS
      WRITE(*,55)
      CALL CONNECT(KK,NN,NC2,NT2,ND2,NW)
      DO 165 I=1,NFIN
      ZDUM=ZNEW(I)
      CALL TORQ(ZDUM,TFAC)
      ZNEW(I)=SHEAR*TFAC/PI
165   CONTINUE
C
C     ISOLATE THE STRESS-STRAIN DIAGRAM
C
      ZMIN=ZNEW(1)
      DO 190 I=1,NFIN
      IF(ZNEW(I).LE.ZMIN) THEN
        ZMIN=ZNEW(I)
        XMIN=XNEW(I)
        IMIN=I
      ENDIF
190   CONTINUE
      XMIN=ABS(XMIN)
      I=0
```

```
      DO 200 J=IMIN,NFIN
      I=I+1
      ZNEW(I)=ZNEW(J)-ZMIN
      XNEW(I)=XNEW(J)-XMIN
200   CONTINUE
      NFIN=I
210   CONTINUE
      XG=XNEW(NFIN)-XNEW(1)
      ZG=ZNEW(NFIN)-ZNEW(1)
      CALL CLS
      CALL DRAW(XNEW,ZNEW,1,NFIN,6,XG,ZG)
      NL33=0
      NLP=0
      WRITE(*,220)
220   FORMAT(' BEGINING ADJUSTMENT ? (Y/N) ==> ',\)
      READ(*,'(A1)') CK
      IF(CK.EQ.'Y') NL33=1
      WRITE(*,222)
222   FORMAT(' INTERMEDIATE ADJUSTMENT ? (Y/N) ==> ',\)
      READ(*,'(A1)') CK
      IF(CK.EQ.'Y') NLP=1
C
C     BEGINNING ADJUSTMENT
C
      IF(NL33.EQ.1) THEN
        WRITE(*,230)
230     FORMAT(' ENTER BEGINING ADJ. LIMIT ')
        CALL ZLOCHV(NF)
        NL33=NF
        NDIV=NL33/20
        CALL SLOP(XNEW,ZNEW,NL33,INFN,NDIV,0.0001,NL33)
        XGT=XNEW(NL33)-XNEW(1)
        ZGT=ZNEW(NL33)-ZNEW(1)
        CALL CLS
        CALL DRAW(XNEW,ZNEW,1,NL33,3,XGT,ZGT)
        CALL RENK(NL33,INFN,N3)
        WRITE(*,55)
        XMIN=ABS(XNEW(N3))
        ZMIN=ZNEW(N3)
        I=0
        DO 250 J=N3,NFIN
        I=I+1
        ZNEW(I)=ZNEW(J)-ZMIN
        XNEW(I)=XNEW(J)-XMIN
250     CONTINUE
        NFIN=I
        XG=XNEW(NFIN)-XNEW(1)
        ZG=ZNEW(NFIN)-ZNEW(1)
      ENDIF
```

```
C
C     INTERMEDIATE ADJUSTMENT
C
      IF(NL33.NE.0) THEN
        CALL CLS
        CALL DRAW(XNEW,ZNEW,1,NFIN,6,XG,ZG)
      ENDIF
      IF(NLP.EQ.1) THEN
251     WRITE(*,252)
252     FORMAT(' ENTER NO OF PAIRS OF ADJ. LIMITS ==> ',\)
        READ(*,'(I2)') NLP
        K=0
254     K=K+1
        CALL ZLOCHV(NF)
        NP(1,K)=NF
        CALL ZLOCHV(NF)
        NP(2,K)=NF
        NP1=NP(1,K)-10
        NP2=NP(2,K)+10
        NP3=NP(1,K)+1
        IF(NP1.LT.2) NP1=2
        IF(NP2.GT.NFIN) NP2=NFIN
        DO 257 I=NP1,NP2
        CALL LINE(IX(I-1),IZ(I-1),IX(I),IZ(I),6,-1)
257     CONTINUE
        DO 253 I=NP3,NP(2,K)
        CALL LINE(IX(I-1),IZ(I-1),IX(I),IZ(I),4,-1)
253     CONTINUE
        IF(K.LT.NLP) GO TO 254
        WRITE(*,255)
255     FORMAT(' RETRY ? (Y/N) ==> ',\)
        READ(*,'(A1)') CK
        IF(CK.EQ.'Y') GO TO 251
        WRITE(*,55)
        K=0
        NTEMP=0
256     K=K+1
        IF(K.GT.NLP) GO TO 262
        NP(1,K)=NP(1,K)-NTEMP
        NP(2,K)=NP(2,K)-NTEMP
        NTEMP=NP(2,K)-NP(1,K)
        NFIN=NFIN-NTEMP
        XTEMP=XNEW(NP(2,K))-XNEW(NP(1,K))
        ZTEMP=ZNEW(NP(2,K))-ZNEW(NP(1,K))
        DO 258 I=1,NFIN
        IF(I.LT.NP(1,K)) THEN
          TEMPX=0.0
          TEMPZ=0.0
          J=I
        ELSE
          TEMPX=XTEMP
          TEMPZ=ZTEMP
          J=NTEMP+I
```

```
          ENDIF
          XNEW(I)=XNEW(J)-TEMPX
          ZNEW(I)=ZNEW(J)-TEMPZ
258       CONTINUE
          GO TO 256
262       CALL CLS
          XG=XNEW(NFIN)-XNEW(1)
          ZG=ZNEW(NFIN)-ZNEW(1)
          CALL DRAW(XNEW,ZNEW,1,NFIN,6,XG,ZG)
        ENDIF
C
C       END ADJUSTMENT
C
        WRITE(*,259)
259     FORMAT(' END ADJUSTMENT ? (Y/N) ==> ',\)
        READ(*,'(A1)') CK
        IF(CK.EQ.'Y') THEN
          WRITE(*,260)
260       FORMAT(' ENTER END ADJUSTMENT LIMIT ',\)
          CALL ZLOCHV(NF)
          NFIN=NF
          XG=XNEW(NFIN)-XNEW(1)
          ZG=ZNEW(NFIN)-ZNEW(1)
          CALL CLS
          CALL DRAW(XNEW,ZNEW,1,NFIN,6,XG,ZG)
        ENDIF
C
C       DRAW CARTESIAN COORDINATES
C
        IX(1)=75
        IZ(1)=200
        IX(NFIN)=75+NINT(520*XNEW(NFIN)/XG)
        IZ(NFIN)=200-NINT(180*ZNEW(NFIN)/ZG)
        CALL LINE(IX(1),IZ(NFIN),IX(1),IZ(1),3,-1)
        CALL LINE(IX(1),IZ(1),IX(NFIN),IZ(1),3,-1)
C
C       FIND STRAIGHT LINE CONSTANTS BY LEAST SQUARES METHOD
C
        WRITE(*,280)
280     FORMAT(' 1. LOCATE UPPER LIMIT FOR ENLARGEMENT ')
        WRITE(*,332)
332     FORMAT(' 2. LOCATE LOWER LIMIT FOR G2 ')
        CALL ZLOCV(NF)
        NL=NF
        CALL ZLOCV(NF)
        N2=NF
291     CALL CLS
        XG=XNEW(NL)-XNEW(1)
        ZG=ZNEW(NL)-ZNEW(1)
        CALL DRAW(XNEW,ZNEW,1,NL,4,XG,ZG)
        WRITE(*,292)
292     FORMAT(' ENTER LIMITS FOR REGRESSION ANALYSIS ')
        CALL ZLOCHV(NF)
```

```
      N11=NF
      CALL ZLOCHV(NF)
      N1=NF
      WRITE(*,55)
      N1=N1-N11+1
      N2=N2-N11+1
      NL=NL-N11+1
      NS=N1
      EPS=0.00001
      I=0
      XMIN=XNEW(N11)
      ZMIN=ZNEW(N11)
      DO 302 J=N11,NFIN
      I=I+1
      XNEW(I)=XNEW(J)-XMIN
      ZNEW(I)=ZNEW(J)-ZMIN
302   CONTINUE
      NFIN=I
      I=0
310   I=I+1
      IF(XNEW(I).LE.EPS) GO TO 310
      IF((I-1).LT.N1) THEN
        N1=N1-N1/3
        IF(N1.LE.50) THEN
          N1=NS
          EPS=0.00001+EPS
          IF(EPS.GT.0.0001) THEN
            CALL CLS
            CALL DRAW(XNEW,ZNEW,1,NL,4,XG,ZG)
            DO 312 I=10,NL,10
            CALL PSET(IX(I),IZ(I),2)
312         CONTINUE
            WRITE(*,320)
320   FORMAT(' EXCEEDED 10-2 % STRAIN, ',/,
     &'/ENTER NEW LOWER LIMIT (DOTS ARE AT EVERY 10TH POINT) ==> ',\)
            READ(*,'(I5)') N1
            WRITE(*,55)
            GO TO 330
          ENDIF
        ENDIF
        I=0
        GO TO 310
      ENDIF
330   CONTINUE
      EPS=XNEW(N1)
      CALL FIT(XNEW,ZNEW,1,N1,A1,B1,RS1,SIG1)
      CALL FIT(XNEW,ZNEW,N2,NFIN,A2,B2,RS2,SIG2)
      XG=XNEW(NFIN)-XNEW(1)
      ZG=ZNEW(NFIN)-ZNEW(1)
C
C     PREPARE FOR PLOTTING
C
      NSET=NFIN-N1
```

```
340   NSET=NSET-1
      N4=N1+NSET
      P12=A1+B1*XNEW(N4)
      IP12=200-NINT(180*P12/ZG)
      IF(IP12.LE.0) GO TO 340
      N5=N4/5
      P11=A1+B1*XNEW(1)
      IP11=200-NINT(180*P11/ZG)
      P21=A2+B2*XNEW(N5)
      IP21=200-NINT(180*P21/ZG)
      P22=A2+B2*XNEW(NFIN)
      IP22=200-NINT(180*P22/ZG)
C
      CALL CLS
      CALL DRAW(XNEW,ZNEW,1,NFIN,1,XG,ZG)
      CALL LINE(IX(1),IZ(NFIN),IX(1),IZ(1),3,-1)
      CALL LINE(IX(1),IZ(1),IX(NFIN),IZ(1),3,-1)
      CALL LINE(IX(1),IP11,IX(N4),IP12,2,-1)
      CALL LINE(IX(N5),IP21,IX(NFIN),IP22,2,-1)
C
      WRITE(*,350) B1,RS1,100*SIG1
350   FORMAT(' G1 ==> ',F9.3,/,' RS1 ==> ',F6.4,' SIG1 ==>',
     &F6.3,' %')
      WRITE(*,360) B2,RS2,100*SIG2
360   FORMAT(' G2 ==> ',F9.3,/,' RS2 ==> ',F6.4,' SIG2 ==>',
     &F6.3,' %')
      WRITE(*,370) EPS*100
370   FORMAT(' EPS ==> ',G15.8,' %')
      WRITE(*,380)
380   FORMAT(' RETRY ? (Y/N) ==> ',\)
      READ(*,'(A1)') CK
      IF(CK.EQ.'Y') THEN
        CALL CLS
        WRITE(*,272)
272     FORMAT(' FURTHER ADJUSTMENT (Y/N) ==> ',\)
        READ(*,'(A1)') CK
        IF(CK.EQ.'Y') GO TO 210
        IF(CK.NE.'Y') GO TO 291
      ENDIF
C
C     FIGURE THE INTERSECTION POINT AND INITIAL STRAIN RESOLUTION
C
      XINT=(A1-A2)/(B2-B1)
      ZINT=A1+B1*XINT
      ETOT=0.0
      DO 410 I=1,10
      EDIF=ABS(XNEW(I+1)-XNEW(I))
      ETOT=ETOT+EDIF
410   CONTINUE
      XNMIN=ETOT/10
      WRITE(*,400) XINT*100,ZINT,XNMIN*100
400   FORMAT(' XINT ==>',G15.8,' %',' ZINT ==>',F8.4,/,
     &' XMIN ==>',G15.8,' %')
```

```
      WRITE(*,420) XNEW(NFIN)*100,ZNEW(NFIN)
420   FORMAT(' STR RANGE ==>', G15.8,'%',/,
     &' STS RANGE ==>',F8.4,' KPA')
C
      OPEN(9,FILE=DATOUT,STATUS='NEW',FORM='BINARY')
      WRITE(9) NFIN,A1,B1,A2,B2
      WRITE(9) EPS,XINT,ZINT
      WRITE(9) RS1,SIG1,RS2,SIG2
      WRITE(9) (K,XNEW(K),ZNEW(K),K=1,NFIN)
      CLOSE(9,STATUS='KEEP')
      STOP
      END
C
C     ************************************************************
C
C     CALCULATE SLOPE CHANGES ON SAMPLE DATA
C
      SUBROUTINE SLOP(XX,ZZ,NT,INF,M,EPS,NL3)
      DIMENSION XX(1),ZZ(1)
      INTEGER*2 M,INF,I,K,L,NT,NL3
      DIMENSION SLOPE(3),INF(50)
      K=0
      I=1
      SLOPE(1)=(XX(M)-XX(1))/(ZZ(M)-ZZ(1))
300   I=I+1
      L=M*I
      IF(L.GE.(NT-M)) GO TO 310
      IF(L.GT.NL3) EPS=10*EPS
      SLOPE(2)=(XX(L)-XX(L-M))/(ZZ(L)-ZZ(L-M))
      SSD=ABS(SLOPE(2)-SLOPE(1))
      IF(SSD.GT.EPS) THEN
      K=K+1
      INF(K)=L-M
      ENDIF
      SLOPE(1)=SLOPE(2)
      GO TO 300
310   CONTINUE
      SLOPE(2)=(XX(L)-XX(L-M))/(ZZ(L)-ZZ(L-M))
      SSD=ABS(SLOPE(2)-SLOPE(1))
      IF(SSD.GT.EPS) THEN
      K=K+1
      INF(K)=L-M
      ENDIF
      SLOPE(1)=SLOPE(2)
      SLOPE(2)=(XX(NT)-XX(L))/(ZZ(NT)-ZZ(L))
      SSD=ABS(SLOPE(2)-SLOPE(1))
      IF(SSD.GT.EPS) THEN
      K=K+1
      INF(K)=L
      ENDIF
      RETURN
      END
C
```

```
      SUBROUTINE DRAW(XX,ZZ,NB,NE,ICOL,XG,ZG)
      DIMENSION XX(1),ZZ(1)
      COMMON/GRAPH/IX(3500),IZ(3500)
      INTEGER*2 NB,NE,ICOL,I,NBP1,IX,IZ
      IX(NB)=75+NINT(520*XX(NB)/XG)
      IZ(NB)=200-NINT(180*ZZ(NB)/ZG)
      NBP1=NB+1
      DO 100 I=NBP1,NE
      IX(I)=75+NINT(520*XX(I)/XG)
      IZ(I)=200-NINT(180*ZZ(I)/ZG)
      CALL LINE(IX(I-1),IZ(I-1),IX(I),IZ(I),ICOL,-1)
100   CONTINUE
      RETURN
      END
C
C     DRAW CURVE WITH SLOPE CHANGE AREAS IN DIFFERENT COLOR
C
      SUBROUTINE RENK(NT,INF,N1)
      COMMON/GRAPH/IX(3500),IZ(3500)
      INTEGER*2 NT,INF(50),N1,IX,IZ
      INTEGER*2 I,L,IFLAG,ICOL
      CHARACTER*1 CK
      I=1
      ICOL=0
      IFLAG=0
      L=0
380   L=L+1
      ICOL=ICOL+1
      IF(ICOL.GT.7) THEN
      IFLAG=IFLAG+1
      ICOL=L-IFLAG*7
      ENDIF
390   I=I+1
      CALL LINE(IX(I-1),IZ(I-1),IX(I),IZ(I),ICOL,-1)
      IF(I.EQ.INF(L)) THEN
      CALL COLOR(ICOL,-1)
      WRITE(*,60) INF(L)
60    FORMAT(I5,\)
      READ(*,'(A1)') CK
      GO TO 380
      ENDIF
      IF(I.EQ.NT) GO TO 400
      GO TO 390
400   CONTINUE
      CALL COLOR(ICOL,-1)
      WRITE(*,60) NT
      READ(*,'(A1)') CK
      CALL COLOR(7,-1)
      WRITE(*,70)
70    FORMAT(' ENTER LOWER CUT-OFF POINT ==> ',\)
      READ(*,40) N1
40    FORMAT(I5)
      DO 45 I=1,L
```

```
      INF(I)=0
45    CONTINUE
      RETURN
      END
C
C     FIND THE BEGINING AND END POINTS FOR INITIAL CORRESPONDENCE
C
      SUBROUTINE FINDER(ZZ,ZDIR,NST,NB,NE,NFIN)
      DIMENSION ZZ(1)
      INTEGER*2 NB,NE,NFIN,I,NST
      I=NST
      IF(ZZ(I).GT.ZDIR) GO TO 100
      IF(ZZ(I).LT.ZDIR) GO TO 200
      IF(ZZ(I).EQ.ZDIR) GO TO 500
100   I=I-1
      IF(I.EQ.NB) GO TO 500
      IF(ZZ(I).GT.ZDIR) GO TO 100
      GO TO 500
200   I=I+1
      IF(I.EQ.NE) GO TO 500
500   CONTINUE
      NFIN=I
      RETURN
      END
C
C     FIGURE OUT THE CORRESPONDING POINTS ON DATA CURVE TO
C     SUBTRACT THE CAL CURVE FROM
C
      SUBROUTINE SUB(I,J,L,LC,KK,NN,ICR,NT1,ND2,NT2)
      COMMON/POS/X(3500),Z(3500)
      COMMON/CAL/XCAL(1500),ZCAL(1500)
      COMMON/NEW/XNEW(3000),ZNEW(3000)
      DIMENSION KK(1),NN(1)
      INTEGER*2 I,J,L,LC,LL,JJ,KK,NN,NM,NT1,ND2,ICR,NT2
      XFIN=X(I)-XCAL(J)
      IF(XFIN.EQ.0.0) GO TO 300
      LL=NINT(XFIN/ABS(XFIN))
      IF(LL.LT.0.AND.J.EQ.NT2.AND.I.EQ.NT1) THEN
        ZDIF=Z(NT1)-Z(NT1-1)
        XDIF=X(NT1)-X(NT1-1)
        ZINC=ZDIF/XDIF
        NT1=NT1+1
        X(NT1)=XCAL(NT2)
        XDIF=X(NT1)-X(NT1-1)
        Z(NT1)=Z(NT1-1)+(XDIF*ZINC)
        L=L+1
        LC=LC+1
        NN(LC)=NT2
        KK(L)=NT1-ICR
        XNEW(KK(L))=X(NT1)
        ZNEW(KK(L))=Z(NT1)-ZCAL(NT2)
        GO TO 400
      ENDIF
```

```
100   I=I-LL
      IF(I.LE.ND2) GO TO 400
      XFY=X(I)-XCAL(J)
      IF(XFY.EQ.0.0) THEN
         JJ=0
      ELSE
         JJ=NINT(XFY/ABS(XFY))
      ENDIF
      IF(JJ.EQ.LL) GO TO 100
      IF(JJ.GT.0) NM=I-1
      IF(JJ.LE.0) NM=I
      QDIF=XCAL(J)-X(NM)
      PDIF=X(NM+1)-XCAL(J)
      IF(PDIF.GT.QDIF) THEN
        IF((NM-ICR).LE.KK(L)) GO TO 400
      ELSE
        IF(((NM+1)-ICR).LE.KK(L)) GO TO 400
      ENDIF
      L=L+1
      LC=LC+1
      NN(LC)=J
      ZDIF=Z(NM+1)-Z(NM)
      XDIF=X(NM+1)-X(NM)
      ZINC=QDIF*ZDIF/XDIF
      ZINT=Z(NM)+ZINC
      IF(PDIF.GT.QDIF) THEN
        KK(L)=(NM)-ICR
        XNEW(KK(L))=X(NM)+QDIF
        X(NM)=X(NM)+QDIF
        Z(NM)=ZINT
      ELSE
        KK(L)=(NM+1)-ICR
        XNEW(KK(L))=X(NM+1)-PDIF
        X(NM+1)=X(NM+1)-PDIF
        Z(NM+1)=ZINT
      ENDIF
300   IF(XFIN.EQ.0.0) THEN
        IF((I-ICR).LE.KK(L)) GO TO 400
        L=L+1
        LC=LC+1
        NN(LC)=J
        KK(L)=I-ICR
        XNEW(KK(L))=X(I)
        ZINT=Z(I)
      ENDIF
      ZNEW(KK(L))=ZINT-ZCAL(J)
400   CONTINUE
      RETURN
      END
```

```
C
C     ADJUST THE LENGTH OF THE CALIBRATION CURVE
C
      SUBROUTINE ADJUST(NT1,NT2)
      COMMON/POS/X(3500),Z(3500)
      COMMON/CAL/XCAL(1500),ZCAL(1500)
      INTEGER*2 I,NN,NT2,NT1
      XCOR=XCAL(NT2)-X(NT1)
      IF(XCOR.EQ.0.0) GO TO 300
      COR=ABS(XCOR)
      XP=XCAL(NT2)
      I=NT2
100   I=I-1
      XTEMP=ABS(XP-XCAL(I))
      IF(COR.GT.XTEMP) GO TO 100
      XINC=XTEMP-COR
      ZINC=(ZCAL(I+1)-ZCAL(I))/(XCAL(I+1)-XCAL(I))
      ZINT=ZINC*XINC
      ZCOR=ZCAL(I)+ZINT
      IF(XCOR.GT.0.0) THEN
        NT2=I+1
        XCAL(NT2)=XCAL(I)+XINC
        ZCAL(NT2)=ZCAL(I)+ZINT
      ENDIF
      IF(XCOR.LT.0.0) THEN
        NN=NT2-I
        ZINC=(ZCAL(NT2)-ZCOR)/NN
        XINC=COR/NN
        I=0
200     I=I+1
        IF(I.GT.NN) GO TO 250
        XCAL(NT2+I)=XCAL(NT2)+I*XINC
        ZCAL(NT2+I)=ZCAL(NT2)+I*ZINC
        GO TO 200
250     NT2=NT2+NN
      ENDIF
300   CONTINUE
      RETURN
      END
C
C     FIGURE OUT THE POSITION OF REMAINING POINTS ON SAMPLE CURVE
C     BY EXTRAPOLATION BETWEEN KK(L) POINTS
C
      SUBROUTINE CONNECT(KK,NN,NC2,NT2,ND2,NW)
      COMMON/POS/X(3500),Z(3500)
      COMMON/CAL/XCAL(1500),ZCAL(1500)
      COMMON/NEW/XNEW(3000),ZNEW(3000)
      INTEGER*2 KK,NC2,NT2,J,K,L,N,NUM,ND2,NW,LC,NN
      DIMENSION KK(1),NN(1)
      L=0
      LC=0
      J=ND2
      K=NW
```

```
500   LC=LC+1
      IF(NN(LC).EQ.NT2) GO TO 498
      L=L+1
      ZDIF=ZCAL(NN(LC+1))-ZCAL(NN(LC))
      NUM=KK(L+1)-KK(L)
      IF(NUM.EQ.1) GO TO 495
      IF(NUM.LE.0) THEN
      GO TO 500
      ENDIF
      ZINC=ZDIF/NUM
      N=1
490   J=J+1
      K=K+1
      XNEW(K)=X(J)
      ZNEW(K)=Z(J)-(ZCAL(NN(LC))+N*ZINC)
      IF(N.EQ.NUM) GO TO 500
      N=N+1
      GO TO 490
495   CONTINUE
      K=K+1
      J=J+1
      XNEW(K)=X(J)
      ZNEW(K)=Z(J)-ZCAL(NN(LC+1))
      GO TO 500
498   CONTINUE
      RETURN
      END
C
C     LEAST SQUARES FOR LINEAR FIT
C
      SUBROUTINE FIT(XX,ZZ,NB,NE,A,B,RS,SIG)
      DIMENSION XX(1),ZZ(1)
      INTEGER*2  NB,NE,I,NT
C
C     A IS THE INTERCEPT, B IS THE SLOPE OF A STRAIGHT LINE FIT
C
      XS=0.0
      ZS=0.0
      XZS=0.0
      XXS=0.0
      ZZS=0.0
      NT=NE-NB+1
      DO 100 I=NB,NE
      XS=XS+XX(I)
      ZS=ZS+ZZ(I)
      XZS=XZS+(XX(I)*ZZ(I))
      XXS=XXS+(XX(I)*XX(I))
      ZZS=ZZS+(ZZ(I)*ZZ(I))
100   CONTINUE
      A=((XZS*XS)-(ZS*XXS))/((XS*XS)-(NT*XXS))
      B=((ZS*XS)-(NT*XZS))/((XS*XS)-(NT*XXS))
      SSTO=ZZS-(ZS*ZS)/NT
      SSE=0.0
```

```
      DO 200 I=NB,NE
      ZHAT=A+B*XX(I)
      ZDIF=ZZ(I)-ZHAT
      SSE=SSE+(ZDIF*ZDIF)
200   CONTINUE
      RS=1-(SSE/SSTO)
      SIG=SQRT(SSE/(NT-2))
      RETURN
      END
C
C     FIND SPRING CONSTANT FOR STRESS
C
      SUBROUTINE TORQ(ZDUM,TFAC)
      COMMON/AUX1/ANG(20),TOR(20),INFN(200),NP(3,10)
      INTEGER*2 J,INFN,NP
      J=0
10    J=J+1
      IF(ZDUM.GT.ANG(J)) GO TO 10
      IF(J.EQ.1) I=2
      ADIF=ANG(J)-ANG(J-1)
      TDIF=TOR(J)-TOR(J-1)
      TDUM=(ZDUM-ANG(J-1))*TDIF/ADIF
      TFAC=TOR(J-1)+TDUM
      RETURN
      END
C
C     SHIFT DATA HORIZONTALLY
C
      SUBROUTINE HSHIFT(NX,IASC,NT)
      COMMON/GRAPH/IX(3500),IZ(3500)
      INTEGER*2 IX,IZ,IASC,NX,MX,MY,I,NDIF,NT,NDUM
C
      CALL ZLOCOO(MX,MY,NDUM)
      NDIF=IABS(NX-MX)
      IF(IASC.EQ.76) NDIF=-NDIF
      DO 100 I=1,NT
      IX(I)=IX(I)+NDIF
100   CONTINUE
      RETURN
      END
C
C     SHIFT DATA VERTICALLY
C
      SUBROUTINE VSHIFT(NY,IASC,NT)
      COMMON/GRAPH/IX(3500),IZ(3500)
      INTEGER*2 IX,IZ,IASC,NY,MX,MY,I,NDIF,NT,NDUM
C
      CALL ZLOCOO(MX,MY,NDUM)
      NDIF=IABS(NY-MY)
      IF(IASC.EQ.85) NDIF=-NDIF
      DO 100 I=1,NT
      IZ(I)=IZ(I)+NDIF
100   CONTINUE
```

```
      RETURN
      END
C
C     FIND CROSS HAIR POSITION (VERTICAL AND HORIZONTAL)
C
      SUBROUTINE ZLOCHV(NF)
      INTEGER*2 NX,NY,NF,I,IZ,IX,IASC
      COMMON/GRAPH/IX(3500),IZ(3500)
      CALL ZLOCOO(NX,NY,IASC)
      I=0
240   I=I+1
      IF(IZ(I).GE.NY) GO TO 240
      IF(IX(I).LE.NX) GO TO 240
      NF=I-1
      RETURN
      END
C
C     FIND CROSS HAIR POSITION (VERTICAL)
C
      SUBROUTINE ZLOCV(NF)
      INTEGER*2 NX,NY,NF,I,IZ,IX,IASC
      COMMON/GRAPH/IX(3500),IZ(3500)
      CALL ZLOCOO(NX,NY,IASC)
      I=0
240   I=I+1
      IF(IZ(I).GE.NY) GO TO 240
      NF=I-1
      RETURN
      END
```

```
C*************************************************************
C                                                            *
C     RESON.FOR                                              *
C                                                            *
C     THIS IS A FORTRAN PROGRAM TO REDUCE AND PLOT           *
C     RESONANT COLUMN DATA                                   *
C                                                            *
C                  By SIBEL PAMUKCU                          *
C                                                            *
C           Latest revision : February 1986                  *
C                                                            *
C                                                            *
C*************************************************************
C
C
      COMMON/OUT/G(50),STA(50),DAMP(50),STAD(50),F(50)
      COMMON/DAT/T(50),TD(50),A1(50),A1D(50),AMP(50,50)
      COMMON/GRAPH/IX(1000),IY(1000),ISTA(50),IG(50),ID(50)
      COMMON/FITT/X1(50),Y1(50),X(1000),Y(1000)
      REAL LEN,JO,J1,JS
      INTEGER*2 I,J,JLAST(50),NDAMP,NLAST,KFLAG
      INTEGER*2 MIS,NLM1,IX,IY,ISTA,IG,ID,N
      CHARACTER*10 DATIN,DATOUT
      CHARACTER*1 CK
      DATA PI,GO,JO,ACF/3.141592,980.66,28.44,28./
C
C     GO IS ACCELERATION OF GRAVITY IN  CM/SEC2
C     JO IS POLAR MOMENT OF INERTIA OF THE DRIVING END IN GM-CM-SEC2
C     (FOR 3.57 CM DIAM SPECIMEN, CHANGE JO TO 29.97 FOR 7.11 CM DIAM)
C     ACF IS ACCELERATION CALIBRATION FACTOR IN PK-MV/PK-G
C
C     READ IN USER SUPPLIED DATA
C
      CALL CLS
      WRITE(*,10)
10    FORMAT(' ENTER INPUT DATA FILE NAME ==> ',\)
      READ(*,'(A10)') DATIN
      WRITE(*,15)
15    FORMAT(' ENTER OUTPUT DATA FILE NAME ==> ',\)
      READ(*,'(A10)') DATOUT
      OPEN(9,FILE=DATIN,STATUS='OLD')
      READ(9,25) DATIN
25    FORMAT(A10)
      READ(9,20) NLAST,DIAM,LEN,WW,WC,DEN
20    FORMAT(I5,5F10.5)
      READ(9,22) NDAMP
22    FORMAT(I5)
      READ(9,30)  (I,T(I),A1(I),I=1,NLAST)
30    FORMAT(I5,2F10.5)
      IF(NDAMP.EQ.0) GO TO 70
      I=0
50    I=I+1
```

```
      READ(9,55) I,TD(I),A1D(I),JLAST(I)
      READ(9,65) (AMP(I,J),J=1,JLAST(I))
      IF(I.EQ.NDAMP) GO TO 70
      GO TO 50
70    CONTINUE
55    FORMAT(I5,2F10.5,I5)
65    FORMAT(5F5.2)
      CLOSE(9,STATUS='KEEP')
C
      WC=WC/100
      VOL=PI*DIAM*DIAM*LEN/4
      J1= (WW*DIAM*DIAM)/(8.*GO)
      JS=J1/JO
      B=SQRT(JS)
      I=0
80    I=I+1
      A=JS-B*TAN(B)
      B=B+A
      IF(ABS(A).LT.0.000001) GO TO 90
      GO TO 80
90    CONTINUE
      C2=DEN*((2*PI*LEN/B)**2)
      S2=3.68714*(DIAM/LEN)/ACF
C
      DO 100 I=1,NLAST
      F(I)=1000/T(I)
      IF(F(I).LE.5.0) A1(I)=A1(I)*2.828
      G(I)=C2*F(I)*F(I)/98066.
      STA(I)=S2*A1(I)/(F(I)*F(I))
100   CONTINUE
      GMIN=G(NLAST)
      STM=STA(NLAST)
      STAM=STA(1)
      DO 101 I=1,NLAST
      IF(G(I).LT.GMIN) GMIN=G(I)
      IF(STA(I).GT.STM) STM=STA(I)
      IF(STA(I).LT.STAM) STAM=STA(I)
101   CONTINUE
      IF(NDAMP.EQ.0) GO TO 118
C
      DO 110 I=1,NDAMP
      FD=1000/TD(I)
      STAD(I)=S2*A1D(I)/(FD*FD)
      AMPO=AMP(I,1)
      DAMP(I)=0.0
      MIS=0
      DO 120 J=2,JLAST(I)
      IF(AMP(I,J).EQ.0.0) THEN
        MIS=MIS+1
        GO TO 115
      ENDIF
      DUM=(ALOG(AMPO/AMP(I,J)))/(2*PI*(J-1))
      DAMP(I)=DAMP(I)+DUM
```

```
115   CONTINUE
120   CONTINUE
      DAMP(I)=(DAMP(I)/(JLAST(I)-(1+MIS)))*100
110   CONTINUE
118   CONTINUE
C
C
C     CURVE FITTING AND ESTIMATION OF GMAX
C
      DO 150 I=2,NLAST
      Y1(I-1)=(STA(I)-STA(1))/(G(I)-G(1))
      X1(I-1)=STA(I)
150   CONTINUE
      NLM1=NLAST-1
      CALL FIT(X1,Y1,1,NLM1,AA1,BB1,RS1,SIG1)
      AF1=(AA1*AA1)/(AA1+BB1*STA(1))
      BF1=(AA1*BB1)/(AA1+BB1*STA(1))
      GMAX1=G(1)-(STA(1)/(AF1+BF1*STA(1)))
      GG=GMAX1
      DO 152 I=1,NLAST
      IF(G(I).GT.GG) GG=G(I)
152   CONTINUE
      XINC=0.000001
      I=1
      X(1)=0.000001
      IF(STAM.LT.X(1)) THEN
155     X(1)=X(1)/10
        XINC=X(1)
        IF(STAM.LT.X(1)) GO TO 155
      ENDIF
      KFLAG=0
      Y(1)=GMAX1+(X(1)/(AF1+BF1*X(1)))
160   I=I+1
      X(I)=X(I-1)+XINC
      Y(I)=GMAX1+(X(I)/(AF1+BF1*X(I)))
      IF(Y(I).LT.0.0) THEN
        I=I-1
        KFLAG=1
        GO TO 162
      ENDIF
      IF(X(I).EQ.(10.*XINC)) XINC=XINC*10.
      IF(Y(I).LE.(0.85*GMIN).OR.X(I).GE.(2.0*STM)) GO TO 162
      GO TO 160
162   CONTINUE
      N=I
      DO 164 I=1,N
      X(I)=ALOG10(X(I))
164   CONTINUE
      XDIF=X(N)-X(1)
      YDIF=Y(1)-Y(N)
      IF(KFLAG.EQ.1) THEN
       XDIF=ALOG10(STM)-ALOG10(STAM)+0.5
       YDIF=GG-0.85*GMIN
```

```
      ENDIF
      CALL CLS
      CALL LINE(50,215,620,215,3,-1)
      CALL LINE(50,30,50,215,3,-1)
      CALL DRAW(X,Y,1,N,1,XDIF,YDIF)
      DO 170 I=1,NLAST
      DUM=ALOG10(STA(I))
      ISTA(I)=50+NINT(550*(DUM-X(1))/XDIF)
      IG(I)=40+NINT(175*(Y(1)-G(I))/YDIF)
      CALL PSET(ISTA(I),IG(I),2)
      CALL CIRCLE(ISTA(I),IG(I),5,4,-1.,-1.,-1.,-1,-1)
170   CONTINUE
      XP=X(1)
      I=0
172   I=I+1
      DUM=ABS(X(I)-XP)
      IF(DUM.LE.0.000001.OR.X(I).EQ.XP) THEN
      CALL LINE(IX(I),208,IX(I),212,4,-1)
      XP=XP+1.
      ENDIF
      IF(I.EQ.N) GO TO 173
      GO TO 172
173   CONTINUE
      XDUM1=100*(10**X(1))
      XDUM2=100*(10**X(N))
      WRITE(*,174) GMAX1,Y(N)
174   FORMAT(' GMAX ==> ',F10.3,2X,'GLAST ==> ',F10.3)
      WRITE(*,175) XDUM1,XDUM2
175   FORMAT(' ST1 ==> ',G15.7,' % ',2X,' STN ==> ',G15.7,' % ')
C
      READ(*,'(A1)') CK
      OPEN(9,FILE=DATOUT,STATUS='NEW')
      WRITE(9,122) DATOUT
122   FORMAT(A10)
      WRITE(9,124)
      WRITE(9,130) (I,STA(I),G(I),I=1,NLAST)
130   FORMAT(I5,G15.7,F15.3)
      WRITE(9,140)
      IF(NDAMP.EQ.0) GO TO 136
      WRITE(9,132)
      WRITE(9,133) (I,STAD(I),DAMP(I),I=1,NDAMP)
136   CONTINUE
      WRITE(9,135) GMAX1,RS1,100*SIG1
135   FORMAT(/,' GMAX ==> ',F10.3,/,' RS ==> ',F10.6,/,
     &' DEVIATION ==> ',G15.7,' % ')
124   FORMAT(/,'          STRAIN          G (KPA) ')
132   FORMAT(/,'          STRAIN',4X,'    DAMPING RATIO %')
133   FORMAT(I5,G15.8,4X,G15.8)
140   FORMAT(/,' ********************************************',/)
      STOP
      END
```

```
C     ****************************************
C
      SUBROUTINE FIT(XX,ZZ,NB,NE,A,B,RS,SIG)
      DIMENSION XX(1),ZZ(1)
      INTEGER*2 NB,NE,NT,I
      XS=0.0
      ZS=0.0
      XZS=0.0
      XXS=0.0
      ZZS=0.0
      NT=NE-NB+1
      DO 100 I=NB,NE
      XS=XS+XX(I)
      ZS=ZS+ZZ(I)
      XZS=XZS+(XX(I)*ZZ(I))
      ZZS=ZZS+(ZZ(I)*ZZ(I))
      XXS=XXS+(XX(I)*XX(I))
100   CONTINUE
      A=((XZS*XS)-(ZS*XXS))/((XS*XS)-(NT*XXS))
      B=((ZS*XS)-(NT*XZS))/((XS*XS)-(NT*XXS))
      SSTO=ZZS-(ZS*ZS)/NT
      SSE=0.0
      DO 200 I=NB,NE
      ZHAT=A+B*XX(I)
      ZDIF=ZZ(I)-ZHAT
      SSE=SSE+(ZDIF*ZDIF)
200   CONTINUE
      RS=1.-(SSE/SSTO)
      SIG=SQRT(SSE/(NT-2))
      RETURN
      END
C
      SUBROUTINE DRAW(XX,ZZ,NB,NE,ICOL,XG,ZG)
      DIMENSION XX(1),ZZ(1)
      COMMON/GRAPH/IX(1000),IY(1000),ISTA(50),IG(50),ID(50)
      INTEGER*2 NB,NE,ICOL,NBP1,IX,IY,I,ISTA,IG,ID
      NBP1=NB+1
      DO 100 I=NB,NE
      IX(I)=50+NINT(550*(XX(I)-XX(1))/XG)
      IY(I)=40+NINT(175*(ZZ(1)-ZZ(I))/ZG)
100   CONTINUE
      DO 200 I=NBP1,NE
      CALL LINE(IX(I-1),IY(I-1),IX(I),IY(I),ICOL,-1)
200   CONTINUE
      RETURN
      END
```

APPENDIX C

EXPERIMENTAL CURVES

CONSOLIDATION DATA AND FITTED MODEL

Cv DATA

TYPICAL PORE WATER PRESSURE DISSIPATION CURVES

TYPICAL VOLUME CHANGE CURVES

MOTOR SPEED VERSUS ANGULAR ROTATION VARIATION

LOAD-SPRING CALIBRATION CURVES

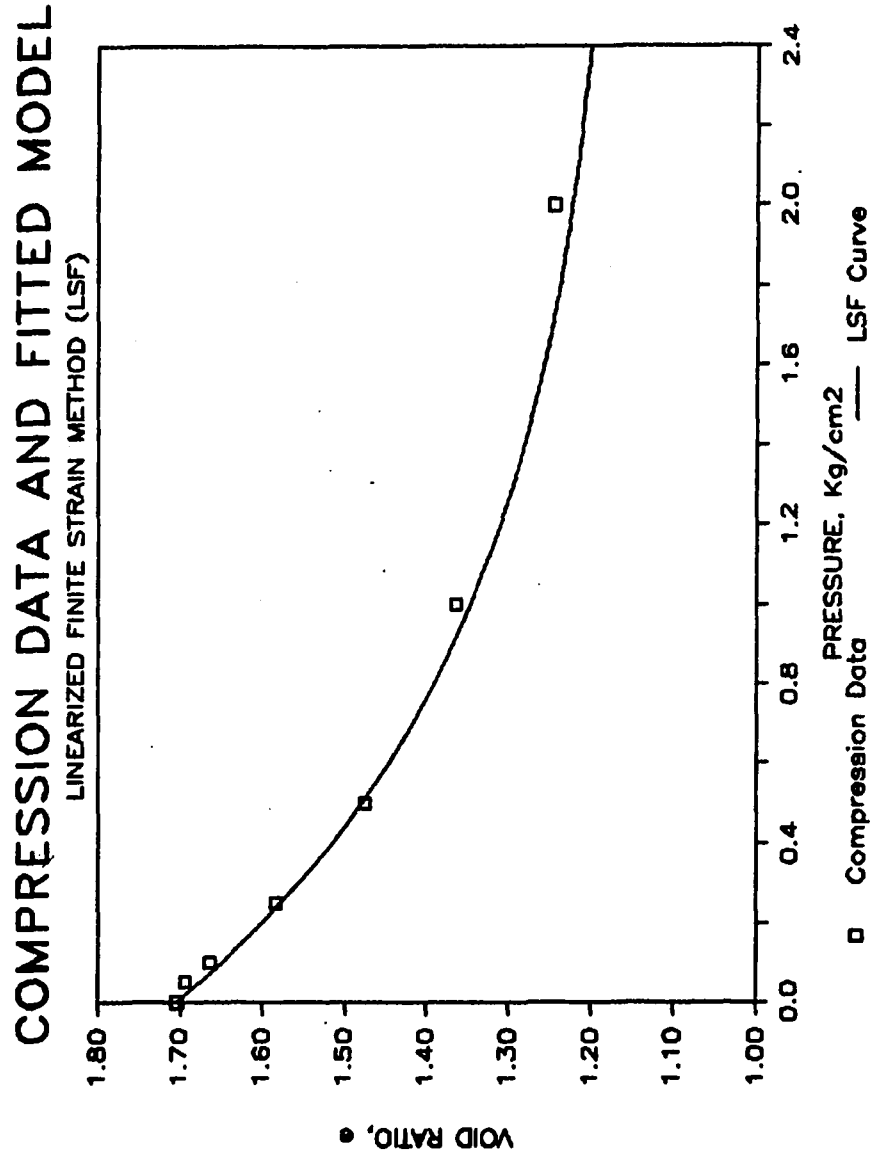

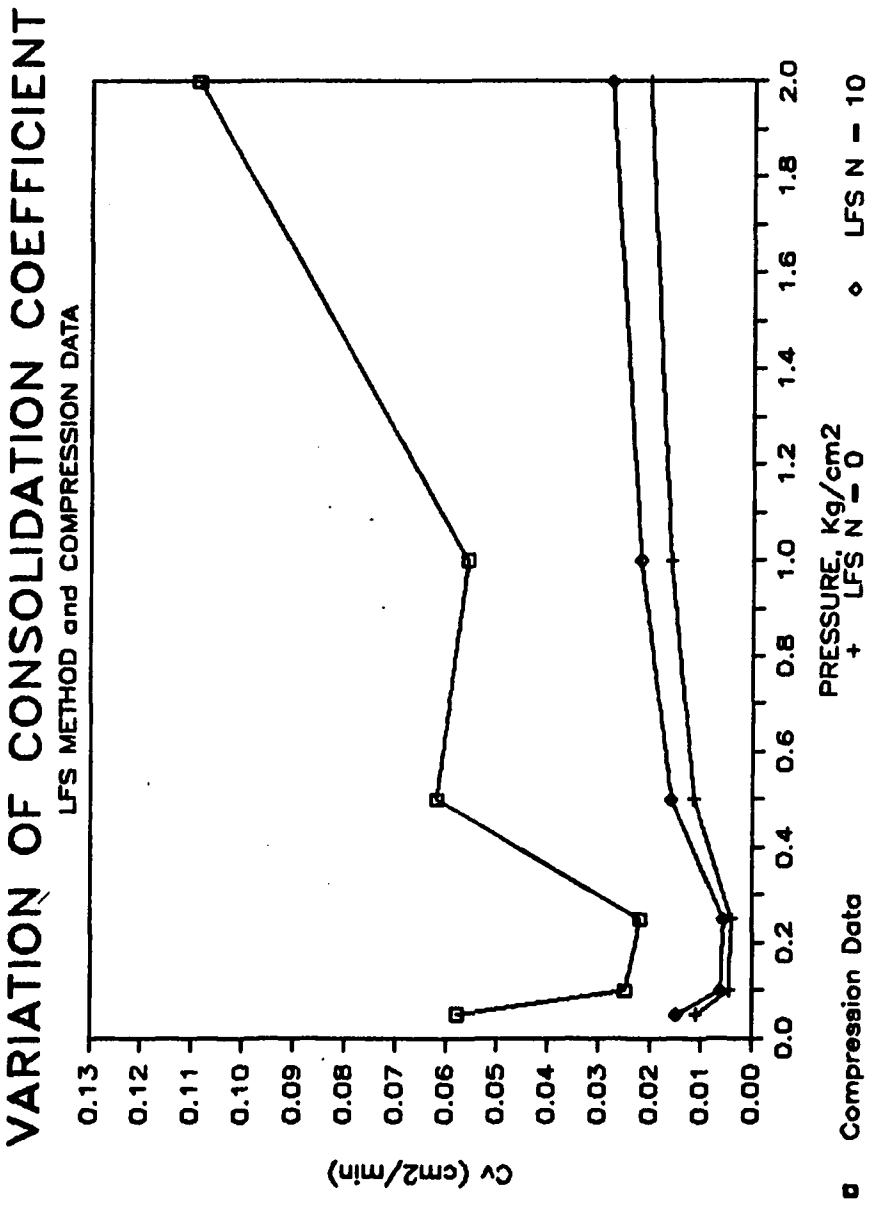

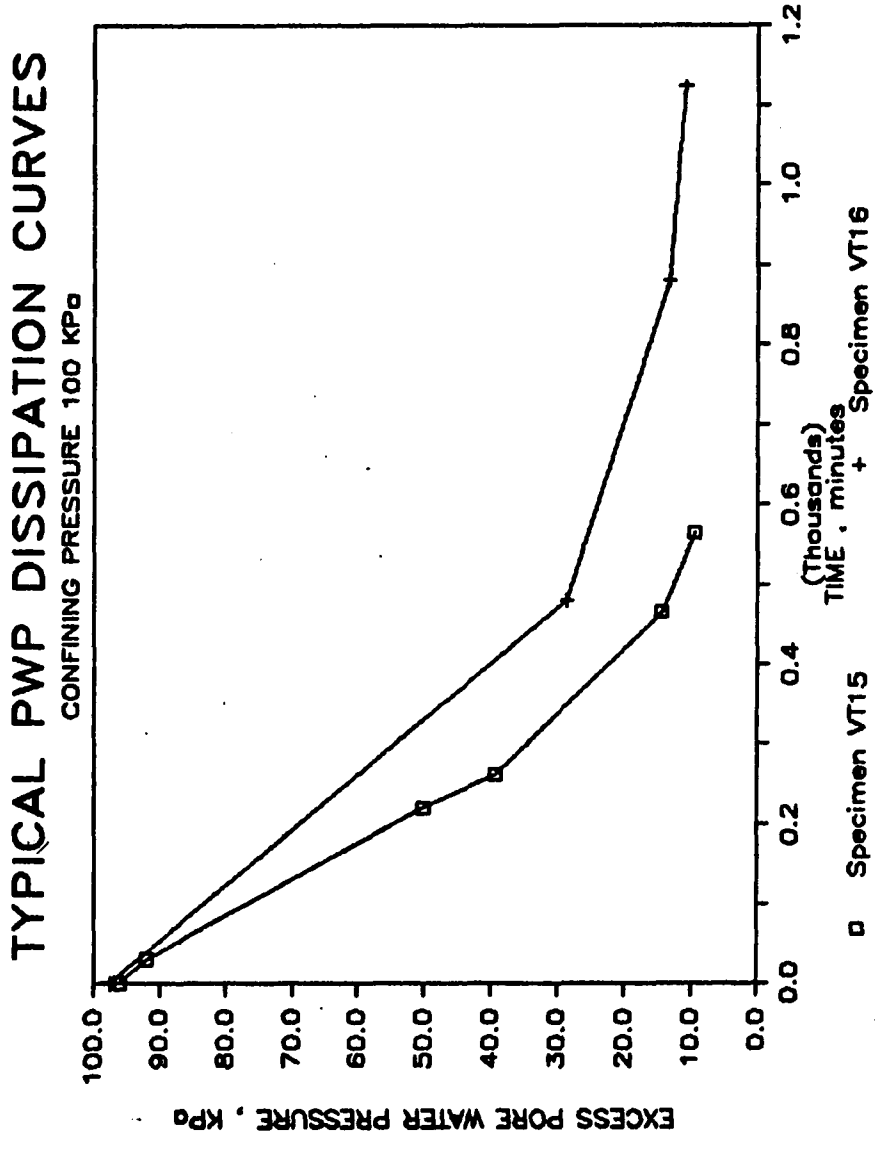

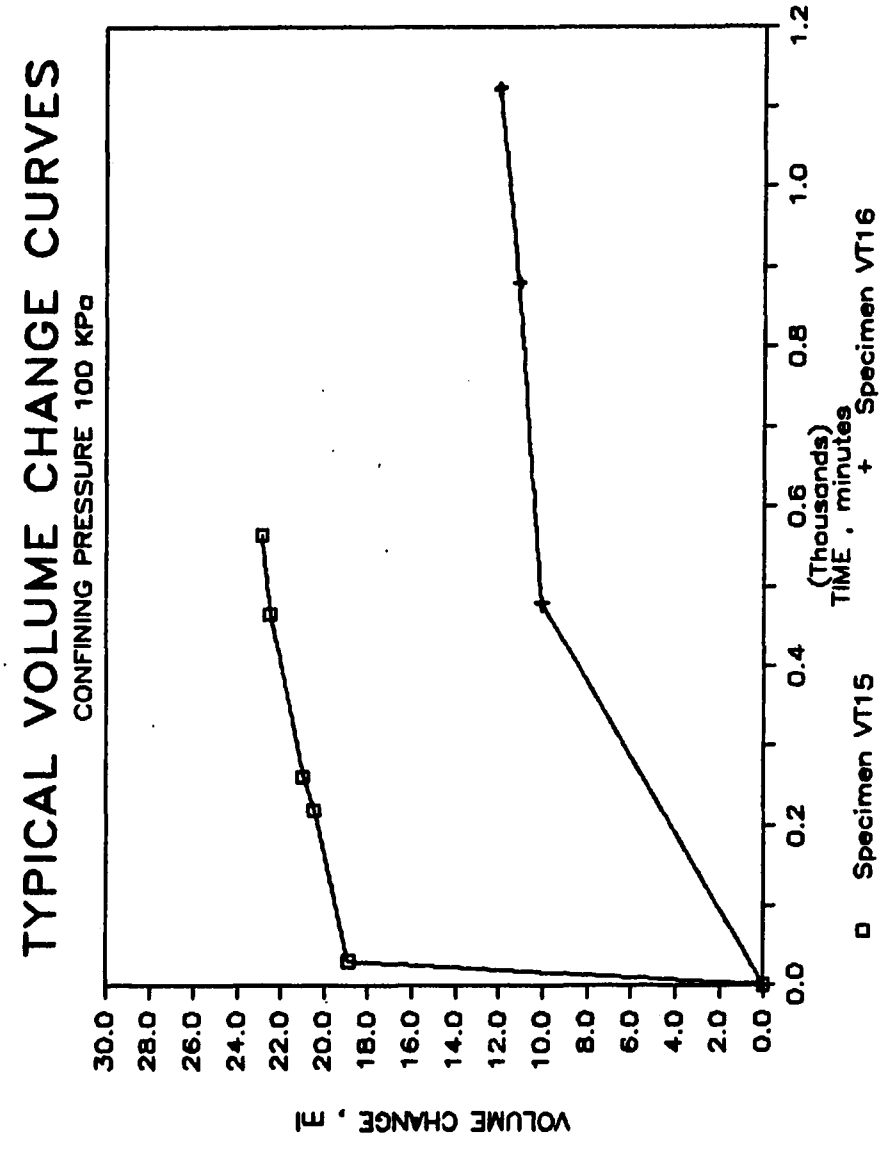

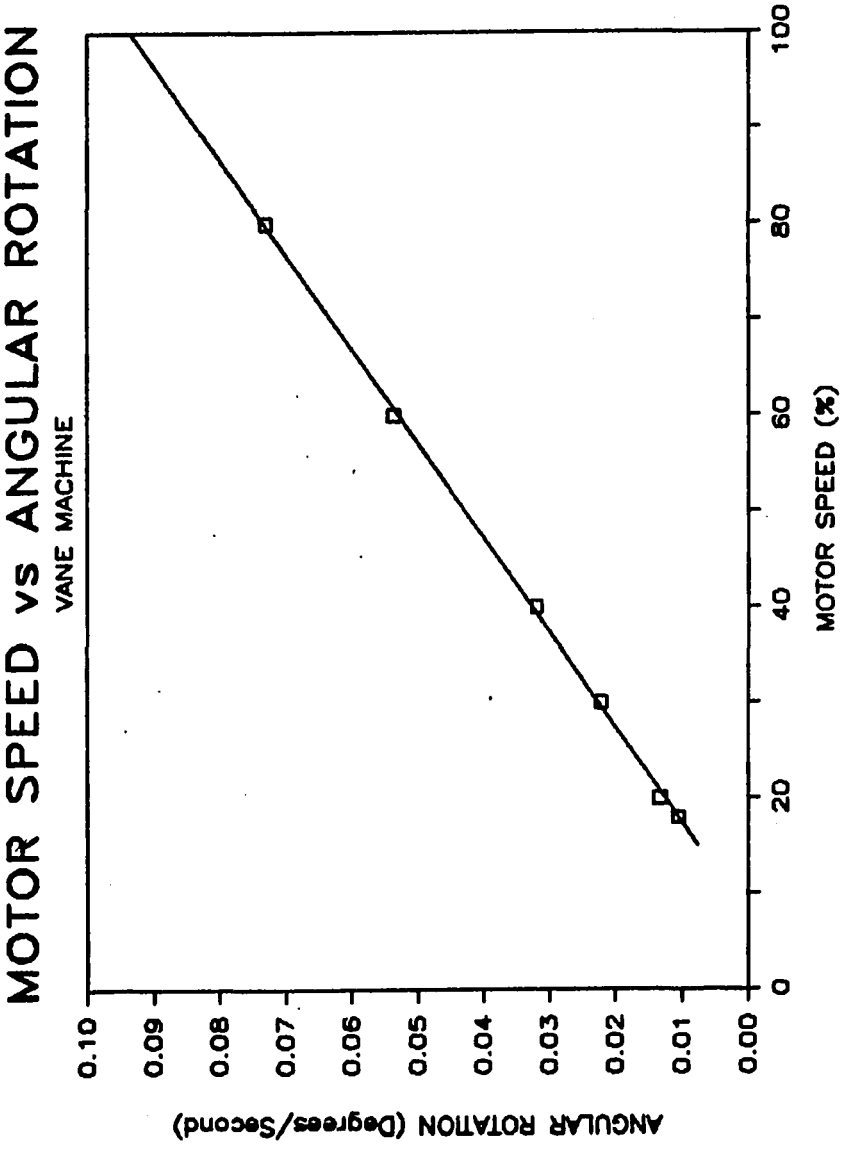

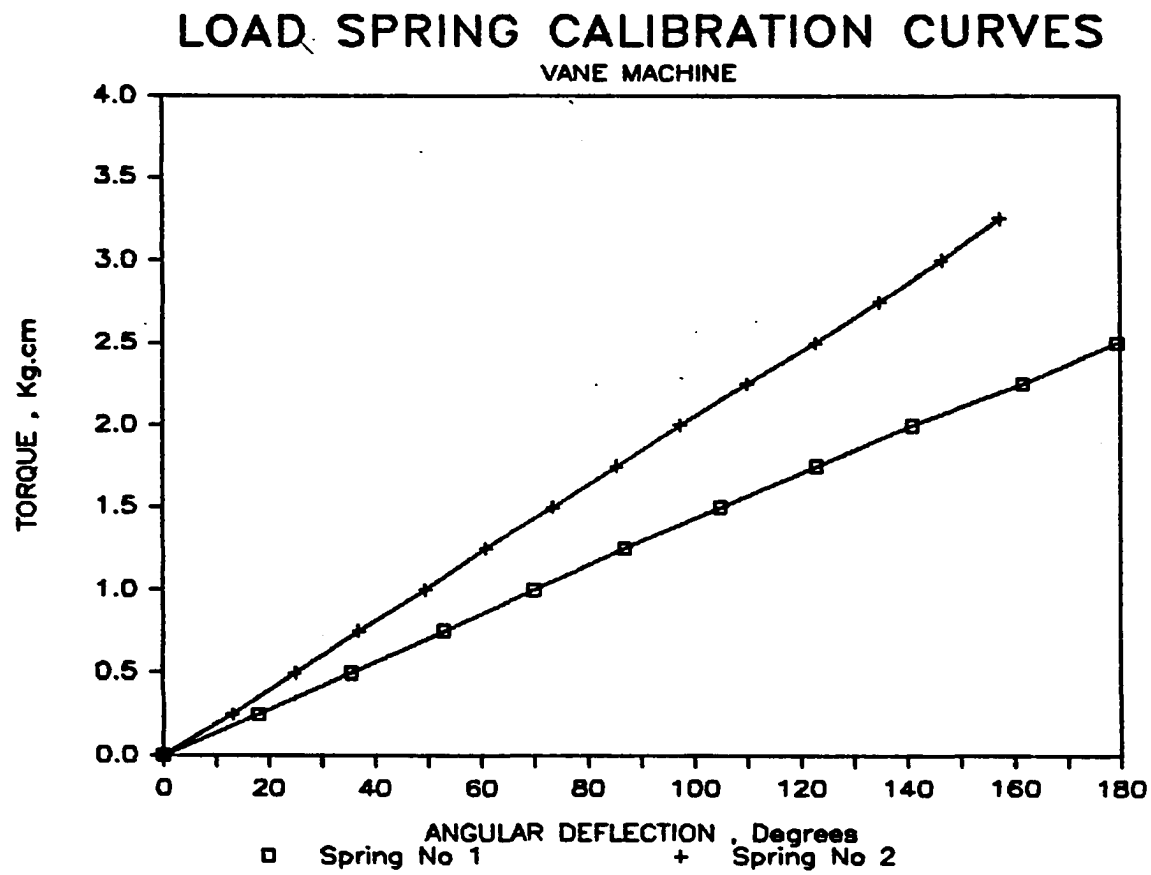

VITA

Date of Birth : February 10, 1956 Artvin, Turkey

1974 - 1978 : BS Civil Engineering
Bogazici University ,Istanbul, Turkey

1979 - 1981 : MS Civil Engineering (Geotechnical)
Louisiana State University, Baton Rouge, LA

The author worked as a Graduate Research and Teaching Assistant in the Civil Engineering Departmant of Louisiana State University during 1979 - 1986.

DOCTORAL EXAMINATION AND DISSERTATION REPORT

Candidate: Sibel Pamukcu

Major Field: Civil Engineering (Geotechnical)

Title of Dissertation: Low Strain Shear Measurements of Soft Sediments Using Triaxial vane Device

Approved:

Joseph N. Suhayda
Major Professor and Chairman

Dean of the Graduate School

EXAMINING COMMITTEE:

G. Steven Gipson

Neal W. Stoltzfus

Date of Examination: April 25, 1986